UiT
THE ARCTIC
UNIVERSITY
OF NORWAY

Faculty of Science and Technology

Department of Geosciences

Comparison and classification of an Arctic Transitional snow climate in Tromsø, Norway

—

Paul Velsand

Master Thesis in Geology — GEO-3900

October 2017

Paul Velsand: *Comparison and classification of an Arctic Transitional snow climate in Tromsø, Norway,* Master of Science, October 2017

SUPERVISORS:
Professor Jan Sverre Laberg, UiT
Associate Professor II Rune Verpe Engeset, CARE UiT
Research Scientist Markus Eckerstorfer, Norut

LOCATION:
Tromsø

SUBMISSION DATE:
October 2017

The cover picture shows the high altitude study plot at Steinskarfjellet with mountains in Ersfjorden, Kvaløya as a backdrop on March 29, 2017. The red stakes were used for depth measurements and orientation at the study plot.

ABSTRACT

Winter tourism in Tromsø has increased significantly over the last years, consequently also the skiing tourism. It is advertised that Tromsø has a mild coastal climate compared to other destinations at similar latitudes. Existing snow climate classes separate covers into a maritime, continental and a transitional class where persistent weak layers are rare in the maritime class. Rain and average air temperatures during snow season are decisive factors whether a snow pack one single winter is classified as maritime or not (Mock & Birkeland, 2000).

In total 76 snow profiles from the winter 2016-2017, in addition to winter meteorological data from 1957 to 2017, have been used to classify the snow cover climate in the Tromsø area. During the winter season 2016–2017, two study plots approximately 25 and 50 km away from open sea were classified as maritime and continental, respectively. Simultaneously, persistent weak layers were observed and forecasted from February to mid-May in both forecasting regions Lyngen and Tromsø. Thus, an *Arctic transitional* snow climate is defined as having multiple rain-induced crusts in relatively warmer years and extensive depth hoar formation in relatively colder years, where the frequency of constructive metamorphism increase inland.

Such a snow cover classification is useful in many ways. Spatial comparison with other areas, both national and international, becomes possible; temporal comparison, making a description of the relationship between weak layers and climate, becomes possible; as well as it provides a better data set for Norwegian avalanche forecasters. Also, this thesis provides the Tromsø area with its own snow cover climate describing typical processes influencing snow and snow stability. At best, the knowledge provided may contribute to prevent fatal accidents in snow covered avalanche terrain.

SAMMENDRAG

Vinterturismen, og også skiturismen, til Tromsøområdet har økt signifikant de siste årene. Det blir reklamert med at Tromsø har et mildt kystklima sammenlignet med andre destinasjoner på samme breddegrad. Eksisterende snøklimaklasser deler snødekker inn i en maritim, kontinental og en overgangsklasse, der vedvarende svake lag er uvanlige i den maritime klassen. Regn og gjennomsnittstemperatur i løpet av vinteren er en avgjørende faktor for om et snødekke en enkelt vinter blir klassifisert som maritimt eller ikke (Mock & Birkeland, 2000).

Til sammen 76 snøprofiler fra vinteren 2016–2017, i tillegg til vinterværdata fra desember 1957 til mai 2017 har blitt brukt for å klassifisere snødekkeklimaet i Tromsøområdet. Vinteren 2016–2017 ble to studielokaliteter om lag 25 km og 50 km unna åpent hav henholdsvis klassifisert som maritimt og kontinentalt. Samtidig ble det fra februar til midten av mai observert og varslet vedvarende svake lag i snødekket i både skredvarslingsregion Tromsø og Lyngen. Et *arktisk overgangsklima* har blitt definert i varme vintre til å ha flere regnskarelag, mens det i kalde vintre har lag av begerkrystaller og kantkorna snø. I både de varme og kalde vintrene er det en økende tendens til oppbyggende omvandling av snøkrystaller lenger vekk fra kysten.

En snødekkeklassifisering for Tromsøområdet er nyttig for flere områder. Sammenligning med andre regioner, både nasjonalt og internasjonalt, blir mulig; sammenligning over tid blir mulig slik at forholdet mellom snøskred og klima kan beskrives; og et bedre datagrunnlag blir tilgjengelig for norske skredvarslere. Samtidig gir oppgaven Tromsøområdet sitt et eget snødekkeklima som beskriver prosessene bak typiske skredproblem en kan finne der. I beste fall vil kunnskapen være med og redde liv.

ACKNOWLEDGMENTS

This thesis would not be what it is today without my supervisors Jan Sverre Laberg, Rune Verpe Engeset, and Markus Eckerstorfer. You have allowed me to do my own project, still raising the quality of it by many levels thanks to fruitful questions and constructive feedback. Especially, thanks to Max. You have been a truly inspiring mentor and teammate, taking this project seriously and always looking out for solutions how to make it better. After every meeting we have had together, I have had a dedicated feeling of *"I can do this, if I work like Max"*.

The Center for Avalanche Research and Education (CARE) at the University of Tromsø is thanked for scholarship making it possible to present this thesis at the Nordic Conference on Snow Avalanches and Mountain Recreation. The Norwegian Water Resources an Energy Directorate (NVE) is thanked for letting me joining their snow observatory course. Karsten Müller at NVE is thanked for answering questions about xgeo. Thanks also to an officer in the Norwegian Army that mailed me field books.

Thanks to all the field assistants: Sam, Fraser, Eef, Ingelin, Gaute, Erik, Daniel, Marie and Marius. Especially Marius, my flatmate, who has dug a large portion of the snow pits. Thanks to Marte and Daniel for proofreading. Also Marius, thanks for maintaining a social life outside our household where I could sneak in during the last weeks of tunnel visioned thesis writing.

Last but not least, I will thank my mother and my father who are a foundation in my life and always keep their home open for me and known and unknown friends. Thanks Linnea, for all conversations putting life into perspective.

Paul Velsand
Tromsø, October 2017

CONTENTS

LIST OF FIGURES

LIST OF TABLES

ACRONYMS

AROME Application of Research to Operations at MEsoscale

ATES Avalanche Terrain Exposure Scale

CARE Center for Avalanche Research and Education

E8 European route 8

EC European Center for Medium Range Weather Forecasting

ECT Extended column test

NVE The Norwegian Water Resources and Energy Directorate

OGRS Observation Guidelines and Recording Standards for Weather, Snowpack and Avalanches

SLF WSL Institute for Snow and Avalanche Research

SWAG Snow, Weather, and Avalanches: Observation Guidelines for Avalanche Programs in the United States

WWAN Westwide Avalanche Network

1 INTRODUCTION

1.1 MOTIVATION

Snow stratigraphy in mountainous areas holds important information about past weather events and future snow avalanche activity (Fitzharris, 1987; Mock & Birkeland, 2000; McClung & Schaerer, 2006; Hägeli & McClung, 2007). The consistent investigation of snow properties in carefully selected snow pit locations is thus critical for the assessment of snow avalanche hazard in space and time. Snow avalanches will from this point be referred to as avalanches.

Avalanches are a threat to people living and traveling in snow covered mountain areas worldwide. The worst consequence of an avalanche accident is obviously death. Fitzharris and Bakkehøi (1986) found that on average nine people died from avalanches every year in Norway in the period 1855–1985. The Norwegian Geotechnical Institute (2016) has registered avalanche fatalities since 1975 and has found that in the period from 1975 to 2015, 5.7 people were killed every year on average. The numbers from The Norwegian Geotechnical Institute (2016) also reveal that the average number of people killed every year has increased between 2009 and 2015, with 9.7 killed. In the winter seasons 2015–2016 and 2016–2017, five and two people were killed, respectively.

According to the The Norwegian Geotechnical Institute (2016), 82% of the fatalities in the 1975–2015 period were during work or recreational activities in the backcountry, while the residual 18% were people driving on a road or staying inside their houses.

Norwegian public avalanche prevention took an important step with the establishment of the Norwegian Avalanche Warning Service Varsom (*E: cautious, careful*) in 2013 (Engeset, 2013). Later, the Center for Avalanche Research and Education (CARE) under the University of Tromsø, has been established in the period from 2015 to 2017. They aim to improve decision making in risky environment for recreationists, professionals and the parts of the Norwegian society exposed to avalanche hazard, hence saving lives.

This thesis aims to provide Varsom and potential readers with valuable data for understanding snow conditions in the Tromsø forecasting area. It describe in what way the snow conditions vary both in time and space, and will make an effort on putting the typical snow conditions in an international context. This is important because it will make comparison to other avalanche winter regimes possible, as well as build a basis for applying different methods of snow investiga-

tion. It may also be important for being able to predict avalanches in Northern Norway during climate changes. Last but not least, it will contribute to the avalanche forecast helping skiers make better decisions in avalanche terrain and therefore reducing the probability for accidents.

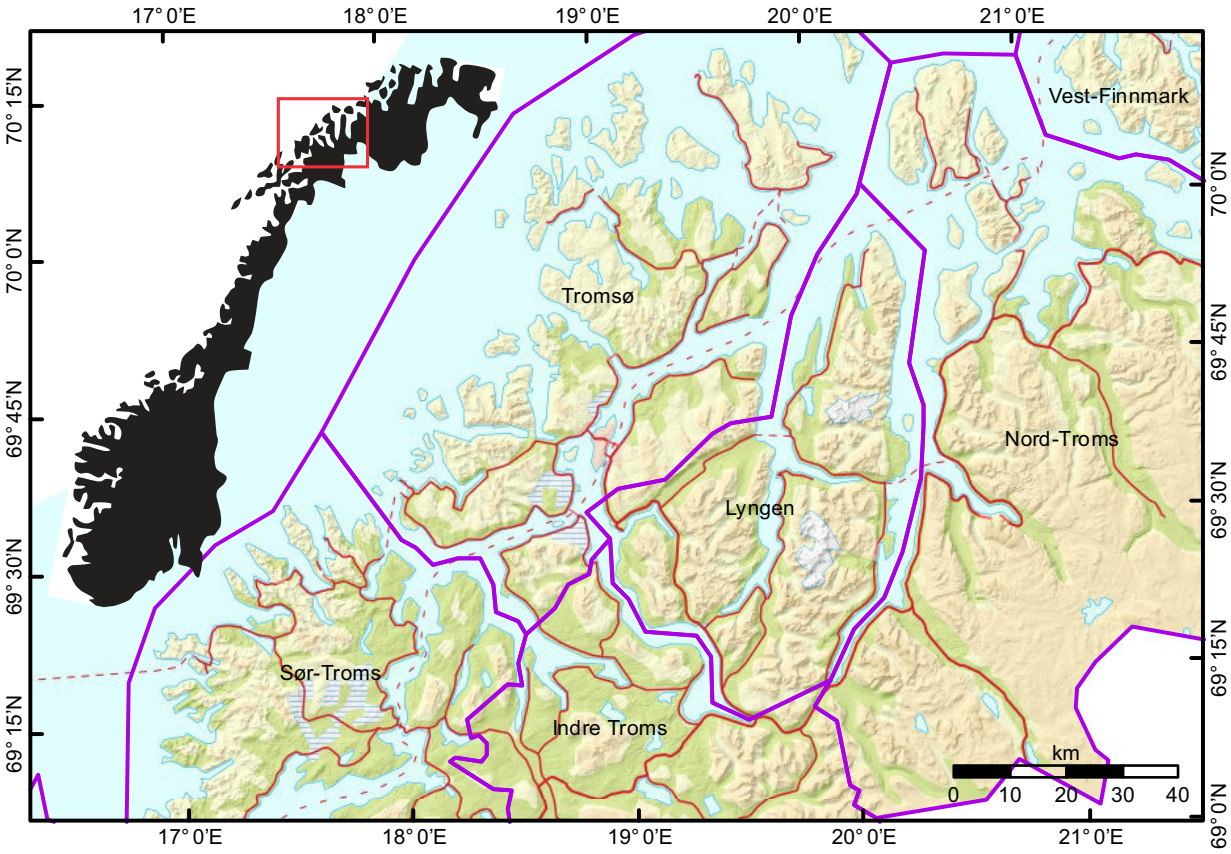

Figure 1.1: Overview map of avalanche forecasting regions in Troms. The purple lines represent avalanche forecasting regions, with its respective name inside.

1.2 OBJECTIVES

The main aim of the project is to classify the snow climate and avalanche winter regime of the avalanche forecasting region Tromsø, as no such classification exists at this time. This will be done by investigating spatial and temporal variance in snow stratigraphy and snow stability with well established snow investigation field methods at selected spots at Steinskarfjellet and Fagerfjellet. Thus, an important objective is to plan and implement safe field work near and in avalanche terrain, so that snow investigations can be conducted.

Another aim is to contribute with relevant information to the Norwegian avalanche forecast service by posting observations on the natural hazard observation site regObs and in the regObs cell phone app.

regObs is a public tool made by Varsom to support crowd sourcing of avalanche relevant data. The purpose of the tool is to improve the data availability for forecasters and information readability for the users. This is done by minimizing the time span between observations and registrations and providing absolute spatial observations together with the regional forecast (Ekker, Kværne, Os, & Humstad, 2013).

A literature review of previous works on snow climate and avalanche classifications will be presented to put the reader in context with state-of-the-art ideas, terms and methods. Together with collected snow and avalanche data from Tromsø, this allows for a comparison between other classified snow region climates in the world.

A final aim is to assess the applicability of *avalanche winter regimes* classifications in mountains in Northern Norway, and also in Norway in general.

Scientific questions to be answered are:

1. What differences do the study plots at Steinskarfjellet and Fagerfjellet display when it comes to snow stratigraphy and snow stability during the winter season 2016/2017?

2. From data collected in well planned and safe field work: into which of the established snow climate classes and what winter avalanche regime do selected study plots at Steinskarfjellet and Fagerfjellet in the winter season 2016–2017 fit, and why?

3. From historical meteorological data: into which of the established snow climate classes do average weather conditions at Steinskarfjellet and Fagerfjellet fit?

2

BACKGROUND AND LITERATURE STUDY

Different regions of the world exhibit different SNOW CLIMATES[1] and AVALANCHE WINTER REGIMES[2]. Snow climates are classified into a maritime and continental class with a transitional class in between (Roch, 1949; McClung & Schaerer, 2006), where the classes represent characteristics of a particular snow cover and its locality.

Tromsø is a city in Northern Norway that lies among fjords and mountains at 69.5° north. The climate in Tromsø is relatively mild and precipitation levels are high compared to other locations at similar latitudes due to the presence of the Norwegian Atlantic Current that brings warmer water northeast along the Norwegian Coast (The Norwegian Meteorological Institute, 2016). Visit Tromsø (2016) advertises Tromsø to foreign travelers as having "... a milder *coastal climate* than other destinations at the same latitude" (italicizing by the author).

At the same time, the snow cover in Tromsø does *regularly exhibit characters of a continental snow cover with layers of persistent weak structures* (The Norwegian Water Resources and Energy Directorate, 2016; Emberland, Medby, & Pedersen, 2015; Matre, 2014).

Winter tourism in Tromsø has increased more than half a magnitude from the winter season 2005–2006 to the winter season 2015–2016 (Aronsen & Benjaminsen, 2016), and ski specific tourism does also increase (Hansen, 2015). Official travel guides advertise skiing in Tromsø and adjacent areas for an international market, and money is invested in better infrastructure for skiers (Wahlgren, 2016). A good avalanche forecast that understands local conditions in the area is important to help skiers make better decisions in avalanche terrain and therefore reducing the probability for accidents. Describing the avalanche winter regime of Tromsø will provide a correction of the discrepancy of Tromsø having a coastal weather climate and *not* having a maritime snow climate.

2.1 HISTORICAL DEVELOPMENT OF CLASSIFICATIONS OF SNOW PACK CLIMATES AND AVALANCHE REGIMES

The snow climate classes that are used today origin from when André Roch, the head of the avalanche protection research at WSL Institute for Snow and Avalanche Research (SLF), described climatic differences

1 *Snow climates* are snow cover characteristic classifications mainly based on meteorological data (McClung & Schaerer, 2006).

2 *Avalanche winter regimes* is a term encompassing both meteorological based snow climate together with snow layer and avalanche characteristics based on standardized snow investigations (Hägeli & McClung, 2007).

in the western U.S.A. in 1947 (Roch, 1949). The zones are shown in Figure 2.1. Roch's classes have evolved into three classes that still make up the basis for snow climate classifications today.

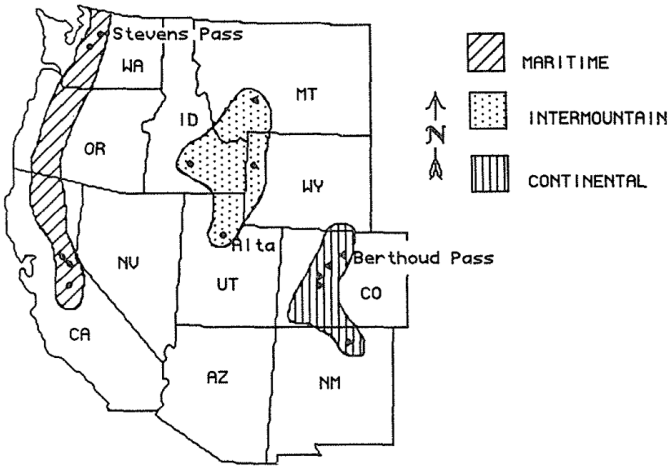

Figure 2.1: The three snow climate zones in the western U.S.A. first identified by Roch (1949) and later described by Armstrong and Armstrong (1987). The place names refer to high elevation data collection sites after 1949 (Armstrong & Armstrong, 1987). The figure is from Armstrong et al.

André Roch described three zones which later have become known as MARITIME and CONTINENTAL together with a TRANSITIONAL[3] zone situated in between the two former. He did not do any systematic research, but his observations lead to high elevation snow and weather study sites being put up by the U.S. Forest Service in each of the three regions. The purpose of the study sites was acquiring continuous data on important meteorological snow data, e. g. temperature, wind direction and speed, precipitation rate and type (Armstrong & Armstrong, 1987).

Data from these high elevation weather stations was the foundation for the first quantitative classification of snowpack climates by LaChapelle (1966). LaChapelle used snowpack climate data for guidance on what type of investigating methods to be used to provide the best avalanche forecast from that specific area.

With data from U.S. Forest Service's Westwide Avalanche Network (WWAN), Armstrong and Armstrong (1987) compared characteristics of all three climate zones quantitatively as well as analyzing the overall stability of the different zones based on avalanche accident data. Computations of monthly temperature gradients were also executed, showing tendencies to presence of more persistent weak layers within

3 The term *intermountain* instead of *transitional* is still extensively used in the U.S.A due to its position between Coast Mountains and Rocky Mountains. McClung and Schaerer (2006) suggests using *transitional* due to its greater applicability for other countries and areas.

the snow cover in the transitional and especially the continental zone. In these zones, a bigger portion of artificially triggered avalanches released in non-storm periods due to these persistent weak layers . This is also supported from the avalanche accident data; avalanches in continental zones tend to release *below the old snow – new snow interface*, while avalanches in the coastal zone release at or above the old snow – new snow interface. Armstrong et al.'s data supported the concept of three distinct zones and emphasized the conclusion that a continental climate will produce a snow cover that is more unstable a longer portion of the winter season. They also noticed a lack in standardization of avalanche event reporting. Hence, information on size and type of release were not possible to statistically compare.

Thirteen years later, Mock and Birkeland (2000) published an article where they also used the WWAN to provide an updated snow avalanche classification of the western United States. Mock and Birkeland did also investigate temporal variability and identified abnormal avalanche winters and their relationship to synoptic climatic patterns. Those winters were further investigated at specific sites by daily plots of different snow climate variables to understand avalanche responses to weather and climate. One specific important product of their research was a flow chart for classifying snow and avalanche climates based on values acquired in the three different climate zones (Figure 2.2). This flow chart has later been used in other snow climate classifications (Hägeli & McClung, 2003; Hägeli & McClung, 2007; Ikeda, Wakabayashi, Izumi, & Kawashima, 2009; Eckerstorfer & Christiansen, 2011).

Mock and Birkeland also conclude like Armstrong and Armstrong (1987); a typical continental winter is conducive to a different avalanche regime than a maritime winter. Avalanches in continental zones have a tendency to release on persistent weak layers within the old snow in the snowpack, while avalanches in coastal zones have a tendency to release on the old snow – new snow interface.

In 2007, observations on spatial variability of persistent weak layers in relation to average weather in the winter months was conducted by Hägeli and McClung (2007). After examining avalanche characteristics in a transitional snow climate in the Columbia Mountains, southwestern Canada (Hägeli & McClung, 2003), Hägeli and McClung (2007) showed that there are significant temporal and spatial variations of the dominating weak layer in areas with the same snow climate characteristics.

A zone is an area that displays similar characteristics (Jewell & Abate, 2010). Thus, a snow climate zone experience similar amounts of snowfall and rainfall, and similar temperatures. In general, the term *snow climate* has been used when measuring and comparing *average meteorological factors* in different zones (LaChapelle, 1966; Armstrong & Armstrong, 1987; Sturm, Holmgren, & Liston, 1995; Mock &

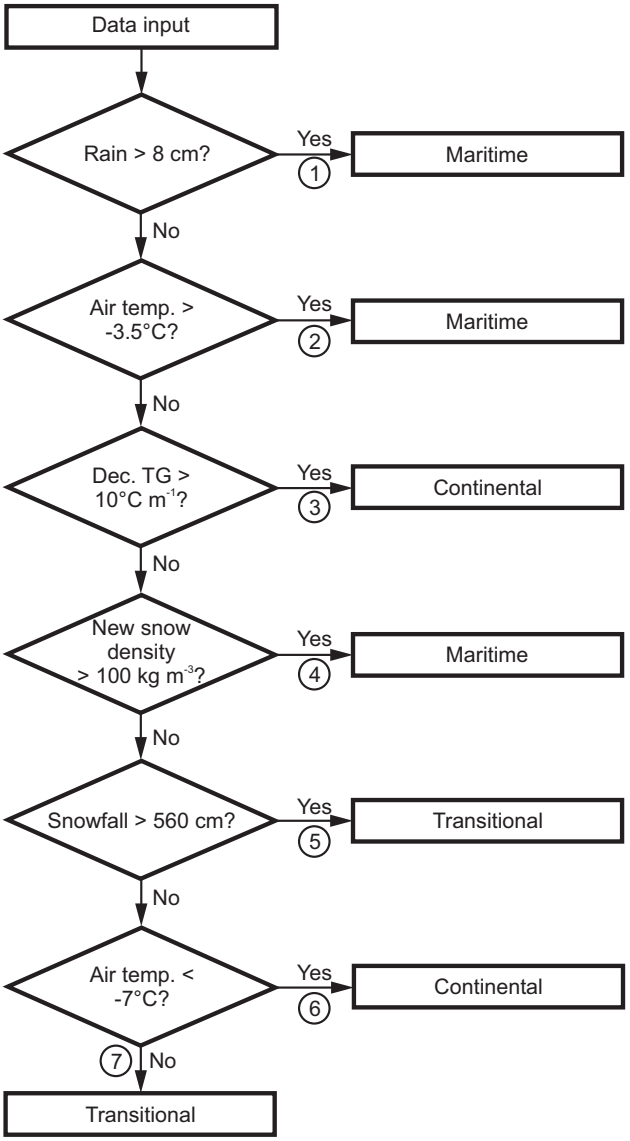

Figure 2.2: Flow chart describing the classification procedure for snow climates. Modified after Hägeli and McClung (2007) and Mock and Birkeland (2000). TG: temperature gradient, SWE: snow water equivalent.

Birkeland, 2000; Sharma & Ganju, 2000; Beniston, Keller, & Goyette, 2003; Höller, 2009).

By including snowpack characteristics that directly relate to avalanche activity, Hägeli et al. suggested *avalanche winter regime* as a new classification term that also took snowpack weaknesses and avalanches into account. Unlike a snow climate zone classification that base on average meteorological data, the classification term and method *avalanche winter regime* is supposed to examine the *snowpack structures* that allow avalanches to happen. The idea is that *process-understanding* of the weak layers in a particular snowpack is of higher value for avalanche forecasting, especially when talking about slab avalanches on persistent weak layers (Hägeli & McClung, 2007).

Avalanche problems explain what snowpack structures that are responsible for the given avalanche danger rating.

To communicate such a process-understanding of avalanches to the public, the term *avalanche problems* was introduced around 2010 (Lazar, Greene, & Birkeland, 2012). Both the American, Canadian, Swiss, and Austrian, as well as the Norwegian forecast service use different avalanche problems as a way of communicating avalanche hazard (Landrø, 2013).

Since weak snowpack structures is a closer proxy to what avalanches that are expected than meteorological factors, Hägeli and McClung (2007) suggests to include the *avalanche winter regime* in snow-climate classifications.

2.2 CHARACTERISTICS OF THE DIFFERENT SNOW CLIMATES

Following in this section is an outline of the different snow climates. Typical meteorological factors will be described and are synthesized in Table 2.1. Typical weak layers are shown in Table 2.2 and will also be described.

Table 2.1: Climate characteristics of maritime, transitional and continental snow climates. From McClung and Schaerer (2006) after Armstrong and Armstrong (1987)

Type	*Total precipitation [mm]*	*Air temperature [°C]*	*Snow depth [cm]*	*New snow density [kg/m³]*
Maritime	1280	-1.3	190	120
Transitional	850	-4.7	170	90
Continental	550	-7.3	110	70

Table 2.2: A compilation of weak layer characteristics of different snow climates from different snow climate classifications. The weak layers mentioned are active unless *inactive* is stated.

	Weak layer characteristics		
Author	*Maritime*	*Transitional*	*Continental*
LaChapelle (1966)	CR	—	DH
Armstrong and Armstrong (1987)	—	—	DH, SH
Mock and Birkeland (2000)	—	—	DH
Hägeli and McClung (2003)	—	FC/CR and SH	DH
Hägeli and McClung (2007)	FC, CR, inactive SH	FC, SH, inactive CR	FC (DH)
Eckerstorfer and Christiansen (2011)	—	—	FC, DH

CR = pure crusts, FC = faceted grains, FC/CR = facet-crust combinations, SH = surface hoar, and DH = depth hoar. ( ) = potentially.

2.2.1 *Maritime Snow Climate*

A maritime snow climate is characterized by abundant precipitation both as snow and as rain (McClung & Schaerer, 2006). The prevalence of mild temperatures cause fast stabilization of the snow that falls, so that instabilities normally not persists. From weather stations with more than 15 years record in the WWAN using the regionalization provided by Armstrong and Armstrong (1987), Mock and Birkeland (2000) found that maritime snow climates have a seasonal temperature of warmer than $-3.5\,^{\circ}\mathrm{C}$, and experience rainfall of between 8 cm and close to 40 cm. Further on, the new snow density exceed $100\,\mathrm{kg/m^3}$.

Direct action avalanches release on weak layers within new snow.

Avalanches in maritime snow climates often takes place during or directly after a storm. Such avalanches may be called DIRECT-ACTION AVALANCHES and fail on snow layers or interfaces near the surface of the snowpack *within* the new snow (LaChapelle, 1966; McClung & Schaerer, 2006; Schweizer, 2008). A notable cause for the avalanches is rain that follows immediately after a new snowfall. Typical weak layer characteristics found in maritime snow climates are rain crusts and near-surface faceting (Table 2.2) which are described underneath.

WEAK INTERFACES AND CRUSTS An avalanche can also slide on bed surfaces due to poor bonding between new and older snow, or on sun or rain crusts. Rain crusts form on all aspects of a mountain from rain that saturates the snow surface before it refreezes. A rain crust is smooth and tends to be non-cohesive to

new snow burying the crust. Subsequent rainfalls may lubricate the rain crust into a sliding surface (McClung & Schaerer, 2006).

NEAR-SURFACE FACETING Near-surface faceting is a generic term for different processes that result in extreme near-surface temperature gradients (Birkeland, 1998). *Melt layer recrystallization* is typically associated with rain events and occurs when rain saturates the snow surface before a subsequent snowfall of cold and dry snow. The saturated wet snow layer creates a strong temperature gradient to the cold overlying snow, which favors the growth of faceted crystals. Melt layer recrystallization temperature gradients of 1°C/cm to 3°C/cm has been observed (Birkeland, 1998).

2.2.2 *Continental Snow Climate*

A continental snow climate is characterized by; compared to maritime snow climates; lower snowfall, notably colder temperatures and a location inland from coastal areas. The snow cover in a typical continental snow climate is shallow and often unstable due to persistent weak layers in the snowpack. Mock and Birkeland (2000) defined a continental snowpack to be characterized by a *December temperature gradient* of more than 10 °C/m and to experience a seasonal mean temperature colder than −7 °C.

A temperature gradient above 10°C/m cause constructive metamorphism.

As with maritime snowpacks, many avalanches in a continental snowpack release on non-persistent weak interfaces in new snow during or immediately after snowfalls (McClung & Schaerer, 2006). However, avalanches released on *persistent weak layers* is a distinctive feature of a continental snowpack.

A weak layer is a layer that cause unstable and avalanche prone snow. *Persistent* weak layers persists as an instability through a significant time. Jamieson (1995) defines a persistent weak layer as a layer containing faceted crystals, depth hoar, or surface hoar, while Hägeli and McClung (2003) consider a weak layer to be persistent if it displays avalanche activity after the second big snowfall after it was buried. Hägeli and McClung (2007) puts a threshold at observed avalanche activity on that layers more than 10 days after burial. Hereafter, the snow crystal specific definition from Jamieson (1995) will be used, as avalanche activity will not be monitored in the field period.

Both layers and interfaces can persist as weaknesses in the snow cover.

A persistent weak *layer* appear as a specific crystal type with a vertical extent from a few mm to many cm. Persistent weak *interfaces* are borders between different layers that can act as gliding planes for avalanches.

Persistent snow crystal forms, hereafter *persistent forms*, are recognized in the snowpack as angular crystals, or *faceted crystals*. The facets form from exotherm deposition of water on adjacent snow crystals due to water vapor pressure differences in the pore space (McClung

& Schaerer, 2006). This reaction release a lot of energy that is not easily transferred back to the snow grains. Thus, faceted crystals tend to persist through time. Persistency do also occur due to anisotropic characteristics of some crystal types. Anisotropic characteristics is to be weak in shear, and resistant to bonding to overburden layers.

Persistent weak layers are prevalent in human triggered avalanches and avalanche accidents (Jamieson & Johnston, 1992; McClung & Schaerer, 2006), and hence receive a lot of attention from avalanche forecast services.

Persistent forms typical in persistent weak layers in a continental snow cover are shown in Table 2.2 and described underneath:

FACETED CRYSTALS (FIGURE 2.3A) Faceted crystals grow due to temperature gradients above 10°C/m in the snow cover. The motion rate of water molecules through the snowpack, and hence the growth rate of faceted crystals, increase with temperature gradient, the air temperature and the available pore space.

DEPTH HOAR (FIGURE 2.3B) Depth hoar are large and strongly faceted crystals that develop near the ground. Strong faceting do ultimately result in a hollow cup shaped form, which is the typical criterion for depth hoar (Fierz et al., 2009). Depth hoar grows at large temperature gradients above 10 °C/m, and normally persist throughout the season (McClung & Schaerer, 2006).

Climax avalanches release on old snow within the snowpack.

Snow that is redistributed by winds can cause local snow accumulations. Due to the presence of persistent weak layers deeper in the snow pack, such snow accumulations may trigger avalanches even a significant time after the last snowfall. Such avalanches may be called CLIMAX AVALANCHES (LaChapelle, 1966; Schweizer, 2008).

Due to the commonness of thin snow covers in continental snow climates, constructive metamorphism can happen throughout the winter. Thus, in continental mountain ranges, one can find almost the entire snow pack to comprise weak faceted crystals.

2.2.3 *Transitional Snow Climate*

The transitional snow climate class displays features of both a maritime and a continental snow climate (LaChapelle, 1966; McClung & Schaerer, 2006). Consequently, a transitional snow climate can occur both in a region that normally exhibits a maritime or continental snowpack. But, Eckerstorfer and Christiansen (2011), Ikeda et al. (2009) have added complexity to the simple statement that "a transitional snow climate is a mixture of a maritime and continental snow climate". Ikeda et al. (2009) described a study plot in the Pacific Sea side mountains in the Japanese Alps where the snow depth and structure displayed continental characteristics, but with a mean snow season

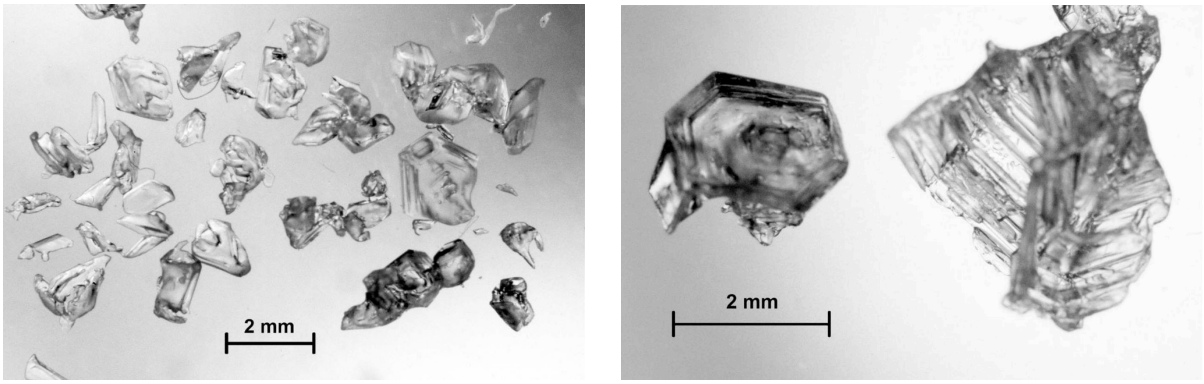

(a) Solid faceted crystals.

(b) Depth hoar crystals with faceted edges.

Figure 2.3: Solid faceted and depth hoar crystals. The facets are the elongated edges on the crystals. Both images are from (Fierz et al., 2009).

rainfall of 75 mm i. e. close to the threshold of 80 mm of a maritime climate. Eckerstorfer and Christiansen (2011) identified a *"High Arctic maritime snow climate"* in the Central parts of the Svalbard archipelago in the Arctic Sea, where the snowpack also exhibited a combination of extreme maritime and continental characteristics, respectively extensive ice layers due to rain-on-snow events and a extensive depth hoar in investigated snow pits.

Thus, one should be careful when imagining the three different snow climates. Instead of utilizing the concept of moving *from* a maritime snow climate, *through* a transitional snow climate *into* a continental climate, one should start with either a maritime *or* continental climate and picture characteristics of the opposite climate as features in the original climates, as shown in Figure 2.4. The overall descriptive term for such a climate could be a *transitional snow climate*.

Transitional snow climate

✓	Mar	Mar
	Mar	Cont
X	Mar	Tran
	Tran	Cont

Figure 2.4: Conceptual model of the characteristics of a transitional snow climate. The check marked row shows the correct conceptualization, while the cross-marked row shows the wrong one. The different cells represent characteristics of a transitional snow climate, where Mar = maritime characteristics, Tran = the faulty transitional characteristics, and Cont = continental characteristics.

A transitional snow climate is conducive to the same type of persistent weak layers as a continental snow climate due to presence of strong temperature gradients. But when continental snow climates

tend do have dry air, the air can be moist in a transitional snow climate. Even though it may occur in any of the three snow climates, *surface hoar* is listed below as a typical persistent weak layer in a transitional snow climate. Surface hoar crystals are shown in Figure 2.5.

Surface hoar may occur in all three snow climates.

SURFACE HOAR Surface hoar grows because of strong outgoing radiation during calm and humid conditions and under a clear sky without sun. The outgoing radiation from the snowpack causes it to cool down, allowing moist from the humid air to condense on the snow surface due to temperature gradients of up to 300°C/cm (McClung & Schaerer, 2006). Surface hoar is very persistent when buried, but wind easily destroys the fragile crystals on the surface. Hence surface hoar appears patchy in windy regions, which decrease the expected avalanche sizes. Surface hoar has a lower preferable failure slope angle than other persistent weak layers (McClung & Schaerer, 2006).

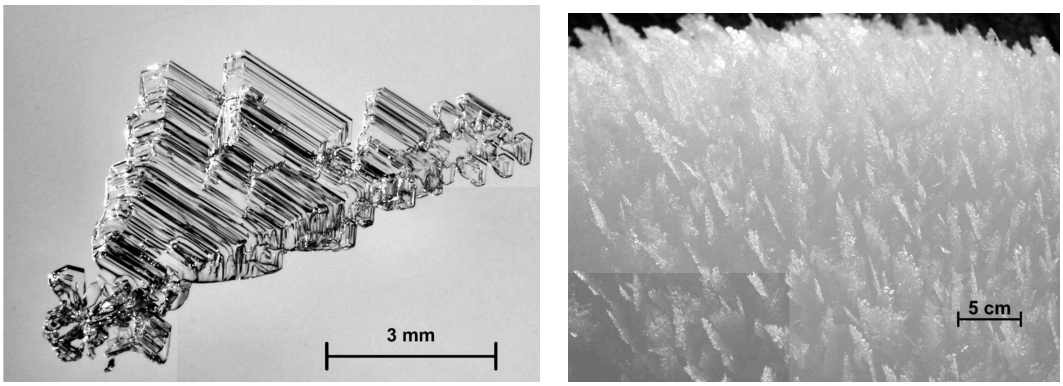

(a) Surface hoar crystal.

(b) Surface hoar crystals on a surface.

Figure 2.5: Surface hoar crystals. Both pictures from Fierz et al. (2009).

3

METHODS

Forecasting avalanches involves continuous evaluation of different factors (McClung & Schaerer, 2006). For making data *valuable* to an avalanche forecasting service, accurate observations recorded in an uniform manner and in a mutual nomenclature is crucial. Following established protocols increases consistency and reduces errors (Greene et al., 2010).

Field work is the established working method for collecting such data. The safety of field workers and observers that choose to go out into avalanche terrain is a top-priority issue. Keeping a low accident ratio for professional snow field workers legitimizes the knowledge of avalanche professionals, and will therefore provide avalanche terrain recreationists with a reason to believe in the forecast and those who produce it.

3.1 FIELD WORK

3.1.1 *Study plots and safety*

Prior to the field work, the routes to the chosen study plots were investigated in different manners. The routes were examined on topographic maps and slope angle maps, before the routes were reviewed in the field, taking especially care of avoiding potential avalanche run-out zones. To avoid undesirable issues during fieldwork, the University of Tromsø requires risk evaluation schemes to be written before such activities. The scheme for the field work in this thesis is shown in Table 3.1.

The risk evaluation scheme together with a reporting routine on *where and when* I was in the field were compared to the safety measure of always bringing an assistant into the field. Together with the administration at the Department of Geosciences, a risk evaluation scheme and reporting routine were considered as a sufficient safety measure. Thus, every field trip — except those together with co-supervisor Markus Eckerstorfer — were reported before and after the field to the administration at the Department.

Choosing appropriate study plots was done after certain criterions before the field period started. The criterions are listed below.

WEATHER INDEPENDENT. The study plots must be reachable in nearly all weather conditions. As sight is a prerequisite for evaluating danger, and thus traveling in avalanche terrain, the study plot and the route should be in simple avalanche terrain after the

Table 3.1: Field work risk evaluation scheme used for field work in avalanche terrain.

Issue/undesirable event	*Cause*	*Measure*
Colliding while driving.	Inattentive for slippery roads and/or other road users. Driving too fast.	Keep the speed limit. Stop if the driver needs to do something that remove attention from the driving.
Knee injuries from torsion when skiing.	Wrong setting on binding preventing proper release. Downhill skiing with bindings in walking mode.	Set proper release values on bindings after weight and boot size of skier.
Wounds.	Wounds from steel edges on skis, knives, boots or poles. Cut wounds from branches.	Wear gloves. Wear thin gloves when finely finger work must be done. Bring helmet and goggles for downhill skiing. Bring strips in first aid kit.
Hypothermia and frostbite due to issues preventing activity.	Injuries on field workers that cause standstill in the mountain.	Bring emergency sleeping mat, emergency sleeping bag and down jacket to keep potential injured people warm.
Snow avalanches.	The field worker underestimate danger and/or overestimates his abilities. Low visibility inhibit the ability to recognize own position and surrounding avalanche terrain.	Read the avalanche forecast and find out if the potential danger exist in or adjacent to the route.
Cornice falls.	Traveling on or below a cornice that hangs off a cliff.	Stay away from cornices. Mark possible cornice areas on the map.
High energy injuries and injuries from falling.	Colliding with trees while skiing, or falling when jumping or skiing fast.	Ski with a lot of turns that limits speed. Do not ski a jump without controlling if the landing are without rocks or with soft snow first. Limit speed in forest.
Getting lost.	Limited visibility inhibit navigation.	Maps, compass and GPS with maps is standard equipment in the field.

Avalanche Terrain Exposure Scale (ATES) (Statham, McMahon, & Tomm, 2006; The Norwegian Water Resources and Energy Directorate, 2015).

SHELTERED. The study plot should be sheltered from two important disturbing agents; wind and backcountry travelers (Greene et al., 2010; The Canadian Avalanche Association, 2014). Precipitation measurements require shelter, wind measurements require wind exposure. The study plots should be placed so that they provide good shelter for precipitation measurements. Wind measurements can be conducted along the route. Choosing the study plots outside the normal route, and downslope from dense trees or rocks tempting to use as jumps or similar will shelter the plots from other backcountry travelers.

COASTAL AND CONTINENTAL LOCATION. To be able to answer the research questions, one location should be located close to the ocean while the other one should be inland.

Study plots reachable in all weather conditions meant that the high altitude study plots needed to be navigable in whiteout conditions. Forest or cliffs that are not covered by snow provide navigation in difficult weather situations. Thus, the high altitude study plots were located close to the treeline. In good weather conditions, test profiles were sometimes conducted at higher elevations.

3.1.2 *Routines*

The field work was conducted after operational routines learned on the avalanche observers course from The Norwegian Water Resources and Energy Directorate (NVE) ensuring consistent data. Guidelines from the American Avalanche Association[1] and the Canadian Avalanche Association[2] were used as references for stability test procedures. "The International Classification for Seasonal Snow on the Ground" by Fierz et al. (2009) was used extensively to recognize different snow crystals and understand the processes behind them.

3.1.3 *Equipment*

On field work days, standard equipment (The Canadian Avalanche Association, 2014; Greene et al., 2010) for doing snow investigation was used. Both snow study specific field equipment and standard skiing equipment are described in Table 3.2.

1 Snow, Weather, and Avalanches: Observation Guidelines for Avalanche Programs in the United States (SWAG) (Greene et al., 2010)

2 Observation Guidelines and Recording Standards for Weather, Snowpack and Avalanches (OGRS) (The Canadian Avalanche Association, 2014)

Table 3.2: Equipment used during field work.

Snow study equipment
Snow shovel
2x collapsible snow probes
Snow saw, 35 cm and 70 cm
Cutter cord
Digital snow thermometer (bias: $\pm$ 0.1°C)
2 m ruler
Loupe, 10x magnification
Crystal card with 1 and 3 mm grid
Snow density gauge
Field book with pencils
Gloves
Inclinometer
Cell phone with GPS and regObs-app.

(a)

Skiing equipment
Skis with skins, poles and ski boots
Mammut Pulse Barryvox avalanche transceiver
ABS Avalanche Airbag backpack
Map and compass
Helmet
Snow goggles
Rugged and warm winter clothing
First aid kit
Emergency sleeping mat and down jacket

(b)

3.1.4 *Data logging in the field*

Arriving at the study plot – time, date, and location data were registered in the field book. Different meteorological data were also registered which are shown in Table 3.3.

Table 3.3: Meteorological data registered in the field.

Data
Air temperature
Sky cover
Precipitation type
New and total snow height
Wind strength and direction
Wind transported snow
Snow surface moisture and temperature
Snow surface penetrability

The snow surface temperature was measured by placing the thermometer in the shade on the snow surface to prevent insolation affecting the temperature reading. Snow surface penetrability was measured by walking some steps on foot into untouched snow, and measuring the depth of the footstep in one of the holes of a felt average depth.

Road stakes were put into the snow, so that I was able to recognize the location where the last snow pit was dug. Thus, I was sure to dig in untouched snow on every field day. Depending if a field assistent had joined or not, he or she started digging the snow pit while I collected the meteorological data.

A snow pit is a pit dug into the snowpack for exposing the snow layering. Thus, the snow layering can be observed and logged, and stability tests performed.

The objectives of the full snow profiles dug in the winter season 2016–2017 were to:

- Identify:
  - Weak and strong layers in the snow pack.
  - Weak interfaces between layers.
- Observe snow temperatures.
- Determine:
  - Thickness of a potential slab avalanche.
  - Relative strength of the different weak layers and interfaces.

  - State of metamorphism of the snow.
  - Density of layers

- Monitor and confirm earlier observed changes of all characteristics of the snow.

3.1.4.1 *Snow pit procedure*

The snow pits were dug parallel to the fall line at the particular spot with a width of approximately 120 cm to make room for both snow data registrations and the stability test. The pit was dug all the way to the ground, but not in the full width for time saving purposes. In some cases with atypical deep snow the pit was only dug into old melt forms.

1. CHOOSING APPROPRIATE WALL. To prevent potential insolation to affect the snow, I ensured to pick a pit wall that was in the shadow and would remain in the shadow through the registration. Sidewalls were preferred, where I could enter tools horizontally into the layers without crossing into other layers.

2. DEPTH AND GRAIN CHARACTERISTICS. Snowpack depth was measured at a road stake at a static point at every study plot, and also in the particular pit that was dug every field day. After a fast screening of the entire snowpack, layer thickness and snow grain type, size, hardness and moisture were registered from top to bottom. Layer boundaries were revealed by scraping with a crystal card and feeling with the hands. Layers were marked for easy measuring of the distance to ground. Significant weak layers were also marked by a scoop with my fingers. Layer boundaries were marked in the field book by distance from the ground. I paid extra attention if there was any hoar frost at the surface and faceted crystals adjacent to crusts.

The main classes of different snow grains are shown in Table 3.4. Subclasses were registered in the field, but the main classes are mainly used in the discussion. Exceptions are the snow grain subclasses «graupel» (PPgp), «rounding faceted particles» (FCxr) and «faceted rounded particles» (RGxf). Graupels are heavily rimed particles, while rounding faceted and faceted rounded particles are particles that either undergo destructive metamorphism *from* facets *to* rounds, or in a constructive metamorphism *from* rounds *to* facets. FCxr and RGfx will both be referred to as «mixed particles» hereafter.

Snow hardness was measured with the hand hardness test (de Quervain, 1950; Fierz et al., 2009; McClung & Schaerer, 2006). Hardness is how well a material resists penetration of an object. By pushing objects of different sizes with the same force, or objects of the same size with different force, one can obtain the hardness of a material. The different objects and terms are shown in Table 3.5.

Table 3.4: Grain form classes. From Fierz et al. (2009)

CLASS	SYMBOL	CODE
Precipitation particles	+	PP
(Machine made snow)	◎	MM
Decomposing and Fragmented precipitation particles	⟋	DF
Rounded Grains	•	RG
Faceted Crystals	□	FC
Depth Hoar	∧	DH
Surface Hoar	∨	SH
Melt Forms	○	MF
Ice Formations	▬	IF

Table 3.5: Hand hardness index from Fierz et al. (2009).

SYMBOL	HAND TEST	TERM
F	Fist in glove	Very low
4F	Four fingers in glove	Low
1F	One finger in glove	Medium
P	Sharp end of pencil	High
K	Knife blade	Very high
I	Too hard to insert knife	Ice
N/O	Not observed	

In the field work for this thesis, a pressure equal to pressing the index finger towards the temporal bone and feeling slight pain was used.

3. TEMPERATURE. Snowpack temperatures were measured at 10 cm intervals from the snow surface to the bottom of the snowpack. During spring, with a lot of incoming shortwave radiation, shading the thermometer was done to obtain correct measurements. At isothermal snow packs, the temperature was measured at larger intervals, paying extra attention around crusts.

4. DENSITY. Snow density was measured with a snow density gauge. Snow layers thinner than the gauge and frozen crusts were not measured, as correct volume without additional packing was hard to achieve.

3.1.5 *Stability tests*

The Extended column test (ECT) test was chosen as the primary stability test for the field work due to its ability to test crack propagation, its ability to produce a valid result on low angled slopes, and its reported accuracy (Simenhois & Birkeland, 2009; Schweizer & Bruce Jamieson, 2010; Birkeland, Simenhois, & Heierli, 2010; Van Herwijnen & Birkeland, 2014).

The ECT test has limitations in the ability to reveal weaknesses in softer than F+ layers in the upper part of the column (The Canadian Avalanche Association, 2014), as well as reveal weaknesses deeper than approximately 1 m (Simenhois & Birkeland, 2009).

Table 3.6: Extended column test results description from (Simenhois & Birkeland, 2009).

Result	*Description*
ECTPV	A fracture propagates across the entire column in a weak layer or interface during isolation.
ECTP##	A fracture initiates and propagates across the entire column on the ## tap *or* the fracture initiates on the ## tap and propagates across the column on the ##+1 tap.
ECTN##	A fracture initiates on the ## tap, but *does not* propagate across the weak layer or interface on either the ## or the ##+1 tap.
ECTX	No fracture initiates nor propagates on the weak layer during the test.

The test procedure for the ECT test is after Simenhois and Birkeland (2009). The test begins with isolating a vertical column 90 cm long in the cross-slope dimension and 30 cm in the up-slope dimension. The column has to be deep enough to both expose and isolate the weak layer the observer wants to test, but not deeper than 1.3 m.

One end of the column is loaded with progressively harder taps with a shovel blade. The loading procedure is by tapping the shovel by releasing the arm into a free fall ten times from three different pivot points, the wrist, the elbow and the shoulder, where the wrist taps are the lightest taps and the shoulder taps the hardest. The observer notes the number of taps required to initiate a fracture in a layer below the shovel. Also, the observer notes if the fracture propagates through the column or not. A description of the test result notation is shown in Table 3.6. During the field work, to improve the accuracy of the tests, the ECTs were carried out twice.

3.1.6 *Post field data registration*

Data collected in the field was digitalized after each trip. The data from each visit at each study plot were both registered in a Microsoft Excel data sheet, and in a snowpit visualization tool from www.snowpilot.org. The meteorological data and snow pit data were uploaded to regObs, together with my evaluation of signs of instabilities, most important avalanche problems and an avalanche hazard evaluation for the area. For every field trip, I also put an avalanche danger level for the given area and upcoming days.

The avalanche danger level was evaluated and set after the levels in the European Avalanche Danger Scale (European Avalanche Warning Services, 2017). The Avalanche Danger Scale uses snowpack stability and avalanche triggering probability for setting the avalanche danger level. By moving in the terrain I was able to experience signs of instabilities, observe potential previously triggered avalanches, snow accumulations, and weather and snowpack state. Depending if I was alone or not, the additional load needed for potential failure initiation could be testet in safe test slopes. The information obtained in the ECT made it possible to use *process thinking* (Müller, Landrø, Haslestad, Dahlstrup, & Engeset, 2015) for other aspects and altitudes of the surrounding mountains.

3.1.7 *Observation intervals*

The study plots of this study were visited approximately two times a week. To maintain a high safety level, and to ensure conditions favorable for good observations, days with good forecasted visibility and low wind strength were chosen as field days. To maintain a good relationship with family and partner, the observation routine was put

on hold during the Christmas holidays. The observation intervals is visualized in Figure 5.1 on page 41 in the Results chapter.

3.2 METEOROLOGY DATA

3.2.1 *Weather station data and model data*

Xgeo.no is a freely available emergency preparedness, monitoring and warning tool for floods, landslides and snow avalanches in Norway. The tool is a joint responsibility of NVE, The Norwegian Public Roads Administration, The Norwegian National Rail Administration, The Norwegian Meteorological Institute and The Norwegian Mapping Authority ("About xgeo.no," n.d.). The service presents interpolated weather data in 1 km by 1 km resolution from weather stations on a map over Norway. The data in the map updates eight times a day, and includes a nine day forecast based on two models[3]. The AROME-model makes a prognosis for the two first days while the EC model calculates the seven last. Modeled snow cover properties together with incident and field reports are also presented in xgeo. The interpolated weather data makes it possible for the end user to get data from particular points in the terrain, e. g. snow investigation study plots.

In Figure 3.1A, a comparison between interpolated and measured weather data from the exact location of Kvaløysletta weather station at 68 m a.s.l. is shown. The two temperature series follow each other to a great degree. The difference between the mean measured and mean interpolated temperature is calculated to be -0.16°C. Figure 3.1B shows a comparison between measured temperatures at Kvaløysletta weather station and interpolated temperatures at the high elevation study plot at Steinskarfjellet (Figure 4.2). The interpolated temperature data from Steinskarfjellet high are, as expected, slightly colder than the measured data and show that the interpolation takes meters above sea level into account. Also, the interpolated data reveal air temperature inversions.

Clicking the map to obtain temperature and precipitation data from different locations is convenient. Alternatively, an argument on why weather stations at other locations and elevations than my study plots could be representable would be needed. Thus, the already interpolated data from xgeo are used as datasets for analyses in this thesis.

Also visualized in xgeo are snow data from the seNorge snow model (Saloranta, 2012). The model use the interpolated daily temperature and precipitation data as input forcing for calculating, among others, snow water equivalent (SWE), snow density and snow depth.

3 The Application of Research to Operations at MEsoscale (AROME)-model and the European Center for Medium Range Weather Forecasting (EC)-model.

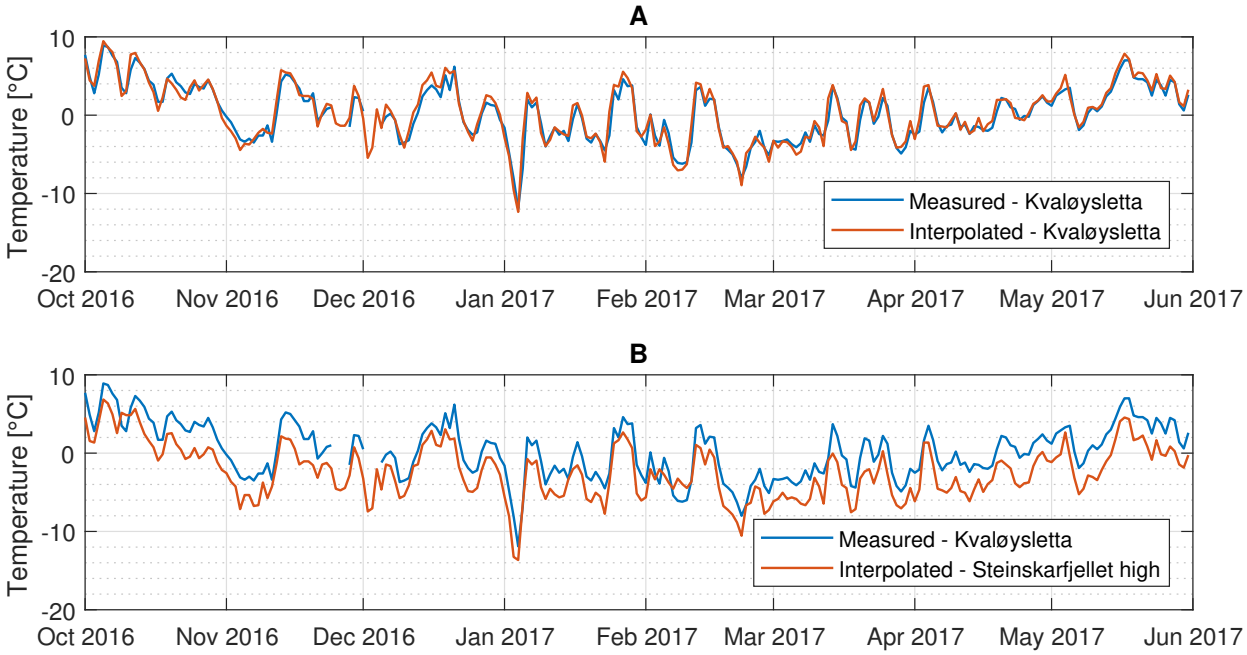

Figure 3.1: *A*: Measured and interpolated daily temperature plots from Kvaløysletta weather station. *B*: Measured (blue) daily temperature plots from Kvaløysletta weather station and interpolated (red) temperatures from the high altitude study plot at Steinskarfjellet at 464 m a.s.l. (Figure 4.2). Both figures represent daily plots from October 2016 through May 2017. Kvaløysletta weather station is located at 69.6988°N 18.8772°E and is 68 m a.s.l.

3.2.2 *Snow climate classification*

The snow climate classification is done by utilizing the flow chart from Mock and Birkeland (2000) on weather data from xgeo and the seNorge model for the four different study plots in the 60 winters from 1957–1958 to 2016–2017. To calculate rain data from the precipitation data, xgeo's own threshold air temperature of 2°C was used. December temperature gradients were calculated by dividing the average air temperature difference between the snow surface and snow basal temperature by the average December snow depth. The snow basal temperature at all the study plots was assumed to be 0°C. The amount of snowfall was obtained from the «fresh snow» layer in xgeo. Millimeter water equivalent is the unit used in the «fresh snow» layer. Thus, snowfall had to be derived either from a calculation of new snow density, or a snow density had to be assumed. The seNorge model includes an equation giving new snow density based on air temperature (Saloranta, 2012, p. 1325). This equation is used for obtaining new snow density values. The equation is shown below:

$$\rho_{ns} = \rho_{nsmin} + \left(\frac{\max(T_{fahr}, 0)}{a_{ns}} \right)^2, \tag{3.1}$$

where ρ_{ns} is density of new snow, ρ_{nsmin} is the minimum density of new snow, a_{ns} is a coefficient for density of new snow, and T_{fahr} is the air temperature in Fahrenheit units, i. e. $T_{fahr} = \frac{9}{5}T + 32$. ρ_{nsmin} is set as 0.050 kg/L and a_{ns} is 100.

Armstrong and Armstrong (1987) used *new snow density* for discriminating the amount of weight added to the snow cover during a typical snowfall in the different climate zones, while Mock and Birkeland (2000) and Hägeli and McClung (2007) used SWE to achieve information on added weight. Both Mock and Birkeland, and Hägeli and McClung are somewhat unclear what time interval and arithmetic operation of SWE values they used. Mock and Birkeland claimed to use daily SWE in the text, but is using SWE *above* 100 cm to discriminate winter seasons into different snow climates. Thousand mm SWE in one day is only a number for records and do not show up in average values. Hägeli and McClung claims to use *total* SWE, which I interpret as *accumulated difference* of SWE through one winter season. Initial calculations on data from seNorge show that none of the study plots exhibit season wise accumulated differences of above 100 cm SWE. Thus, new snow density instead of snow water equivalent is used for step 4 in Mock and Birkeland's flow chart. From the data of Armstrong and Armstrong (1987), a threshold value is set to *100* kg/m^3, where average values *above* classifies a winter season to a maritime snow climate and values *below* let the winter move further on in the flow chart.

During preliminary testing of formulas and data, both a calculated new snow density and an assumed density of 100 kg/m^3 were used. With the assumed densities, only two winters during the 60 year period had more snowfall than the threshold value of 560 cm in the classification scheme. With calculated densities, none of the winters exceeded the threshold. Compared to newspaper articles about record snowfall in Tromsø, both snowfall from calculated and assumed new snow densities fell behind the measured values. Thus, an assumed new snow density of 100 kg/m^3 was chosen for calculating snowfall measurements.

4

STUDY SITE DESCRIPTION

4.1 GENERAL TERRAIN AND LANDSCAPE IN THE REGION

A map over the Tromsø area is shown in Figure 4.1. Puschmann (2005) classifies the landscape of the investigated study area into the terrain class «Fjord villages in Nordland and Troms». The terrain class comprises high but rounded mountains that occasionally have steep mountain walls and cliffs. Valleys are u-shaped due to glacial carving, and lateral moraines, and some cirque glaciers and cirques without ice are present. Pointy peaks are often in the backdrop from both the fjords and the rounded mountains in the area. Smaller tributary fjords cut into the landscape and continue above sea level as u-shaped valleys. Screens are present under coulouirs in steep slopes, and both nutrition rich soils and moraines dominate in gentler slopes and valley floors.

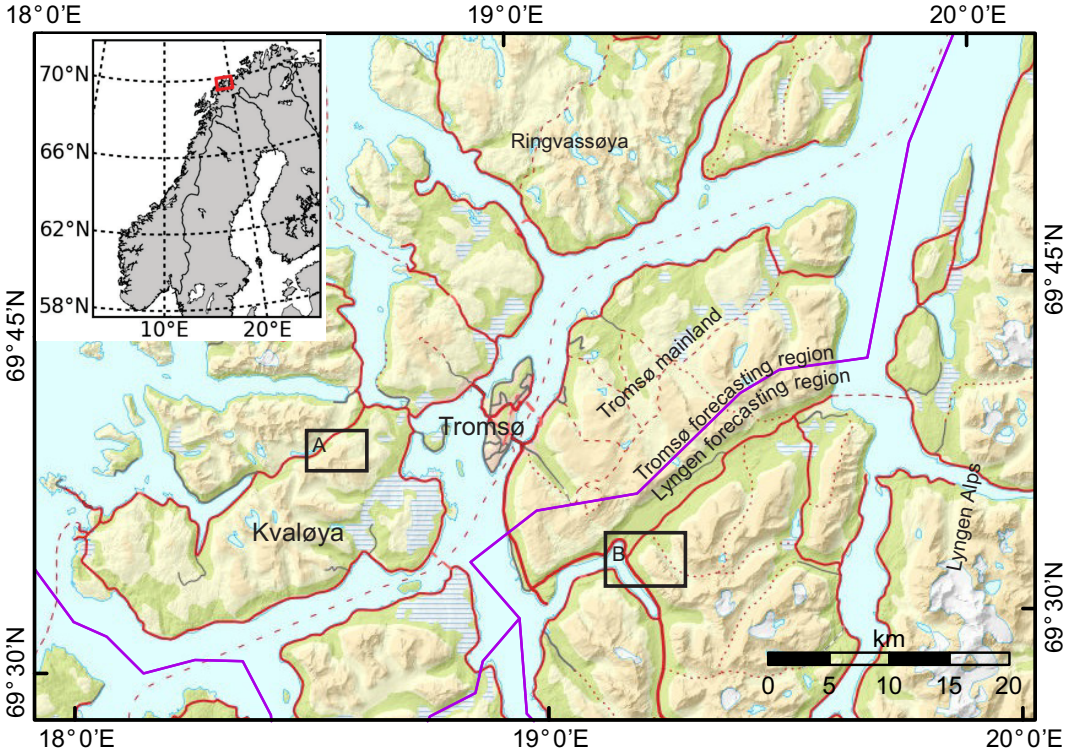

Figure 4.1: Overview map of the surroundings around the city of Tromsø. Box A shows the outline of Steinskarfjellet in Figure 4.2, while box B shows the outline of Fagerfjellet in Figure 4.7.

The coast proximate areas are heavily influenced by the ocean through higher air temperatures. The air temperatures change fast from the outer coast towards the inland (The Norwegian Meteorological Institute, 2016). The following sections will give a description of the study sites used for data collection in this thesis.

4.2 STUDY PLOTS

4.2.1 *Steinskarfjellet*

Steinskarfjellet can be translated to *The Rock Pass mountain*. The name may refer to the view of the mountain from the city of Tromsø, or the numerous draws that exist on the mountain.

HIGH ALTITUDE STUDY PLOT — SSHI The high altitude study plot is situated at 464 m a.s.l. in a north-south stretching shallow valley. The valley is approximately 200 m long, 100 m wide and between 15 and 30 m deep. Hereafter, the study plot will be referred to as *SShi*.

LOW ALTITUDE STUDY PLOT — SSLO The low altitude study plot is situated at 233 m a.s.l. at the foothill north of Steinskarfjellet. The plot is on a mire to the west of a forest encompassing a beck that runs down from the mountain. Hereafter, the study plot will be referred to as *SSlo*. SShi and SSlo are both shown in a topographic map in Figure 4.2, page 31, and on pictures in Figure 4.3 and Figure 4.5, on page 32 and page 34, respectively.

4.2.1.1 *Location*

Steinskarfjellet is located in the north face of the valley Kattfjordeidet that is stretching in a east-west direction on the island Kvaløya at the location N69.655° E18.60°, shown in box A in Figure 4.1 and Figure 4.2. The mountain is approximately 14 km west-southwest of the city of Tromsø with county road 862 running along the valley floor connecting the villages on the western, ocean facing side of Kvaløya to the European route 8 (E8) that ends in Tromsø. Steinskarfjellet is approximately 25 km away from the open ocean outside Kvaløya.

4.2.1.2 *Safe access*

Figure 4.4 on page 33 shows a map of Steinskarfjellet with avalanche starting zones marked with red areas. The upper study plot was placed so that no terrain steeper than 30° had to be crossed to reach it. Since 20 m contours can hide vertical features with enough snow to bury a human, the route was thoroughly explored before the snow season started. The route was also travelled with particularly care the first field trips to be acquainted with the terrain.

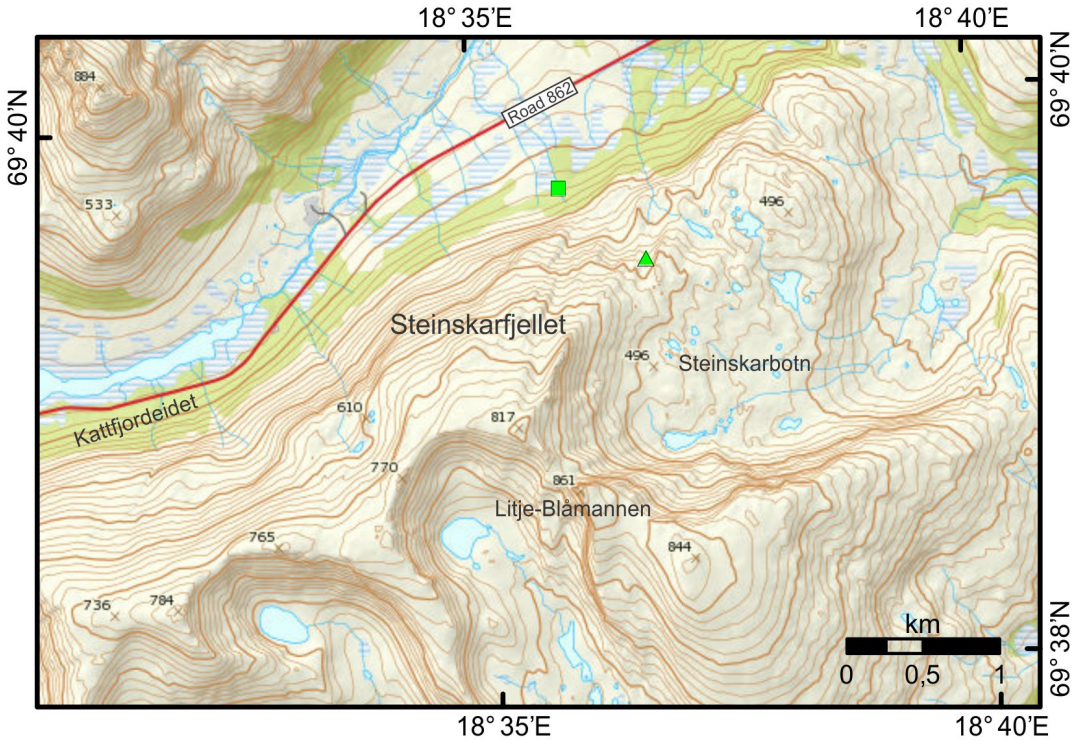

Figure 4.2: Map over the study plot at Steinskarfjellet. The green triangle marks the high altitude study plow at 464 m a.s.l., while the green square marks the low altitude study plot at 233 m a.s.l., respectively Figure 4.5a and b.

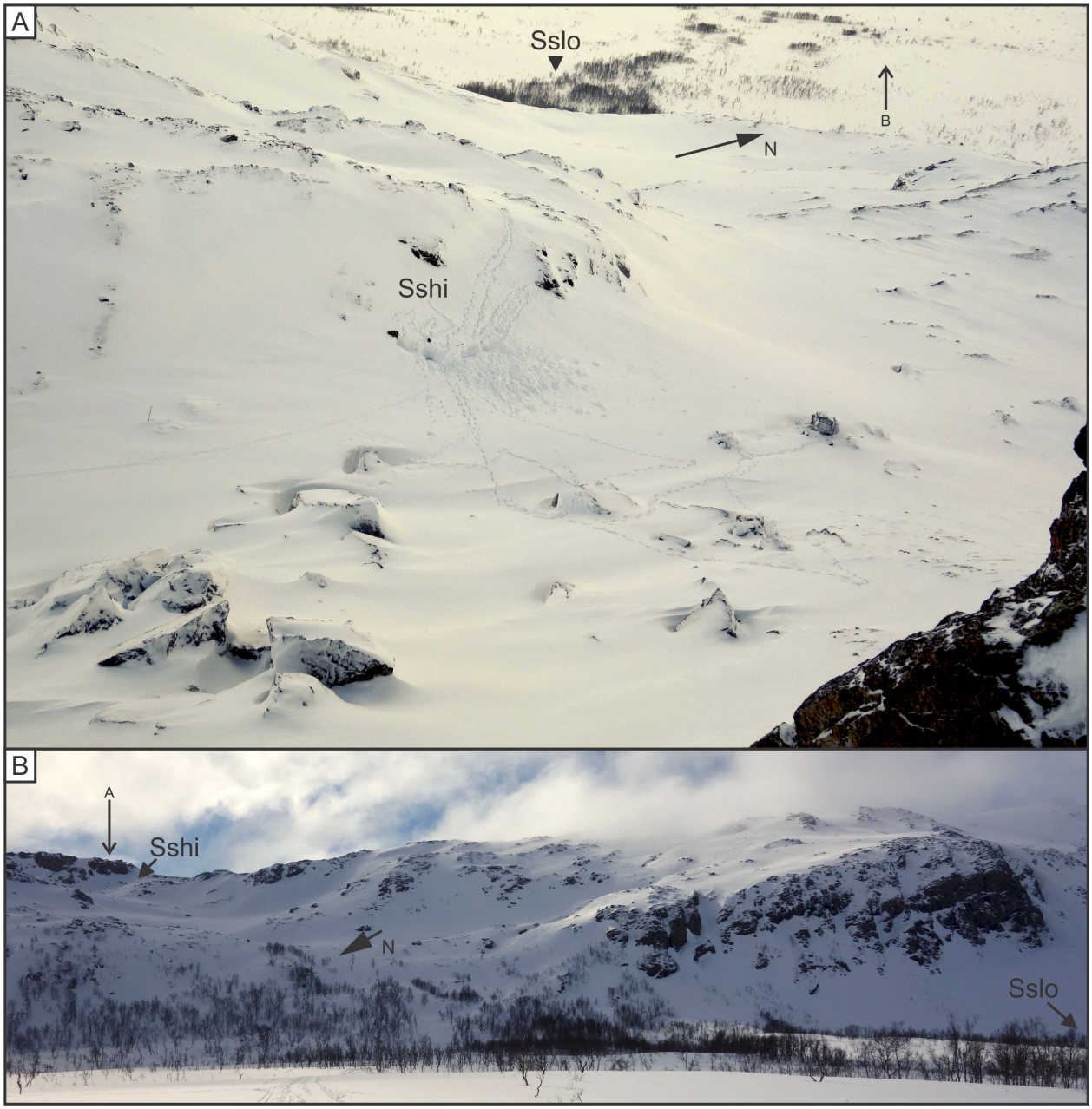

Figure 4.3: Overview winter pictures of the study plots at Steinskarjellet. The viewpoint of each picture are shown in the other picture. *A*: Picture taken March 10, 2017. The snowpits dug at SShi were mostly dug to the left of the pictured snowpit. *B*: Picture taken May 9, 2017.

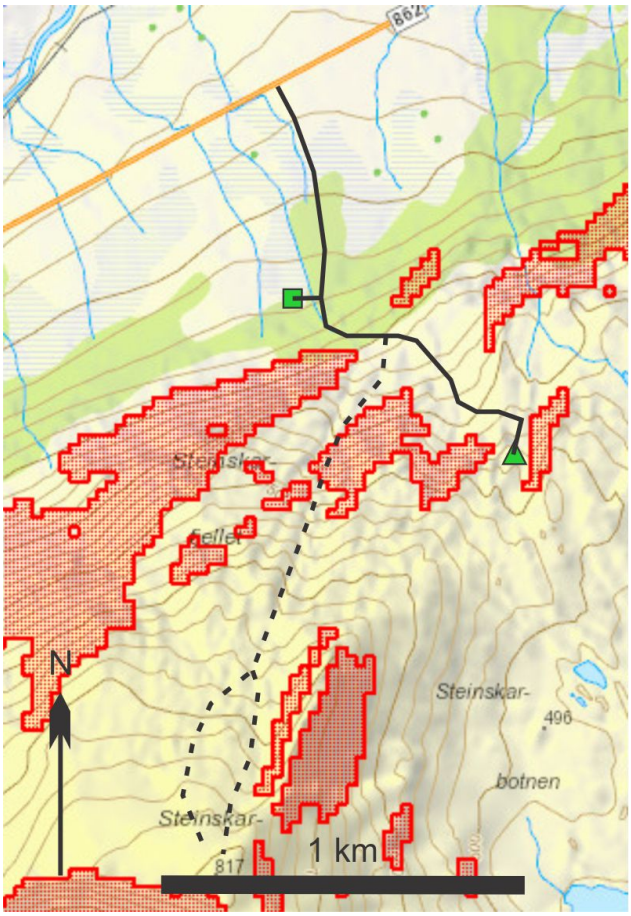

Figure 4.4: A map showing the north face of Steinskarfjellet. Dotted fields within red areas are avalanche starting zones. The solid line represents approximately the chosen route during the field season, while the broken line represents the normal route to the summit of Steinskartinden. Map from The Norwegian Geotechnical Institute (2017a).

4.2.1.3 *Ground surface*

HIGH ELEVATION STUDY PLOT The ground surface at the high elevation study plot on Steinskarfjellet is shown in Figure 4.5a. The ground surface includes mainly rock slabs with scattered angular boulders. Also scattered are patches of moss and grass in between the exposed rock slabs.

LOW ELEVATION STUDY PLOT The ground surface at the low elevation study plot on Steinskarfjellet is shown in Figure 4.5b. The ground is a flat, grass covered mire which is dryer in the left (east) part of Figure 4.5b and wetter in the right (west) part.

Figure 4.5: Ground surface at the study plots at Steinskarjellet. *A*: The high elevation study plot. The dark rock facing the viewer in the middle of the picture is 30°–35° steep. *B*: The low elevation study plot at Steinskarfjellet. The snow pits were dug between the photographer and the birch with the red stake.

4.2.1.4 *Wind and sheltering*

HIGH ELEVATION STUDY PLOT With a treeline at around 325 m a.s.l. at Steinskarfjellet, the study plot at 463 m a.s.l. was not sheltered by trees. The study plot was placed in a north-south stretching shallow valley and experienced snow loading mostly from south and west at many different larger scale wind directions.

LOW ELEVATION STUDY PLOT Due to sparse Northern Norwegian birch, the low elevation study plot was only slightly sheltered from wind, and thus experienced both snow loading and erosion. During the field work, the wind directions often followed the Kattfjordeidet valley, making western or south-western wind directions normal.

4.2.1.5 *Accessibility and accidents*

Kattfjordeidet is a popular valley for snow sport recreation due to easily available mountains on both sides of county road 862 and its vicinity to the city of Tromsø. Many mountain tops with different descend routes from mellow flanks to steep couloirs can be found in the valley (Nordahl, 2010).

Three fatal avalanche accidents killing in total five people have occurred at Kattfjordeidet since registration of fatal avalanche accidents in Norway started (The Norwegian Geotechnical Institute, 2017b). None of the accidents were on Steinskarfjellet, but all on mountains less than 8 km away. One of the accidents was on the same mountain ridge as Steinskarfjellet, but approximately 3 km further southwest.

4.2.2 *Fagerfjellet*

Fagerfjellet translates directly to *The good-looking mountain* in Norwegian. The village at the mountain foot is named Fagernes (*N: The good-looking point* or *headland*, and it is likely that the mountain got its name from the village or the other way around.

HIGH ALTITUDE STUDY PLOT — FFHI The high altitude study plot is situated 469 m a.s.l. on the west face at Fagerfjellet just above the treeline. Hereafter, the study plot will be referred to as *FFhi*.

LOW ALTITUDE STUDY PLOT — FFLO The low altitude study plot is situated at 44 m a.s.l. on an old grassland at the foothill of Fagerfjellet. From now on, the study plot will be referred to as *FFlo*. FFhi and FFlo are shown on a topographic map in Figure 4.7, page 37, and on pictures in Figure 4.6, page 36.

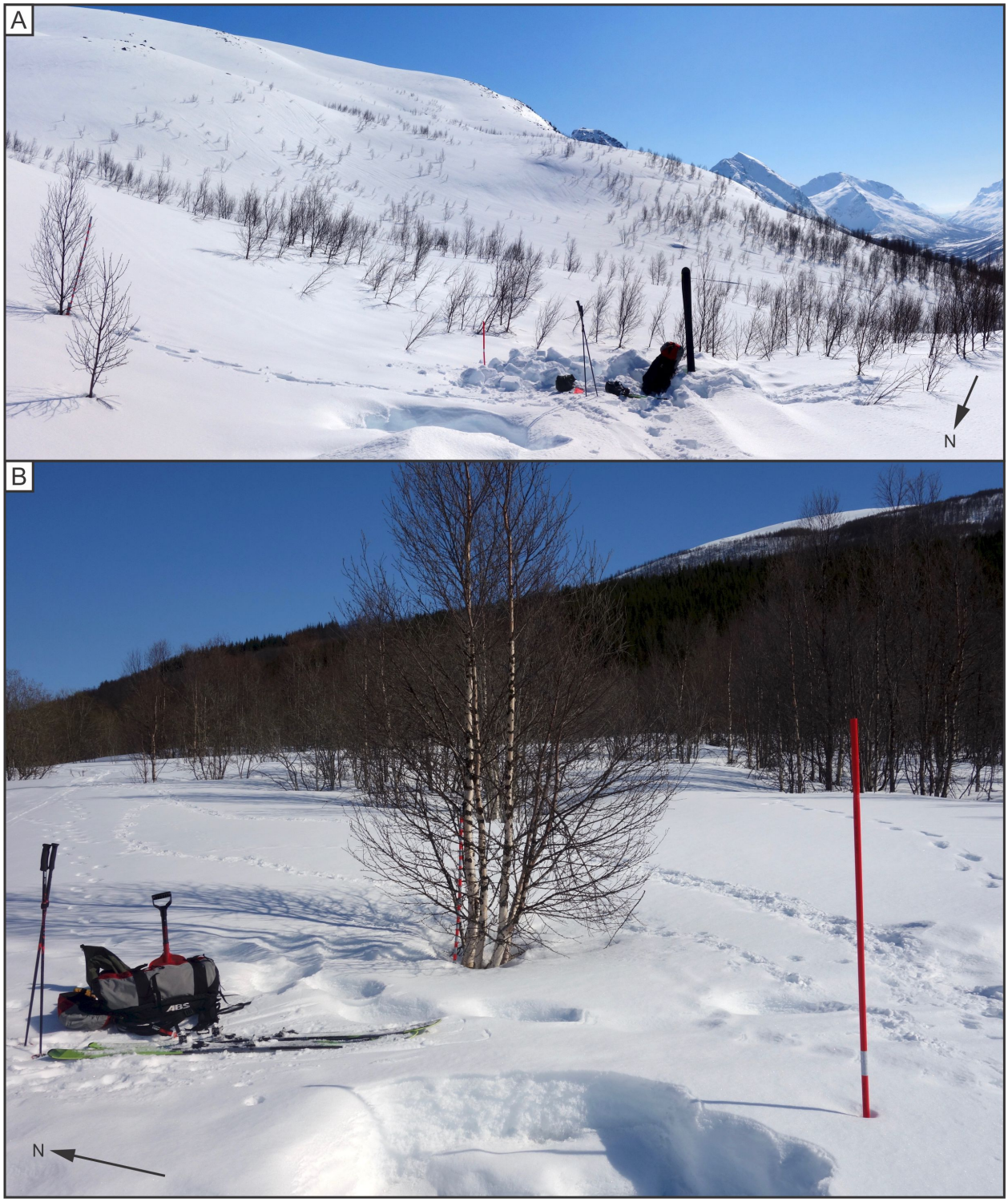

Figure 4.6: Overview winter pictures of the study plots at Fagerjellet. Both pictures are taken April 25, 2017 *at* the respective study plot. *A*: FFhi. All pits were dug in the glade in front of the photographer. *B*: FFlo. The snow pits were dug mainly to the right of the red road stake in the picture.

4.2.2.1 *Location*

Fagerfjellet, shown on a map in Figure 4.7 is located at the south-eastern side of the junction of the east-to-south curving fjord Ramfjorden and the NE–SW facing valley Breivikeidet at location N69.56° and E19.20°. The mountain is about 17 km south-east of Tromsø. Ramfjorden defines the western fringe of the mountain, and Breivikeidet defines the northern side.

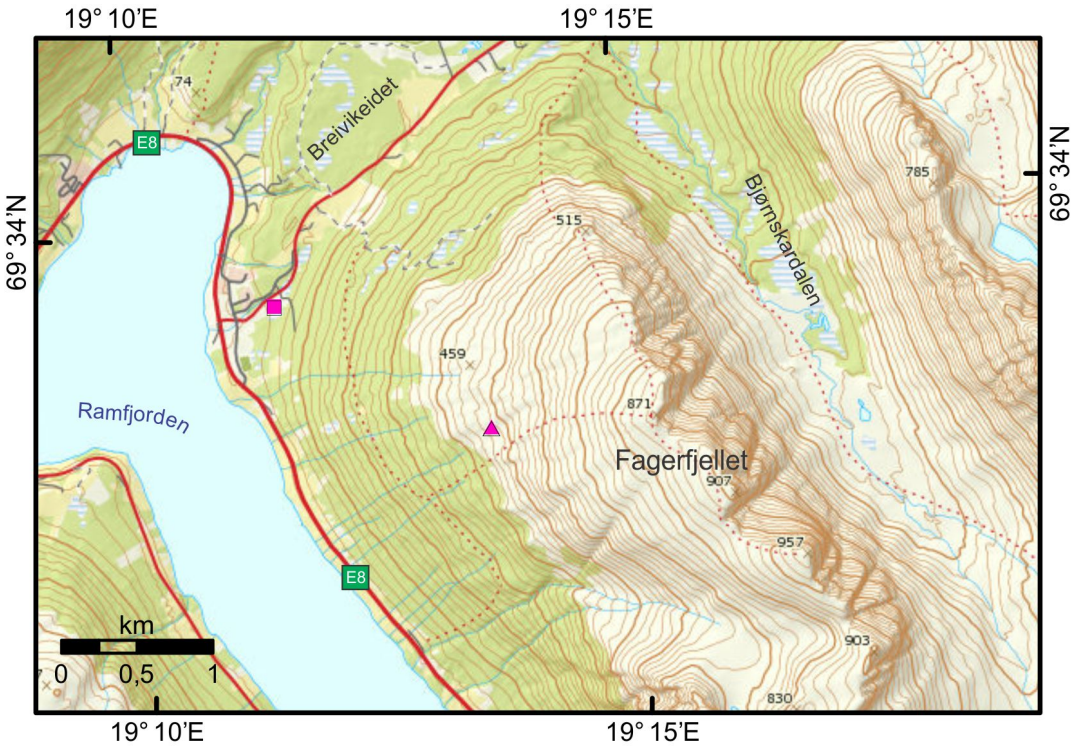

Figure 4.7: Map over the study plot at Fagerfjellet. The pink triangle marks the high altitude study plow at 469 m a.s.l., while the pink square marks the low altitude study plot at 44 m a.s.l., respectively Figure 4.9a and b.

4.2.2.2 *Safe access*

Figure 4.8 shows a map over Fagerfjellet with avalanche starting zones marked in red. As with Steinskarfjellet, the upper study plot was placed so that no terrain steeper than 30° had to be crossed. On Fagerfjellet, avoiding runout zones in general is possible, making weather the limiting factor for reaching the study plot.

4.2.2.3 *Ground surface*

HIGH ELEVATION STUDY PLOT The high elevation study plot on Fagerfjellet is shown in Figure 4.9a. The ground is flat, grass covered soil adjacent to a crest. Birch trees from knee height to around 3 m tall grow in the vicinity of the study plot. The smallest trees were

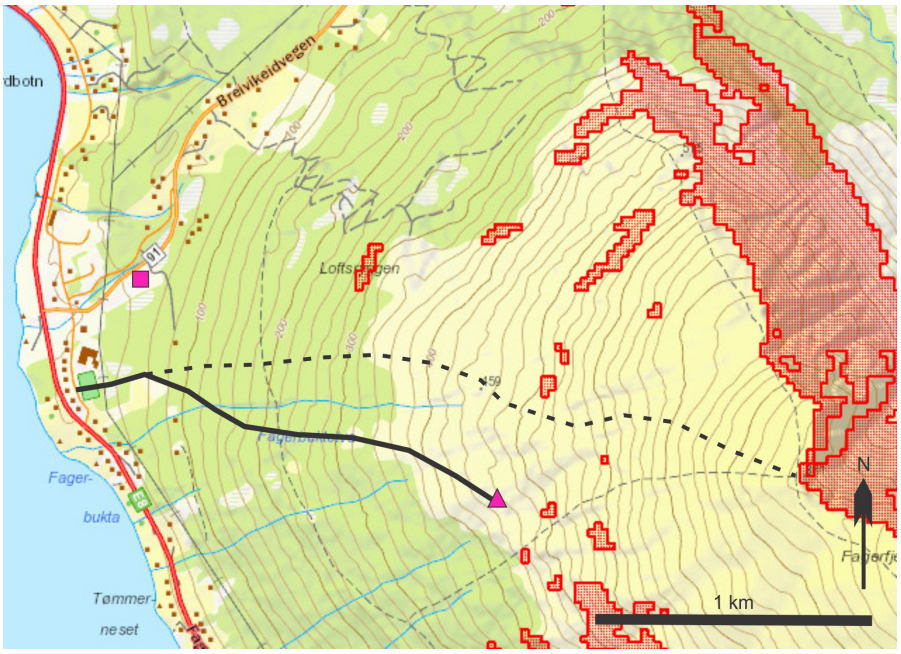

Figure 4.8: A map showing the western, northern and north-eastern face of Fagerfjellet. Dotted fields within red areas are avalanche starting zones. The solid line represents the approximately chosen route in the field season, while the broken line represents the normal route to the 871 m a.s.l. summit of Fagerfjellet. Map from The Norwegian Geotechnical Institute (2017a).

removed in the autumn 2016 to prevent branches making air pockets in the snow pits.

LOW ELEVATION STUDY PLOT The low elevation study plot on Fagerfjellet is shown in Figure 4.9b. The study plot is on a former grassland with grass that reaches knee height in fall if not mowed through the growing season. Birches, all of them around 4–5 m tall, grow around the study plot. The study plot is smooth, even and gently inclined.

4.2.2.4 *Wind and sheltering*

HIGH ELEVATION STUDY PLOT The high elevation study plot was placed in a slightly tree sheltered hollow. The trees surrounding the hollow were sparse and small Northern Norwegian birches, making the plots experiencing some snow loading through the winter season, mostly from the south.

LOW ELEVATION STUDY PLOT The low elevation study plot was placed well sheltered with tall and dense forest surrounding it. At the same time, there was enough room to accommodate the snow pits dug through the winter.

Figure 4.9: Study plots at Fagerfjellet. *A*: High elevation study plot (469 m a.s.l.) on Fagerfjellet. The snow pits were dug between the photographer and the red stake in the picture. The 871 m a.s.l. summit on Fagerfjellet is visible with a cairn in the background. Before the winter field season started, the stake was moved close to a birch to just left of the picture. *B*: The low elevation study plot (44 m a.s.l.) on Fagerfjellet. During the winter, snow pits were dug behind and to the left of the birch and the backpack in the picture.

4.2.2.5 *Accessibility and accidents*

Breivikeidet is a popular valley for ski touring by the same reasons as Kattfjordeidet. Many descend routes described by Nordahl (2010) are gentler than 30°, but these are often on mountains that also have much steeper and still skiable terrain.

One fatal accident occurred in the convex south western face of Fagerfjellet in 2010, and two fatal accidents have occurred by cornice falls down the east face of Tromsdalstinden on the north side of Breivikeidet 7 km away (The Norwegian Geotechnical Institute, 2017b).

5 RESULTS

In the following chapter meteorology and snow data from the 2016–2017 winter season are presented. The meteorology data from xgeo.no are described in Section 3.2, page 24, while the snow data used were collected by myself.

The field data were collected at Steinskarfjellet and Fagerfjellet on the dates shown in Figure 5.1. The total number of pits examined were,

— SShi: 17 pits, FFhi: 20 pits, SSlo: 20 pits, FFlo: 19 pits.

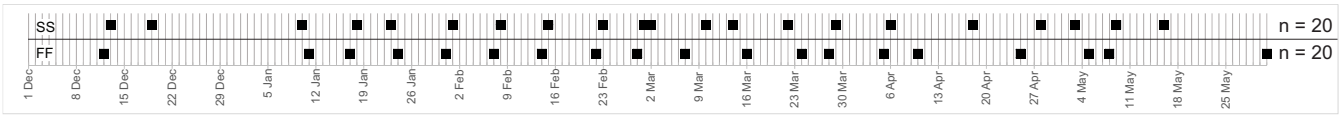

Figure 5.1: Field days 2016-2017. SS = Steinskarfjellet, FF = Fagerfjellet. Every vertical bar symbolizes one day.

5.1 METEOROLOGY DATA

5.1.1 *SShi*

Plotted air temperature and precipitation data are displayed in Figure 5.2. Mean air temperatures and monthly precipitation data are presented in Table 5.2 and Table 5.3.

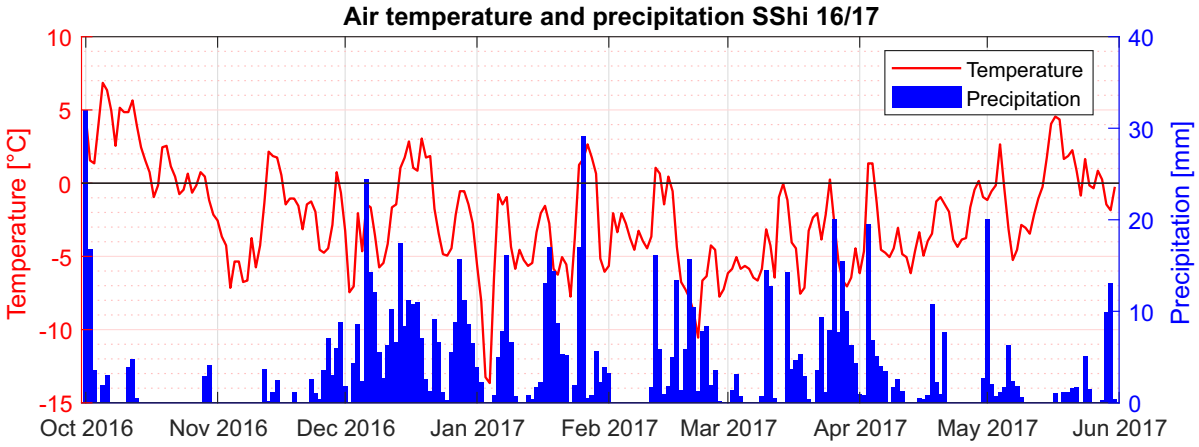

Figure 5.2: Air temperature and precipitation data for SShi from October 2016 through May 2017. A single blue bar represents the precipitation for one day.

AIR TEMPERATURE Monthly mean air temperatures were mostly below 0°C except for October, which had a mean value of 2.1°C. The monthly mean for May was -0.2°C. The rest of the months had negative mean air temperatures with March as the coldest month, measuring -4.5°C in average.

The warmest day of the winter season was October 5 with 6.9°C, while the coldest was January 4 with -13.7°C. Thus, the air temperatures during the winter season spanned over 20.6°C.

SShi had air temperatures lower than -10°C January 3 and 4, with respectively -13.3°C and -13.7°C; and February 22 with -10.6°C. SShi did not experience air temperatures higher than 5°C during the period of snow covered ground. The mean air temperature from October 2016 through May 2017 was -2.4°C.

PRECIPITATION December had the most precipitation with 242.4 mm, while November had least precipitation with 41.3 mm. The first snowfall occurred October 29, but the resulting snow cover was less than 25 cm thick and melted away November 14. The first snowfall persisting through the winter occurred on November 23.

After November 23, air temperatures above zero combined with precipitation above 5 mm occurred six times:

December 14 to 19

January 25, 26 and 29

February 12 and 13

April 3 and 4

May 24

5.1.2 *SSlo*

Air temperatures and precipitation data are displayed in Figure 5.3 with key numbers presented in Table 5.2 and Table 5.3.

AIR TEMPERATURE Since the air temperatures are based on interpolated data from surrounding weather stations, the air temperature plot from SSlo follows more or less the same pattern as the plot from SShi. The mean air temperature at SSlo was -0.6°C, which is 1.8°C higher than at SShi.

On October 9 and 10, temperature inversions[1] took place. More occasions of temperature inversions, both on Steinskarfjellet and Fagerfjellet, are shown in Table 5.1.

1 Temperature inversions occur when cold, heavy air sinks and pools in valleys underneath warm, light air. Hence, the air temperature will *increase* with higher elevations. The phenomenon may happen on clear and calm winter days, where snow radiates heat into the atmosphere, or when a warm front overruns cold air (Tremper, 2008).

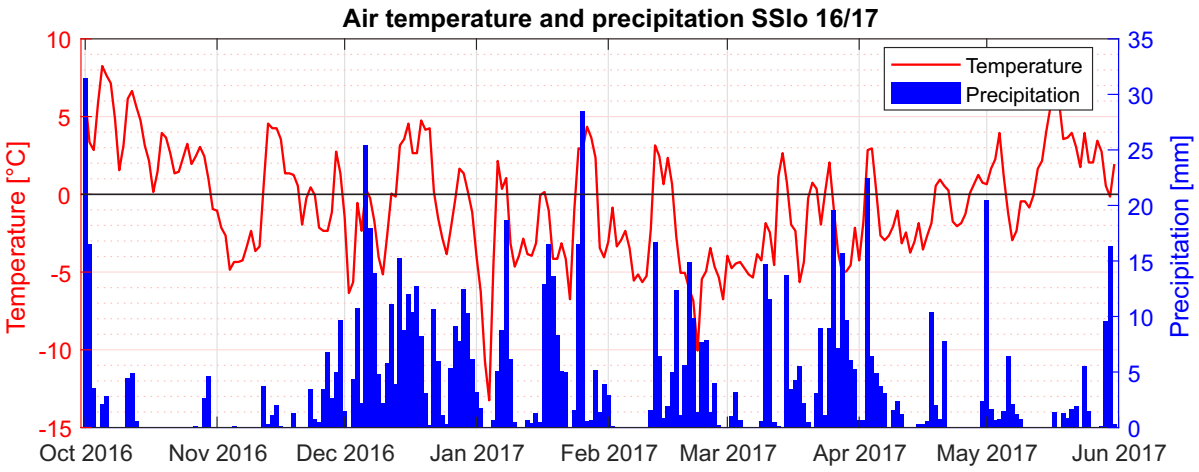

Figure 5.3: Air temperature and precipitation data for SSlo from October 2016 through May 2017. A single blue bar represents the precipitation for one day.

Measured from mean air temperature values, October was the warmest month with 3.5°C, and February the coldest with -3.5°C. November through April had negative mean air temperatures, while May had positive mean air temperature in contrast to SShi. The warmest and coldest day were the same as on SShi i. e. October 5 and January 4 with 8.3°C and -13.3°C, respectively. This gives an air temperature span of 21.6°C.

SSlo experienced air temperatures lower than -10°C January 3 and 4 (-10.8°C and -13.3°C) and February 22 (-10.1°C). Air temperatures higher than 5°C were registered prior to the snow season in early October, and May 16 through 18 (5.7°C, 6.6°C and 6.0°C).

PRECIPITATION Since precipitation data are interpolated, SSlo show similar trends to SShi. At SSlo, November was the month with least precipitation, — 41.3 mm, and December was the month with most precipitation, — 244.1 mm. The snowfall November 23 persisted through the season.

After November 23, air temperatures above zero together with precipitation above 5 mm occurred 14 times, which is 8 times more often than at SShi:

November 29 and 30.

December 6, 12, 14 to 19, 22, and 28 to 30.

January 7 and 8, 17, 25, 26 and 29.

February 12 and 13.

March 15 and 25.

April 3 to 5 and 21.

May 1, 24 and 29.

Table 5.1: Days with temperature inversions in the winter season 2016–2017. The numbers represent the temperature differences between the low and high altitude study plots. The values in the header represent the height difference between the high and low location.

	Temperature difference [°C]	
Date	*SShi vs SSlo [231 m]*	*FFhi vs FFlo [425 m]*
09.10.2016	3.6	
10.10. —	1.7	1.5
15.01.2017		0.4
03.02. —		0.9
04.02. —	0.9	1.1
06.02. —		0.7
07.02. —	1	1.5
08.02. —	1.9	2.9
09.02. —	1.7	2.4
10.02. —	0.8	1.8
26.02. —	0.1	
06.03. —		0.4
No. of days	8	10

5.1.3 *FFhi*

Air temperature and precipitation data from the winter season 2016–2017 are plotted in Figure 5.4 with key numbers presented in Table 5.2 and Table 5.3.

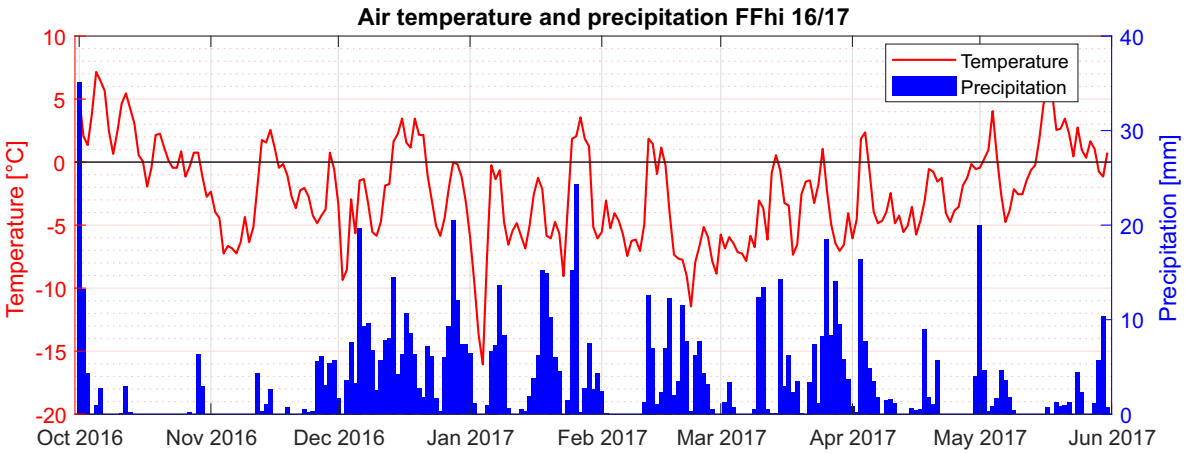

Figure 5.4: Air temperature and precipitation data for FFhi from October 2016 through May 2017. A single blue bar represents the precipitation for one day.

AIR TEMPERATURE The air temperature at FFhi varied in more or less the same pattern as at SShi. It differs on two apparent occasions; temperature inversions and cold temperatures without precipitation. In both situations, FFhi showed *lower* temperatures than SShi. A look at xgeo.no revealed that air temperature differences during the temperature inversions may have been due to placement of the temperature interpolation box models. The lower air temperatures at FFhi during cold periods without precipitation may have been due to the fact that FFhi is a more continental location.

October had the highest mean air temperature with 1.9°C, while February had the lowest with -5.3°C. The warmest day of the winter season was October 5 with 7.2°C and the coldest was January 4 with -16.1°C. Thus, the temperature span was 23.3°C.

FFhi had air temperatures colder than -10°C at January 3 and 4, -13.7°C and -16.1°C respectively, and air temperatures warmer than 5°C from October 5 through October 7 (7.2, 6.5 and 5.7°C) and May 17 and 18 with 5.5°C both days.

PRECIPITATION FFhi experienced the largest amount of precipitation in December (218.7 mm) and the least in November (35.8 mm). The first snowfall was October 30, which melted gradually until November 14. The next snowfall was November 26, lasting through the entire winter.

After November 26 at FFhi, air temperatures above 0°C and daily precipitation of more than 5 mm occurred nine times, which was three times more than at SShi. At FFhi, days with air temperatures above 0°C and precipitation above 5 mm were:

October 29.

November 29.

December 14 and 16 to 19.

January 25, 26 and 29.

February 12 and 13.

March 25.

April 3 and 4.

5.1.4 *FFlo*

Air temperature and precipitation data from the winter season 2016–2017 is plotted in Figure 5.5.

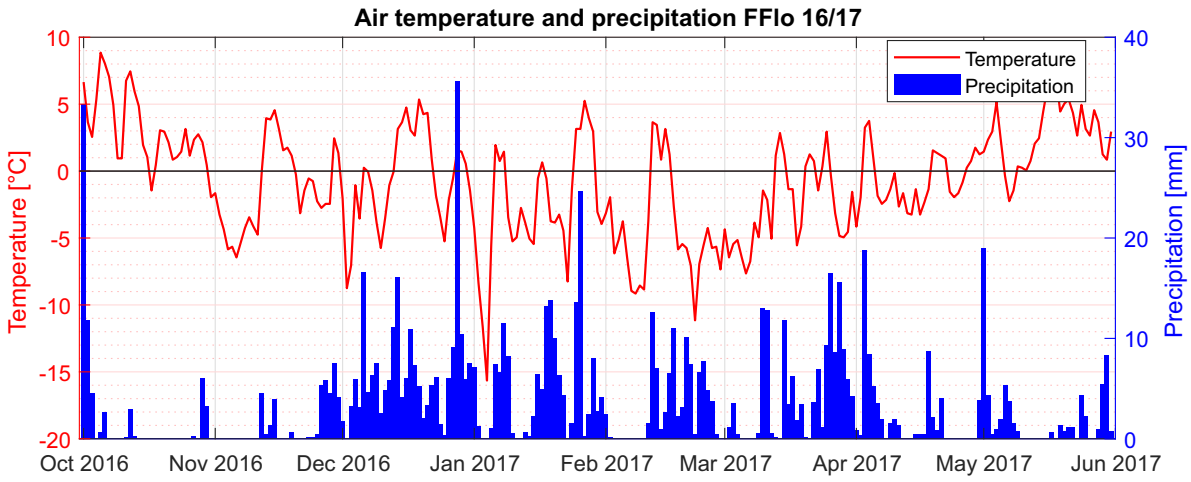

Figure 5.5: Temperature and precipitation data for FFlo from October 2016 through May 2017. A single blue bar represents the precipitation for one day.

AIR TEMPERATURE October had the highest mean air temperatures at FFlo with 3.1°C, while February had the lowest with -4.5°C. May had a mean air temperature above zero, at 2.8°C. October 5 was the warmest day with 8.9°C and January 4 was the coldest with -15.7°C. Thus, the temperature span was 24.6°C.

Fagerfjellet had temperature inversions ten days during the 2016-2017 season, compared to eight at Steinskarfjellet.

PRECIPITATION FFlo experienced the largest precipitation in December (215.6 mm) and the least in November (38.5 mm). The first

snowfall was October 30, melting gradually until November 12. The next snowfall was November 26, lasting through the entire winter.

After November 26, FFlo had air temperatures above 0°C and daily precipitation of more than 5 mm 17 times, which is eight more than at FFhi, and three more than at SSlo. Days with air temperatures above 0°C and precipitation above 5 mm were:

October 29.

November 29.

December 6, 14, 16 to 19, 22, and 28 to 30.

January 6 to 8, 25 to 26, and 29.

February 12, 13 and 16.

March 15 and 25.

April 3 and 5.

May 1, 29 and 30.

Table 5.2: Mean air temperatures at Steinskarfjellet and Fagerfjellet in the 2016–2017 winter season.

	Mean air temperature [°C]								
Location	*Oct*	*Nov*	*Dec*	*Jan*	*Feb*	*Mar*	*Apr*	*May*	*Mean*
SShi	2.1	-2.7	-2.0	-4.1	-4.4	-4.5	-3.1	-0.2	-2.3
FFhi	1.9	-2.9	-2.1	-4.4	-5.3	-4.4	-2.9	0.6	-2.4
SSlo	3.5	-0.7	-0.3	-2.5	-3.5	-2.6	-1.2	1.9	-0.6
FFlo	3.1	-1.4	-0.6	-2.8	-4.5	-2.6	-0.7	2.8	-0.8

Table 5.3: Total precipitation at Steinskarfjellet and Fagerfjellet in the 2016–2017 winter season.

	Precipitation [mm]								
Location	*Oct*	*Nov*	*Dec*	*Jan*	*Feb*	*Mar*	*Apr*	*May*	*Sum*
SShi	73.5	41.3	242.4	172.9	104.4	150.5	72.1	73.5	930.6
FFhi	68.8	35.8	218.7	166.9	97.2	141.7	62.6	67.5	854.9
SSlo	73.9	41.1	244.1	167.7	105.9	147.9	71.8	76.2	924.7
FFlo	65.4	38.5	215.6	162.6	95.1	139.2	64.2	64.3	840.8

5.2 SNOW DATA

Through the snow season of 2016–2017, 76 snow pits were dug in total at SShi, SSlo, FFhi and FFlo. Summing the depth of all the snow pits dug, in total 90.97 m of snow pit data were collected. The mean snow

Table 5.4: Numbers of rainy days at Steinskarfjellet and Fagerfjellet in the winter season 2016–2017. A rainy day is defined as precipitation and air temperature above 2°C.

	No. days with rain.								
Location	*Oct*	*Nov*	*Dec*	*Jan*	*Feb*	*Mar*	*Apr*	*May*	*Sum*
SShi	6	1	2	1	0	0	0	3	13
FFhi	7	1	5	2	0	0	1	7	23
SSlo	10	5	8	6	3	1	2	10	45
FFlo	10	4	8	5	3	1	2	13	46

pit depth at the high locations, SShi and FFhi, were 176 cm and 170 cm, respectively. The mean snow pit depth at the low locations, SSlo and FFlo, were 78 and 60 cm, respectively.

5.2.1 *Snow depths*

A comparison between *modeled* snow depths from xgeo at the study plots is shown in Figure 5.6. The snow depths *measured* at the study plots compared to the modeled snow depth are shown in Figure 5.7.

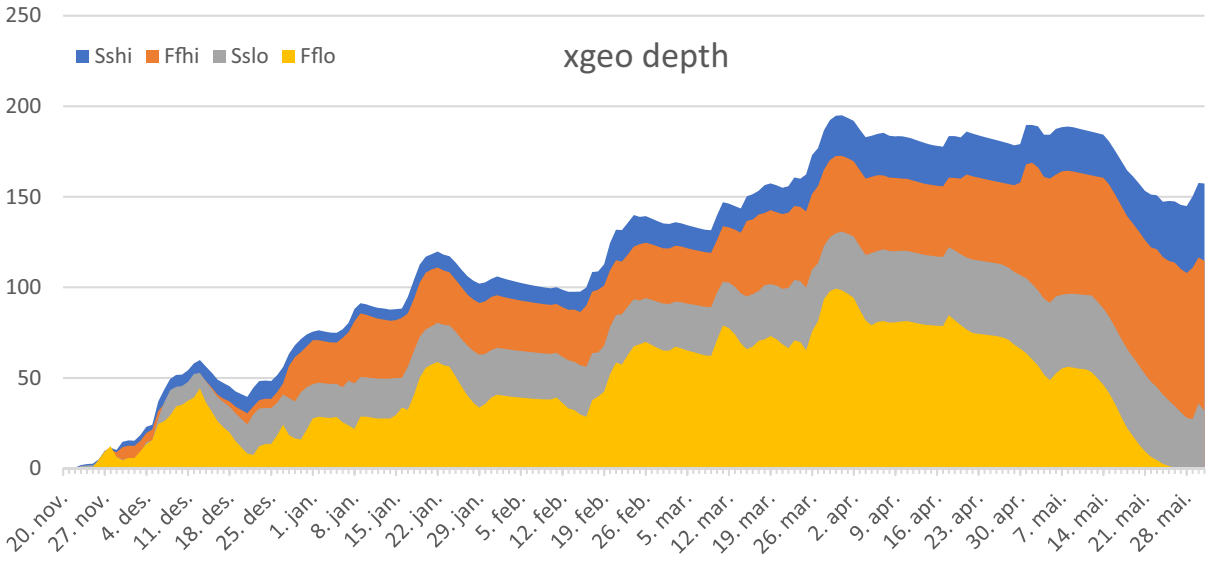

Figure 5.6: Modeled snow depths from interpolated weather data for the winter season 2016–2017 at the different study plots.

Since the snow model in xgeo base on interpolated data, all the study plots in Figure 5.6 exhibit similar trends during the winter. Three apparent differences occurred; — one between December 7 and December 13, one between December 28 and and January 9, and one

Table 5.5: Modeled snow depth summary based on xgeo data from the snow season 2016–2017. Values from November 20 2016 to May 31 2017 are averaged.

	Snow depth			
	SShi	*FFhi*	*SSlo*	*FFlo*
Average [cm]	120.1	105.4	71.4	44.9
Difference [%]	14		59	
	94			
Maximum [cm]	195	172.6	130.8	99.3

Maximum depth at all plots: March 31, 2017.

between May 1 and May 3. At December 7 to 13, the snow depth at SSlo was deeper than at FFhi despite that FFhi is situated 236 m above SSlo. Over those seven days, the snow depth was in average 1.6 cm deeper at SSlo than at FFhi. Between December 28 and January 1, and between January 6 and January 9, the high altitude study plots had a much greater increase in snow depth than the low altitude plots, indicating a possible rain limit between 233 m a.s.l. and 463 m a.s.l. . May 1 and May 3 were similar: snow depth at SShi and FFhi increased, while the snow at SSlo and FFlo melted. Average and maximum modeled snow depths, as well as differences between the study plots are shown in Table 5.5.

Table 5.6 shows a summary of average differences of measured depths at the study plots. The model underestimated the snow depth through the season at SShi and FFhi — Figure 5.7a and Figure 5.7b, respectively. The average snow depth at the stake at SShi was 85% deeper than the modeled snow depth and the average snow depth in the pits was 46% deeper than the model. The stake at SShi disappeared below the snow and many field days were used to localize it, resulting in fewer measurements. The average snow depth at the stake at SShi was 27% deeper than in the pits. Few data points from the stakes are probably the reason for the deviation between the averaged measured values.

FFhi showed a better compliance between snow depth measurements at the stake and in the pits, with a 5% deeper snowpack at the stakes. The measurements also seemed to agree with snowfall events during the winter e. g. January 18 to January 27, February 24, and March 26 to March 30. The model expected a snowmelt between January 25 and January 29 when the snow pit depths showed a gradual increase. Figure 5.4 shows that those days had temperatures between 0°C and 4°C combined with precipitation. Temperatures close to 0°C may result in rain, sleet or snow, while the measured snow depths may indicate that snow were the correct precipitation type during this

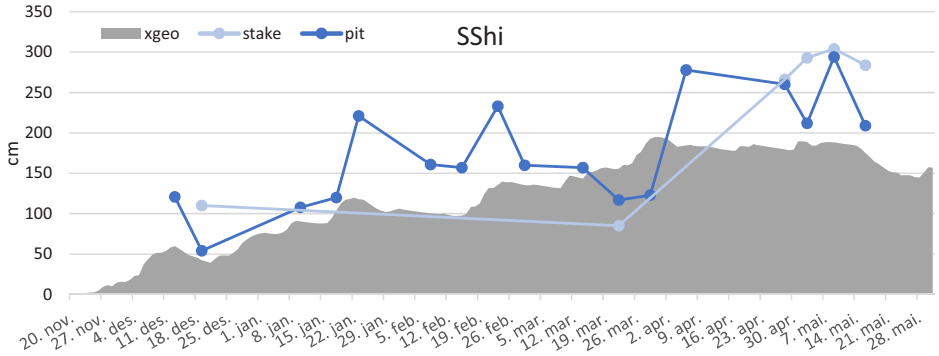

(a)

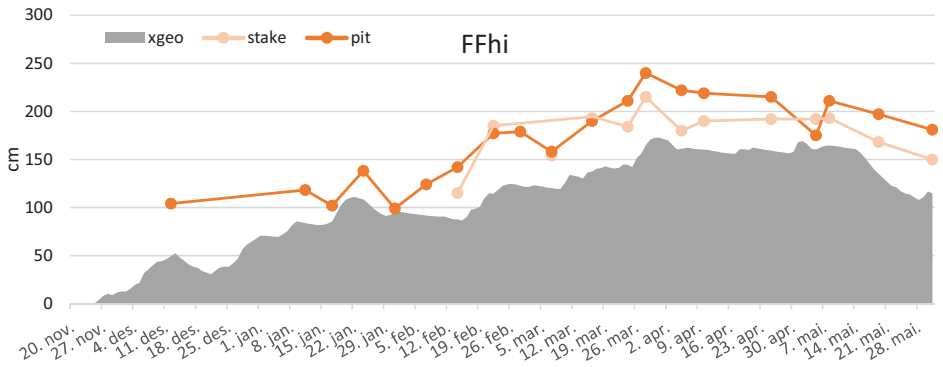

(b)

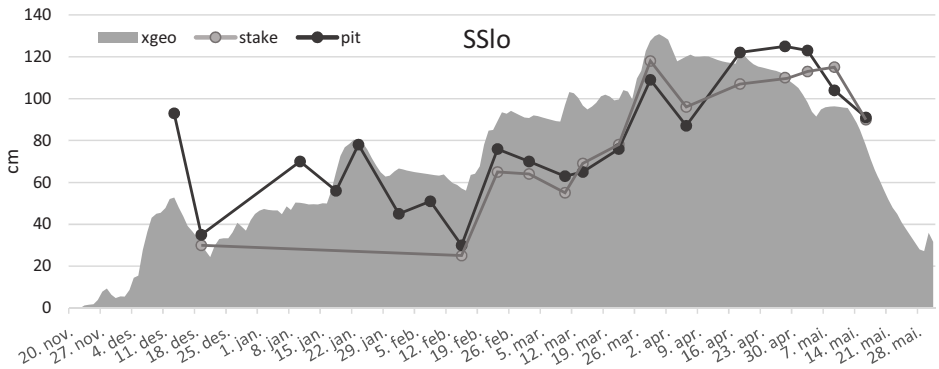

(c)

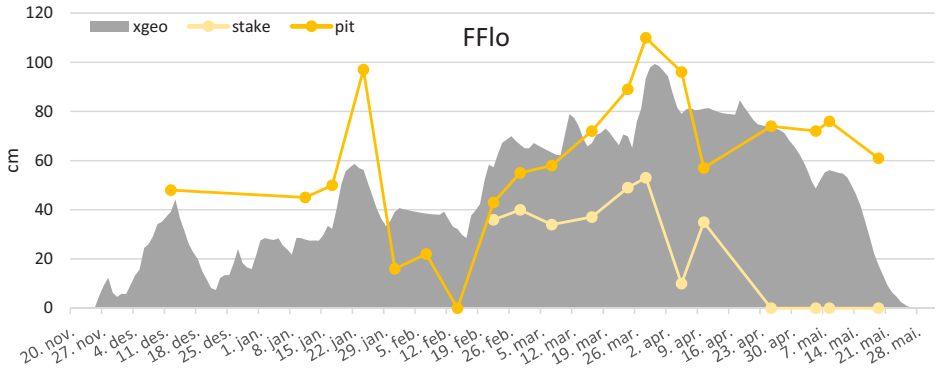

(d)

Figure 5.7: Measured (stake and pit) snow depth together with modeled snow depth data at all study plots in the winter season 2016–2017. Note that the scale on the y-axes are different.

Table 5.6: Measured snow depth summary from pits and depth stakes in the snow season 2016–2017.

	Snow depth			
	SShi	*FFhi*	*SSlo*	*FFlo*
Pit average [cm]	176	170	78	60
Difference [%]	3		31	
	150			
Pit maximum [cm]	294	240	125	110
n	17	20	20	19
Stake average [cm]	222	178	81	25
Difference [%]	25		231	
	279			
Stake maximum [cm]	304	215	118	53
n	8	13	14	12

period. In average, the snow depth at the stakes was 69% deeper than the modeled snow depth.

The model also seemed to underestimate the average snow depth at the low altitude study plots, shown in Figure 5.7c and Figure 5.7d. Snowfall events were also underestimated, e. g. December 13 at SSlo and January 22 and March 28 at FFlo. December 13 at SSlo, the snow depth in the pit was 76% deeper than in the model. With the average stake depth measurement at SSlo 3% deeper than the average pit measurement, it seems to be a good compliance between the data.

The depth stake at FFlo was leaning on a tree with a canopy that clearly affected the snow depth measurements (Figure 4.6b, page 36), hence the fast melt after April 10. Thus, the average snow depth measured at the stake was not representative for the snow depth at 44 m a.s.l. at Fagerfjellet during this winter season. FFlo was at a consistently smooth and even area (Figure 4.9a, page 39), therefore the snow pit depth could be representative for the general snow depth in the area. The average snow pit depth at FFlo was 34% deeper than the modeled snow depth.

AVERAGED RELATIVE SNOW DEPTH COMPARISON. When averaging the measured and modeled relative snow depths between November 20 and May 31, SShi had a 14% deeper snowpack than FFhi. SShi and FFhi were at approximately the same altitude — 463 m a.s.l. vs 469 m a.s.l. SSlo had a 78% deeper snowpack than FFlo. Important to notice is the error from the depth stake at FFlo. When excluding the depth stake measurements at SSlo and FFlo, SSlo had a 43% deeper

snowpack than FFlo, at 233 m a.s.l. vs 44 m a.s.l. , respectively. Averaging SShi and SSlo and comparing with the average of FFhi and FFlo (excluding stakes at FFlo), the coast proximate Steinskarfjellet had a 23% deeper snowpack than the inland Fagerfjellet.

The high altitude study plots had in average 169% deeper snow than the low altitude study plots. Again, FFlo include an anomalously low average stake depth measurement. Comparing the high and low altitude study plots without the stake measurements, the difference is 154%. Thus, the biggest difference in snow depth occurs with altitude.

5.2.2 *Grain types*

The grain type distribution for the winter season 2016–2017 is shown in Figure 5.8, with the relative amount of the different grains in Figure 5.8a, and the relative times registered in Figure 5.8b.

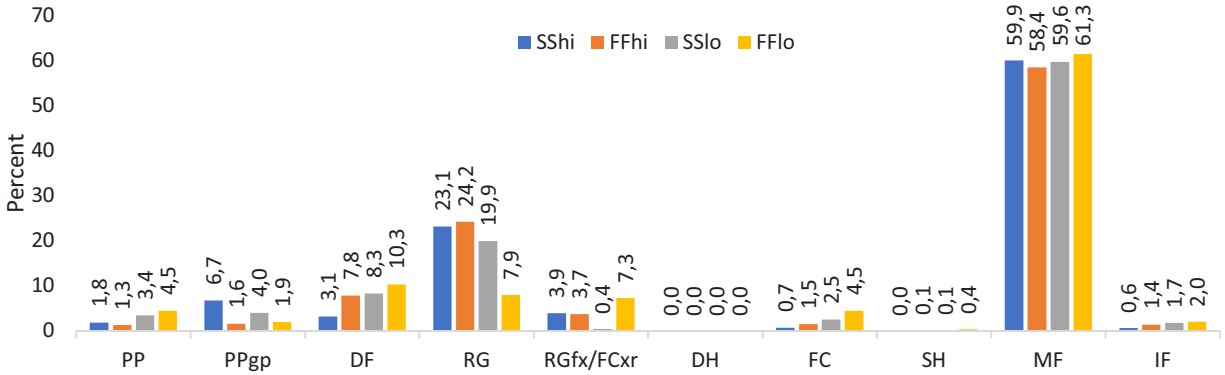

(a) Relative amounts in percent of snow grain types.

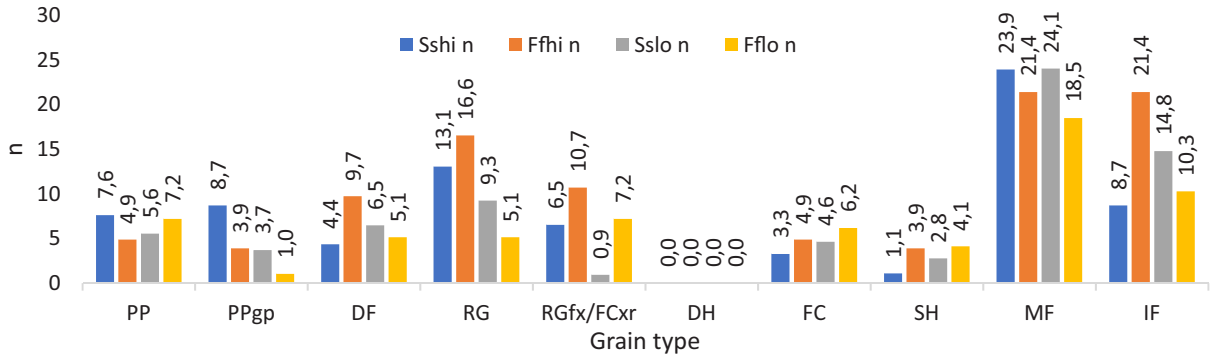

(b) Relative number of snow grain types. Corrected to 19 registered pits.

Figure 5.8: Relative amounts (a) and numbers (b) of snow grain types in the snow season 2016–2017 in the four different locations. Grain type abbreviations are explained in Table 3.4 on page 21.

The most dominating grain type in all locations were melt forms (MF) with approximately 60% presence at each location. Depth hoar (DH) was never observed. Second most occurring were rounded grains (RG), present on average in 22% of the snow pits at SShi, FFhi and

SSlo. Differing substantially were the presence of rounded grains at FFlo, with 7.9% in contrast to 22% at the other locations.

Faceted crystals (FC) and mixed forms (RGfx/FCxr) are crystals that either undergo constructive or destructive metamorphism *and* have clear facets. Seen in the FC group, the amount of faceted crystals *increased* with decreasing altitude and *increased* when moving inland. The same amount of mixed forms were registered at the high locations, with 3.8%, but hardly none at SSlo, with 0.4%. Contradictory, mixed forms were present 7.3% of the time at FFlo. Looking at the number of times observed, mixed forms were distinctively more often observed at FFhi than SShi, with 10.7 and 6.5 times, respectively.

Decomposing and fragmented particles (DF) were also *increasingly* present when moving to lower altitudes, and when moving inland. DF-grains were present 63% less at SShi than SSlo and present 24% less at FFhi than FFlo.

The amount of graupel (PPgp) differed distinctly with respect to location. Graupel was present 1.75% of the time at FFhi and FFlo, and 5.35% of the time at SShi and SSlo.

Precipitation particles (PP) were present in larger amounts at the low altitude locations than at the high locations. This may be due to the high altitude location's exposure to wind. Slightly less precipitation particles were observed at FFhi than at SShi (1.8% vs 1.3%, respectively), and slightly more precipitation particles were observed at FFlo than at SSlo (4.5% vs 3.4%, respectively).

Both ice layers and surface hoar occurred as thin layers in snowpacks, with an average thickness of 3.2 mm and 0.9 mm, respectively. Hence, they account to small amounts of the total snowpack but still appear often. Ice layers were the snow grain type being registered second most often, with 56 registrations (after melt forms with 88). Figure 5.8b displays the number of times different grain type layers were observed corrected to a mean. After correction, ice layers were registered 21.4 times at FFhi compared to 8.7 at SShi. At the low locations the distribution was more similar, 10.3 and 14.8 times at FFlo and SSlo respectively. Interestingly, ice layers were registered *more often* at the low locations at Steinskarfjellet, and *less often* at the low location at Fagerfjellet. Surface hoar was registered 12 times in total during the 2016–2017 season. It was registered two times in a row only one time; February 28 and March 7 at FFlo. At both pits, the surface hoar was the top layer. As displayed in Figure 5.8b, surface hoar was registered more often at FF than at SS and more often at the low locations than at the high locations.

5.2.3 *Hand hardness*

The hand hardness (Fierz et al., 2009) of the registered snow pits is shown in Figure 5.9. Layers harder than one finger (1F) were registered

in more than 50% of the snow pits at all locations except for FFlo. Of the snow layers harder than 1F-P, layers of pencil (P) hardness dominated at the low locations, while the relationship between P hardness and harder layers were more equal at the higher locations.

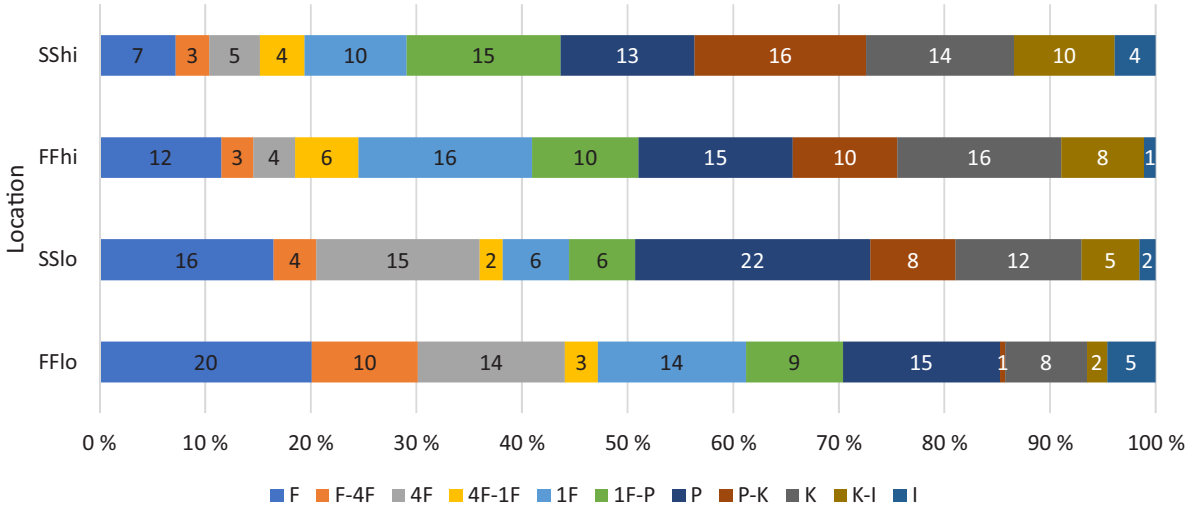

Figure 5.9: Hand hardness in studied snow pits in the snow season 2016–2017.

The amount of soft layers (fist to four-fingers-to-one-finger, F – 4F-1F) were observed more often at the low than the high locations, 47% and 37% to 25% and 19% of the time, respectively. Far more often observed at the low locations were snow of 4F and F hardness. FFlo showed significantly more snow of F-4F hardness than the other locations. Medium hard layers (1F and 1F-P) remained constant at SShi, FFhi and FFlo, observed 25%, 26% and 23% respectively. SSlo stood out with medium hard layers registered approximately half as often, 12% of the time, approximately half the amount of SShi, FFhi and FFlo. Pure ice layers (I) and very hard refrozen layers (knife to ice, K-I) were both observed in 7% of the snow pits at FFlo and SSlo, where I dominated at FFlo and K-I dominated at SSlo. At the high locations, K-I and I layers were observed in 14% of the snow pits at SShi and 9% at FFhi.

5.2.4 *Hand hardness profiles*

The hand hardness profiles in Figure 5.10 are from the classification scheme of Schweizer and Wiesinger (2001). The dominating profile in total was profile 6, observed in 26.7% of the pits. Profile 6 was the typical hand hardness profile for both of the low altitude locations, but was also observed often at the high locations. The second most observed hand hardness profile was profile 7, observed in 18.7% of

the pits. Profile 7 was the most registered profile at FFhi due to a persistent weak layer that developed under a rain crust after a warm period in February and persisted to the end of April. Following close, and observed in 16% of the pits, was profile 8. Profile 8 was observed in 29% of the snow pits at SShi, and was the typical hand hardness profile here, closely followed by profile 6 that was observed in 24% at the pits at SShi.

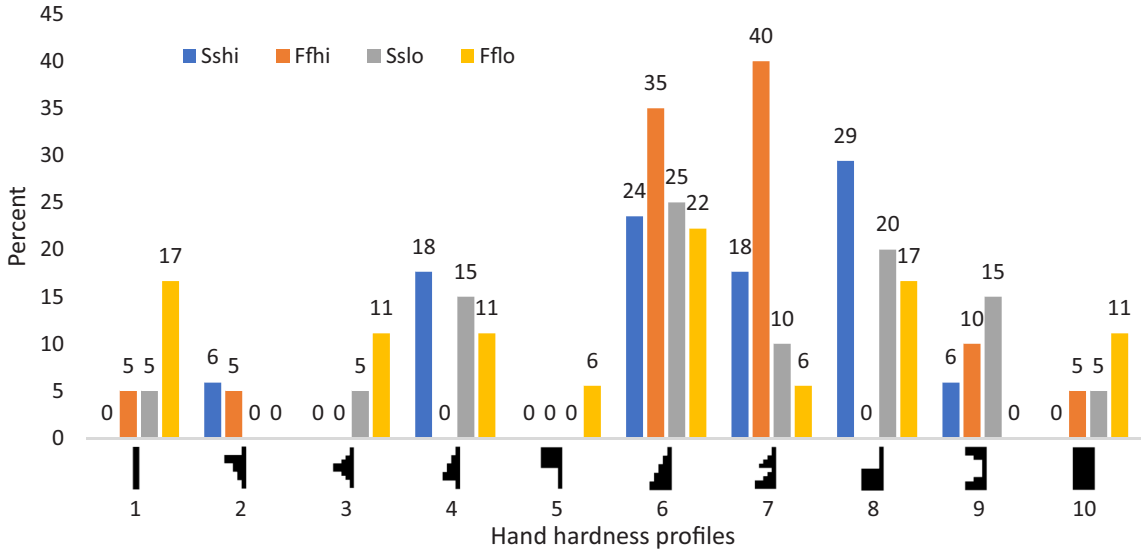

Figure 5.10: Hand hardness profiles (Schweizer & Wiesinger, 2001) in studied snow pits in the snow season 2016–2017. Total number of snow pits compared with hand hardness profiles was 75.

Profile 6 is considered as a stable profile as the hardness decreases in small steps higher in the snow pack. Profile 8 also displays the favorable decrease in hardness closer to the snow surface, but the hardness leap may indicate a weak interface, e. g. between a rain crust and new snow. Profile 7, on the other hand, displays potential instability with a probable persistent weak layer underneath a consolidated snow surface. Important to mention is that that particular persistent weak layer at FFhi often was below well consolidated and dense layers, and that no ECTs propagated on that persistent weak layer through the field season.

Of the standardized hand hardness profiles, profiles 1–5 represent snowpacks with *weak* bases and profiles 6–10 represent snowpack with consolidated, hard and *strong* bases. During the winter season 2016–2017 profiles 1–5 were registered in approximately 20% of the pits at SShi and SSlo, and 10% of the pits at FFhi. In contrast, weak based profiles were registered in 44% of the profiles at FFlo. Thus, strong based hand hardness profiles dominated this winter season at SShi, FFhi and SSlo.

The low locations had a wider distribution of snow profiles than the high locations, with SSlo exhibiting all profiles except 2 and 5, and FFlo exhibiting all except 2 and 9. The *mean snow pit registration depth* was respectively 75 cm and 60 cm at SSlo and FFlo, and 176 cm and 170 cm at SShi and FFhi. The smaller snow depth at the low locations may have made the snow pack more susceptible to different weather conditions and events, making them *change more*.

5.2.5 *Densities*

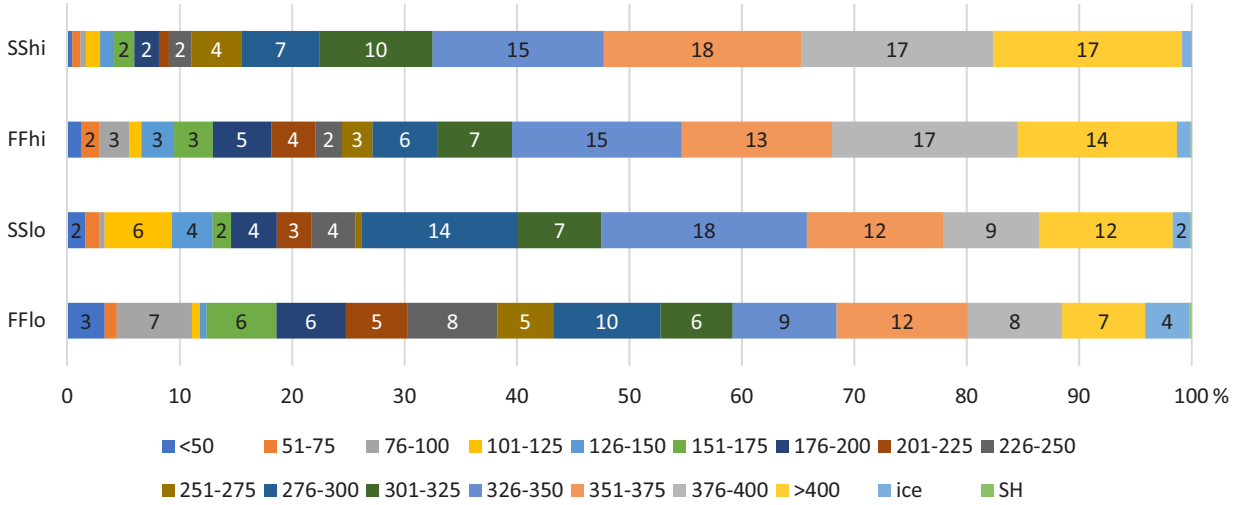

Figure 5.11: Snow density distribution in percent at the study plots in the snow season 2016–2017. Labels representing values less than 2% are omitted on the density intervals. Thus, thin bars without label have a value between «0» and «1», and thick bars between «1» and «2».

The distribution of different snow densities are shown in Figure 5.11. The overall dominating snow density in the winter season 2016–2017 was higher than 325 kg m^{-3}, represented in 57.1% of all the profiles., SShi had the most snow with a density above 325 kg m^{-3} measuring 66.7%. The amount decreased with height and moving inland with FFhi, SSlo and FFlo displaying 59.1, 50.8, and 36.7 %, respectively. The large amount of high density snow could be recognized in type of hand hardness profiles, with profile 6–10 registered in approximately 80% of the snow pits at SShi, FFhi and SSlo.

For densities below 101 kg m^{-3}, FFhi and FFlo had the highest amounts with 5.5 and 11.1 %, respectively. In contrast, 1.6% and 3.3% of the snow pits had snow below 101 kg m^{-3} at SShi and SSlo, respectively. For densities between 101 and 325 kg m^{-3} the amount varied mostly with altitude. SShi and FFhi had 30.9 and 34.0 % with

101 to 325 kg m^{-3} , respectively. SSlo and FFlo had 44.2 and 48.1 %, respectively.

5.2.6 *Avalanche problems*

Registered avalanche problems are shown in Figure 5.12. The dominating avalanche problem was persistent slabs occurring in 31% of all the snow profiles, followed by storm slabs occurring in 21%. No cracks indicating possible glide avalanches were observed neither at the study plots nor in the surroundings during the field period. Cornice falls were not registered nor anticipated in the surroundings of the study plot, but abrupt temperature increases and radiation in spring may make this an avalanche problem.

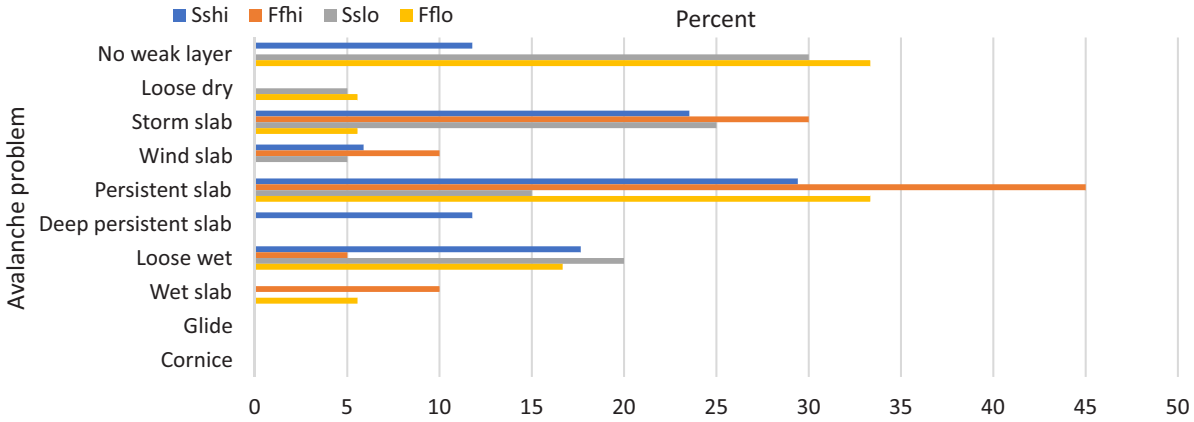

Figure 5.12: Relative amount of avalanche problems in the 2016–2017 snow season. N: SShi: 17, FFhi: 20, SSlo: 20, FFlo: 18, thus 5% reflect approximately one registration.

Persistent slabs were considered the main avalanche problem in approximately 45% of the snow profiles from FFhi. At SShi and SSlo, respectively, persistent slabs were considered the main avalanche problem in 29 and 15 % of the snow profiles. Deep persistent slabs were only registered at SShi in 12% of the snow profiles. Storm slabs were considered the main avalanche problem in 23% of the snow profiles at SShi and 30% of the snow profiles at FFhi. At SSlo and FFlo, storm slabs were considered the main avalanche problem in 25% and 6% of the snow profiles. No weak layer — hence no particular avalanche problem — was registered most often in the snow profiles at the low altitude locations, with 30 and 33 % at SSlo and FFlo.

The loose wet avalanche problem was considered most important at SShi in 18% of the snow profiles, and at SSlo in 20% of the snow profiles. At FFhi, this was considered most important in 5% of the profiles. A warmer snow pack due to rain and insolation is the release reason for both the avalanche problem loose wet and wet slabs. They

differs in the way that wet slabs have apparent layers in its snowpack that are conducive to failure. Wet slabs were considered to be most important in 10% at the snow profiles at FFhi, and none at SShi. At the low locations, wet slabs were considered the most important in approximately 5% of the snow profiles.

WEAK LAYER POSITION. In what third of the snow pack the weakest layer was found in is shown in Figure 5.13.

At SShi, the avalanche problem with its associated weak layer grain type was found in the higher third of the snowpack in 67% of the registrations. When the avalanche problem was in the higher third, melt forms were the most occurring weak layer found in 30% (three times) of the snow pits. Two of these occasions were on the two last field days in May, while the third was on April 6. On three other occasions, — also in 30% — dry crystals in some stage of destructive metamorphism were considered to be the main avalanche problem. Mixed forms were considered the weakest layer in the middle third in 20% of the snow pits. In 13% of the pits (2 pits), facets in the lower third were the main avalanche problem in the snow pack.

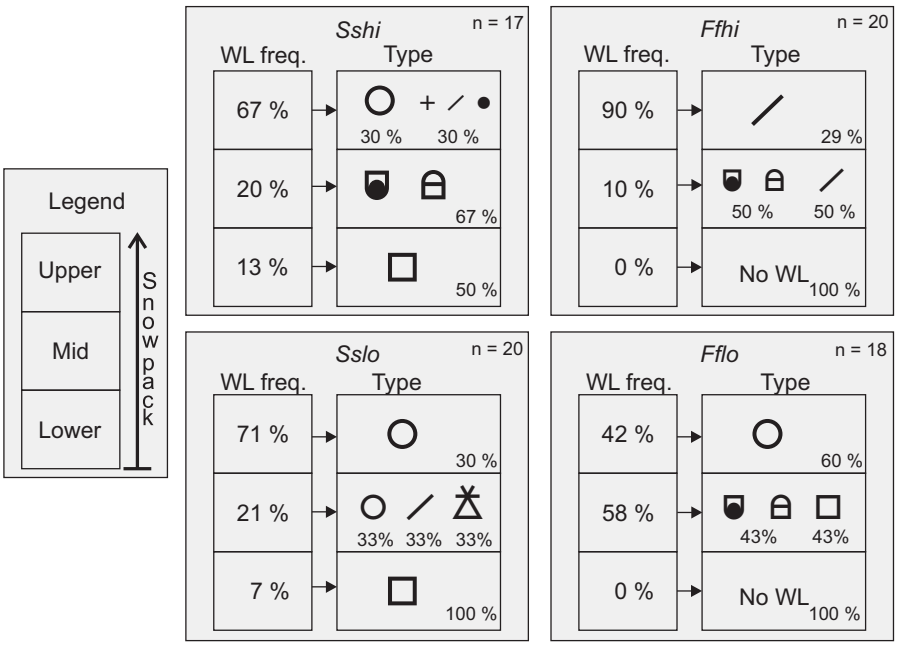

Figure 5.13: Relative frequency of weak layer position at the study plots in the 2016–2017 snow season. «WL freq» (weak layer frequency) shows how often the weakest layer was present in which third of the snow pack. «Type» shows which grain type and frequency of the most frequent weak layers.

At FFhi, the considered avalanche problem was found in the higher third in 85% of the snow pits. In the higher third, 29% (five pits) of the avalanche problems were due to hardness differences within decomposed and fragmented crystals. Mixed forms, found in 24%

(four pits), was the second most occurring weak layer in the upper third of the snowpack. In 15% of the snow pits, the weakest layer was in the middle third, and 67% (two pits) of these weak layers were mixed forms. The weak layer in the third pit was a weak interface between a crust and decomposed and fragmented particles. The weakest layer was never found in the lower third during the winter season.

SSlo had its weakest layers in the upper third of the snowpack in 71% of the pits. Thirty percent (three pits) of these were melt forms. The weakest layers were in the middle third in 21% of the pits. Weak melt forms and weak interfaces in graupel and decomposed and fragmented particles occurred in one pit each. The weakest layer was present in the bottom third once, as faceted grains.

FFlo was the only study plot that had the weakest layer most often in the mid third, in 58% of the pits. Mixed forms and faceted crystals were the weak layer in 86% of these pits, and were found two times each. FFlo did never exhibit the weakest layer in the bottom third.

WEAK LAYER HARDNESS DIFFERENCES. Hardness differences between weak layer and slab and weak layer and bed are shown in Figure 5.14 and Figure 5.15, respectively.

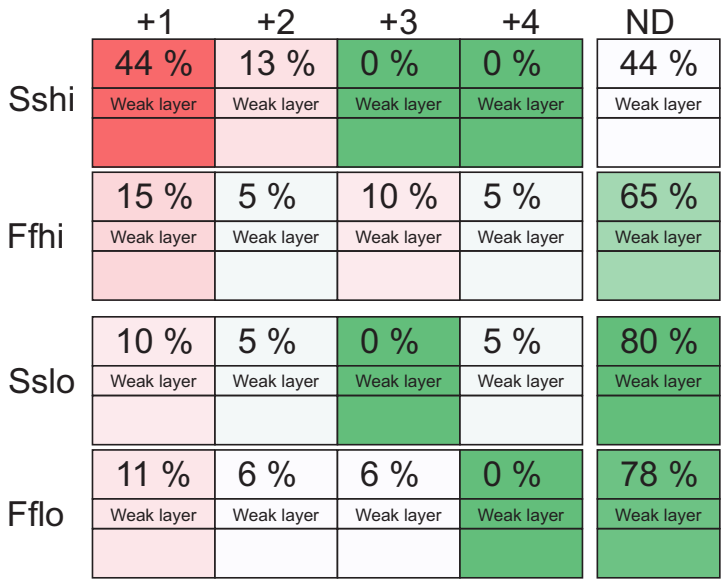

Figure 5.14: Hand hardness differences (Fierz et al., 2009) between weak layer and slab for snow season 2016–2017. Study plots are shown in the rows and hardness difference are shown in the columns. «ND» is short for «no difference». Red color indicates high frequency of hardness differences, green indicates low frequency.

SShi had hardness differences between the overlying slab and the weak layer in 56% of the snow pits. Forty-four percent of the pits showed a hardness difference of 1 step, and 13 % a difference of 2 steps. Hardness differences between weak layer and bed over 2 steps were not observed. Faceted and mixed forms were the most observed

weak layer with a hardness difference of 1 or 2 to the slab. Weak graupels were second most observed.

FFhi displayed no hardness difference more often than at SShi, with no differences between weak layer and slab in 65 % of the pits. Faceted or mixed forms were the weak layers at all situations with hardness differences. Hardness differences between weak layer and slab occurred less often at FFhi than at SShi. But, when present, the hardness differences were more profound.

Both at SSlo and FFlo, hardness differences between the weak layer and overlying slab were present less often than at the high locations. A situation with a 1 step hardness happened two times at both low locations, where three of those four times were with weak facets.

An overlying slab was 4 steps harder than the weak layer two times at all the pits. Both February 14 at FFhi and March 22 at SSlo, a thin rain crust had formed above new snow that experienced strong temperature gradients.

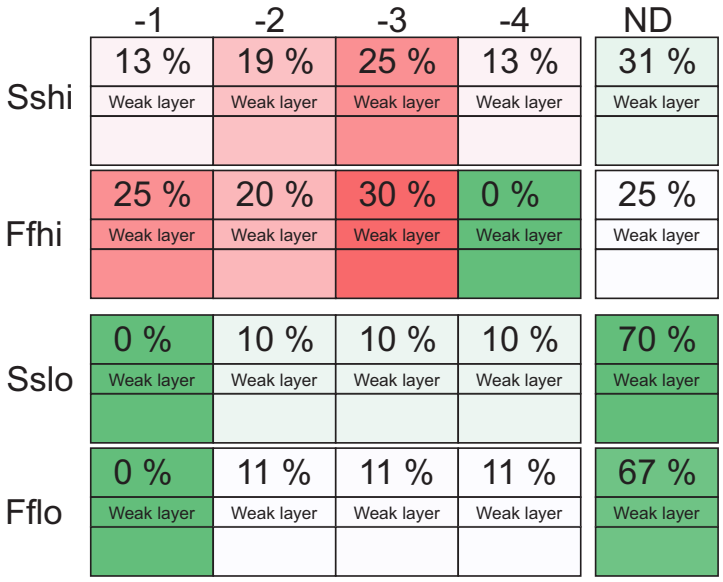

Figure 5.15: Hand hardness differences (Fierz et al., 2009) between weak layer and bed for snow season 2016–2017. Study plots are shown in the rows and hardness difference are shown in the columns. «ND» is short for «no difference». Red color indicates high frequency of hardness differences, green indicates low frequency.

Figure 5.15 shows the frequency of hardness differences between the weak layers and the underlying bed.

At SShi, there was a bed noticeably harder than the weak layer in 69 % of the pits. In 25 % of the pits, the underlying bed was 3 steps harder than the weak layer. All of these weak layers were faceted or mixed forms, where most of them had crusts as beds. In situations with a bed 2 steps harder than the weak layer, most weak layers were graupel on crusts. When the bed was 1 step harder, the bed was of the same crystal type as the weak layer at both occasions.

FFhi displayed a noticeably harder bed slightly more often than at SShi. In 75 % of the pits, the bed was between 1 and 3 steps harder than the weak layer. In situations with a 3 step difference, most weak layers were facets lying on crusts happening before May. Two situations with a 3-step weak layer–bed difference happened in May with new snow lying on top of crusts. Also, at the 1-step weak layer–bed difference situations four of five weak layers were lying on crusts. At 2-step weak layer–bed differences, faceted forms lying on different bed types were observed. The March 16 surface hoar was lying on top of rounded grains, while at other dates both in the beginning and in the end of the snow season, mixed forms were lying on top of either crusts or rounded grains. At one situation, a 2-step weak layer–bed situation was observed with decomposed and fragmented forms both as weak layer and bed.

The same trends of less hardness differences with adjacent snow layers could be observed at the low altitude locations. SSlo and FFlo displayed no hardness differences between the weak layer and underlying slab 70 and 67 % respectively. Hardness differences of between 2 and 4 were found six times at both study plots, two times of each difference. SSlo displayed hardness differences between faceted forms and graupel on a harder slab, while FFlo displayed only faceted or mixed forms on harder beds.

5.2.7 *Extended column test results*

STEINSKARFJELLET HIGH – SSHI The stability test results from SShi are shown in Figure 5.16.

Rain stabilized dry snow conditions with facets on the ground in mid December. From then, no tests propagated through the whole column until March 22 (P30 and N29). In that period, two warm events with precipitation as rain occurred; one in late January, and one in the beginning of February. March experienced three storms with precipitation as snow. During April, two stability tests were conducted with the temperature staying below 0°C the whole time in between. In early May, at two separate field days, tests propagated through the column again. The most unstable test through the year happened May 3 with the column propagating at tap 17 on a weak layer of rounding faceted particles below a crust.

During the winter, 21% of the tests propagated through the whole column. All these fractured on faceted or rounding faceted particles, five of seven on a bed of melt forms, and five of seven with rounded particles in the slab (Figure 5.13). In the two tests in May 9, the slab consisted of melt forms. In average, the P-results required 22.4 taps.

Thirty-two percent of the columns had a failure initiation without propagation, hence a N-result. Of these, four of eleven failed on a weak layer of graupel and three of eleven failed on rounded grains

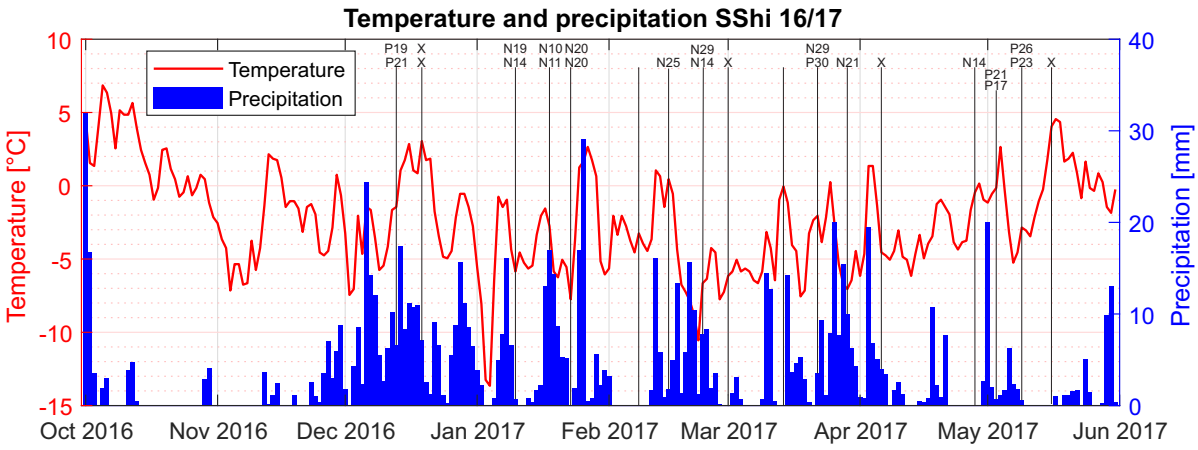

Figure 5.16: Extended column test results plotted on top of interpolated temperature and precipitation data from SShi in the snow season 2016–2017. The vertical lines visualize when the tests were conducted. The test results for the particular day are written above. The test results follow conventions from Simenhois and Birkeland (2009), described in Table 3.6, but are simplified for readability.

(Figure 5.13). Rounded grains as bed surface occurred in four of eleven pits, and melt forms in three. Graupel was registered as a bed twice, where the ECT initiated a fracture within a layer of graupel or graupel/rounded forms mixture. In ten of eleven tests, the slab comprised of dry grains either as graupel, deformed and fragmented particles, or rounded grains. Once the rounded grains were faceting. In average, the N-results required 18.6 taps.

Fifteen percent of the columns did not initiate a fracture, thus indicating stable conditions at that particular spot. Common for all columns that *did not* fracture were that snow adjacent to ice layers and crusts was moist. In two of five columns, dry snow that did not initiate fracture had precipitated on top of the moist, older snow.

FAGERFJELLET HIGH – FFHI The stability test results from FFhi are shown in Figure 5.17.

The test results at FFhi through the winter season 2016–2017 follow a similar pattern as for SShi. Rain in mid December stabilized a facet-on-ground snowpack from early December. Temperatures below 0°C persisted through December until the end of January, providing columns that only initiated fractures or did not fracture at all. January 17, one column initiated a fracture 6 cm below the surface in decomposed and fragmented particles, while the second column did not fracture. The first propagation through the whole column in 2017 occurred March 7, requiring 16 taps. After, three warming events with precipitation both as snow and rain, another propagating column occurred April 10 requiring 27 taps. Two significant warming events

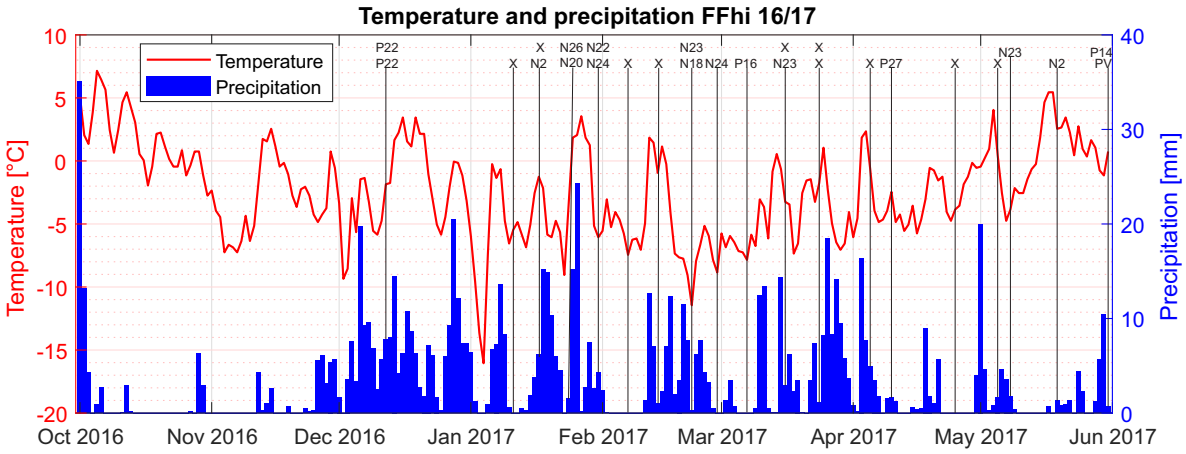

Figure 5.17: Extended column test results plotted on top of interpolated temperature and precipitation data from FFhi in the snow season 2016–2017. The vertical lines visualize when the tests were conducted. The test result for the particular day are written above. The test results follow conventions from Simenhois and Birkeland (2009), described in Table 3.6, but are simplified for readability.

occurred after mid-April to the end of May, one with precipitation, the other without. No propagating columns were registered until the very end of May, where one column propagated during isolation.

At two propagating occasions a second ECT was not conducted, thus producing a relative bias towards the two ECTs conducted May 31. To correct for this, propagating ECTs at FFhi are averaged out into one ECT per snow pit. After the correction, 10 % of the columns propagated through the whole column. Three of four columns propagated on weak layers of facets or mixed forms, while the last propagated on melt forms. Melt forms were the bed surface in two out of four times, facets and rounded grains the two other. Rounded grains were the slab in three out of four columns, while the last one were melt forms. In average, the P-results required 17.1 taps.

Thirty percent of the columns had a failure initiation without propagation. Of these twelve columns, four initiated on a weak interface in decomposed and fragmented particles, and four initiated on melt forms. Two of twelve initiated on faceted crystals, and one each initiated on an ice layer and on surface hoar. In four of twelve columns, the bed layer comprised of decomposed and fragmented crystals. Rounded grains and melt forms were the bed crystal type in three of twelve columns. In two of twelve columns, the bed were either faceted crystals or melt forms. In half of the columns, the slab comprised of decomposed and fragmented crystals, while in five of twelve the slab comprised of melt forms. In one occasion, the slab comprised of graupel. In average, the N-results required 20.1 taps.

Twenty-five percent of the columns at FFhi did not initiate a fracture in the 2016–2017 snow season. Eight of these ten columns comprised of various layers of melt-freeze crusts and ice layers in between dry rounded grains, while the two last ones comprised of moist melt forms and rounded forms.

ECT SUMMARY A summary of the amount of extended column test results is shown in Table 5.7. Example snow profiles for different typical ECT-results are shown in:

	Date & figure	
	SShi	*FFhi*
P	May 3, A.8b	March 7, A.26a
N	January 10, A.2b	January 24, A.23a
X	April 6, A.7b	March 24, A.27a

Table 5.7: Results of extended column tests at SShi and FFhi in the snow season 2016–2017.

	Location	
Property	*SShi*	*FFhi*
Amount P [%]	21	10
WL type	FC/mix	FC/Mix
Depth [cm]	64.3	50.0
Av. taps	22.4	18.6
Amount N [%]	32	30
WL type	Graupel	DF/MF
Depth [cm]	51.3	45.1
Av. taps	18.6	20.1
Amount X [%]	15	25
Characteristic	Moist snow	Type 6 profile
No data [%]	32	35

Common for propagating columns at both SShi and FFhi are that the weak layer included faceted grains, the bed layer included melt forms and the slab included rounded grains. SShi displayed propagating results twice as many times as FFhi through the winter season 2016–2017. At the same time, the average number of taps needed for the columns to propagate was 17.1 at FFhi compared to 22.4 at SShi. In

average, the propagating weak layer at SShi was 14.3 cm deeper than at FFhi.

The same trend accounts for initiating columns in the ECT-tests, except average taps needed. SShi had two percentage points more columns initiating, but with the weak layer in average 6.2 cm deeper. In average, 18.6 taps were needed for initiation at SShi versus 20.1 at FFhi. Columns at SShi did most often initiate within graupels, while columns at FFhi initiated in decomposed and fragmented particles or melt forms.

FFhi had above one-and-a-half more columns *not initiating* than SShi. The characteristics for non-initiating columns at SShi were that they already had not been through a melt-freeze process and were wet. The characteristic for non-initiating columns at FFhi were that the affiliating snow profiles had a type 6 hardness profile (Schweizer & Wiesinger, 2001).

5.2.8 *Avalanche danger levels*

A comparison between forecasted (regional) and registered (local) avalanche danger level at both Steinskarfjellet and Fagerfjellet is shown in Figure 5.18 and Figure 5.19, respectively. The relative amount of time the different danger levels was forecasted and registered is shown in Table 5.8. Note that Steinskarfjellet and Fagerfjellet are situated in different avalanche forecasting regions, Tromsø and Lyngen, respectively.

Table 5.8: Relative regional and local avalanche level at Steinskarfjellet 2016–2017.

Avalanche danger level	*SShi [%]*		*SSlo [%]*		*FFhi [%]*		*FFlo [%]*	
	Local	*Regional*	*Local*	*Regional*	*Local*	*Regional*	*Local*	*Regional*
1	6	0	15	0	5	0	42	0
2	71	71	70	75	60	55	42	53
3	24	29	15	25	35	40	16	42
4	0	0	0	0	0	5	0	5

SShi n = 17, SSlo n = 20, FFhi n = 20, FFlo n = 19

At SShi the forecasted regional avalanche danger level was 2 in 71% of the field days, and at SSlo it was 2 in 75% of the field days. The forecasted avalanche danger was 3 in 29% at SShi and 25% at SSlo. During the field days, the forecasted avalanche danger was never 1 or 4. The avalanche danger was forecasted to level 2 in 55% of the field days at FFhi, and 53% at FFlo. Danger level 3 was forecasted 40% and 42% at FFhi and FFlo, respectively. Danger level 4 was forecasted 5% of the field days at both FFhi and FFlo.

The most noticeably deviation was that danger level 1 was observed at FFlo in 42% of the pits despite that it was never forecasted. Thus, the registered danger level was lower than the forecasted in 63% of the pits at FFlo. The second biggest deviation was observed at SSlo, with danger level 1 registered in 15% of the pits, but forecasted in none. Here, the registered avalanche danger level was lower than forecasted in 25% of the pits. All the study plots had situations where a danger level 1 was registered but not forecasted. A regional avalanche danger level of 4 was forecasted at Fagerfjellet once (5% of the field days), where danger level 3 was registered in the field.

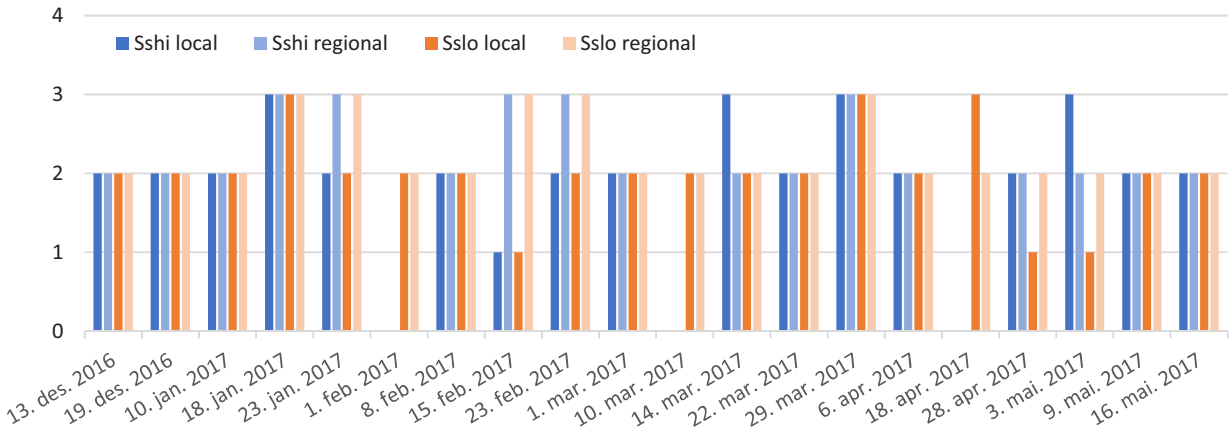

Figure 5.18: A comparison between forecasted avalanche danger level (regional) and registered avalanche danger level (local) at the field days at SShi and SSlo. The vertical axis represents avalanche danger level.

Figure 5.18 and Figure 5.19 display when the local danger level was different from the forecasted regional. At Steinskarfjellet, the first occasion with a different local than regional danger level occurred January 23, when the forecast was level 3 and the observed danger was level 2. A lower danger level was set because wind and precipitation made the new snow form solid bonds and sinter into thick slabs that were not easy to trigger in test slopes. Thus, the avalanches were not anticipated to be larger than the deposits in the specific slopes. The second and third occasions with different danger level happened February 15 and February 23. February 15, the avalanche danger was forecasted to be level 3, but level 1 was observed. A hard omnipresent crust below 500–700 m a.s.l. was the reason for the low danger level. Above that crust, the avalanche danger was considered to be level 2.

March 14, April 18 and May 3, a danger level higher than the forecast was registered at SShi, SSlo and SShi, respectively. At March 14, the snow cover was considered to have weak connections in many leeward slopes above 400 m a.s.l. due to wind transport of snow. Below 400 m a.s.l. the observed conditions agreed with the forecasted danger level. Similar conditions were observed April 18. Thus, the observed

avalanche danger level was set to 3, instead of the forecasted level 2. This day, shooting cracks from the skis were also observed. On May 3, whumpfh-sounds were observed between 400 m a.s.l. and 600 m a.s.l. which indicated that avalanche could initiate and propagate at low additional loads which is a characteristic of danger level 3. The snow profile from May 3 can be seen in Figure A.8b, where the column propagated when conducting ECTs.

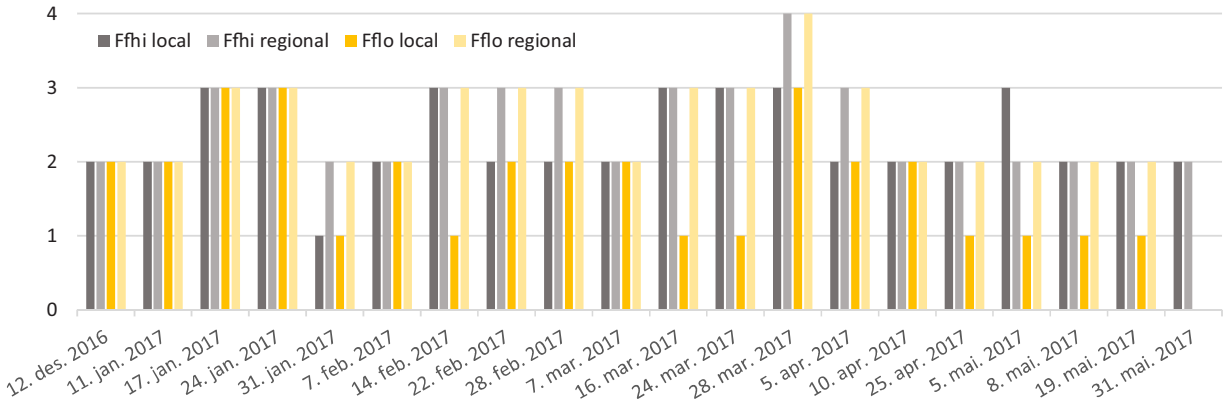

Figure 5.19: A comparison between forecasted avalanche danger level (regional) and registered avalanche danger level (local) at the field days at FFhi and FFlo. The vertical axis represents avalanche danger level.

At January 24 at Fagerfjellet, danger level 3 was both observed and forecasted. This was contradictory to danger level 2 observed and level 3 forecasted at Steinskarfjellet the day before. January 31, the field day after, danger level 1 was observed locally while the regional forecast was danger level 2. Rain up to FFhi at 469 m a.s.l. ahead of the field trip that had refrozen was considered to have stabilized the snowpack. Thus, above the rain limit, the danger level was set to level 2. At February 14, the avalanche danger at FFlo was considered to be level 1, while level 3 was forecasted. Below 500 m a.s.l. the snow was dry and hard, hence the danger level was set to 1. Above 500 m a.s.l. — also above FFhi — fresh wind transported snow resulted in an agreement with the forecasted danger level 3. The two subsequent field days, February 22 and February 28 respectively, the observed danger level was set to 2 despite the forecasted level 3. February 22, weak layers were *not* observed in a fast pit dug near the summit of Fagerfjellet at approximately 800 m a.s.l. . Similar conditions were observed February 28 — I evaluated the snowpack to need big additional loads to release avalanches except from a few slabs in some leeward steep slopes.

The local observations agreed with the forecasted danger level at FFhi on March 16 and 24. At FFlo, the snow was moist and gave stable ECT results both days, hence danger level 1. March 28, danger level 4 was forecasted regionally, while the observed danger level was 3.

Wind and precipitation from polar lows were the reason for the high forecasted danger level (The Norwegian Water Resources and Energy Directorate, 2017). Fagerfjellet faces towards wind from north and northwest which also are the directions where polar lows come from, hence eroding and removing snow from slopes. This is probably the reason why a lower danger level was registered than forecasted at Fagerfjellet March 28.

May 5 was the only occurrence of a higher danger level observed than forecasted at Fagerfjellet. Whumpf-sounds above the treeline indicating susceptible fracture initiation at low additional loading were the main reason for setting the locally observed avalanche danger to level 3 while the regional forecast was 2. Contradictory to the propagating columns at SShi May 3, ECTs at FFhi did not initiate fracture May 5.

6 DISCUSSION

Existing snow climate classes separate snow covers into maritime, continental and transitional classes. Persistent weak layers are rare in the maritime class due to deep snowpacks and snow temperatures close to 0°C due high air temperatures and regular rainfalls. Skiing tourism in Tromsø has increased significantly over the last years, and the Tromsø region is advertised to have mild coast climate compared to other destinations at similar latitudes.

Several snow climate classifications have been conducted throughout the world. The snow climate classes in use today origin from descriptions of climatic differences in mountains in western U.S.A. by Roch (1949). Consequently, the mountains in western U.S.A. and also southwestern Canada have been described in various studies (LaChapelle, 1966; Armstrong & Armstrong, 1987; Fitzharris, 1987; Mock & Birkeland, 2000; Hägeli & McClung, 2003; Hägeli & McClung, 2007), where the latter introduced the term *avalance winter regime* emphasizing snow structure. Internationally, other mountainous regions have been studied such as the Japanese Alps (Ikeda et al., 2009), Svalbard (Eckerstorfer & Christiansen, 2011), and the European Alps (Wakonigg, 1975; Laternser, 2002; Castebrunet, Eckert, & Giraud, 2012). The snow climate in Norway has been briefly mentioned as maritime by Fitzharris and Bakkehøi (1986) in a study primarily focusing on synoptic weather in major avalanche winters.

The purpose of this study was to spatially classify avalanche winter regime in the Tromsø area from field and weather data in the winter season 2016–2017 and temporally classify the snow climate based on weather and snow data from the seNorge model. Also, the study wanted to point out differences in avalanche problems over smaller spatial zones in the 10 km-scale.

6.1 SEASONAL SUMMARY

This section gives an overview in the general conditions in the Tromsø area. Figure 6.1 shows average air temperatures, corrected snow depths, new snow depths and rain from the average of all the four study plots. The figure also shows avalanche cycles and minor avalanche activity.

All subsections are organized to first present air temperatures, precipitation, snow depths and snow structures from xgeo data, snow profiles, and ECT-results. Subsequently, an evaluation and discussion of the conditions during the avalanche cycle 1 to 7 — see Figure 6.1 —

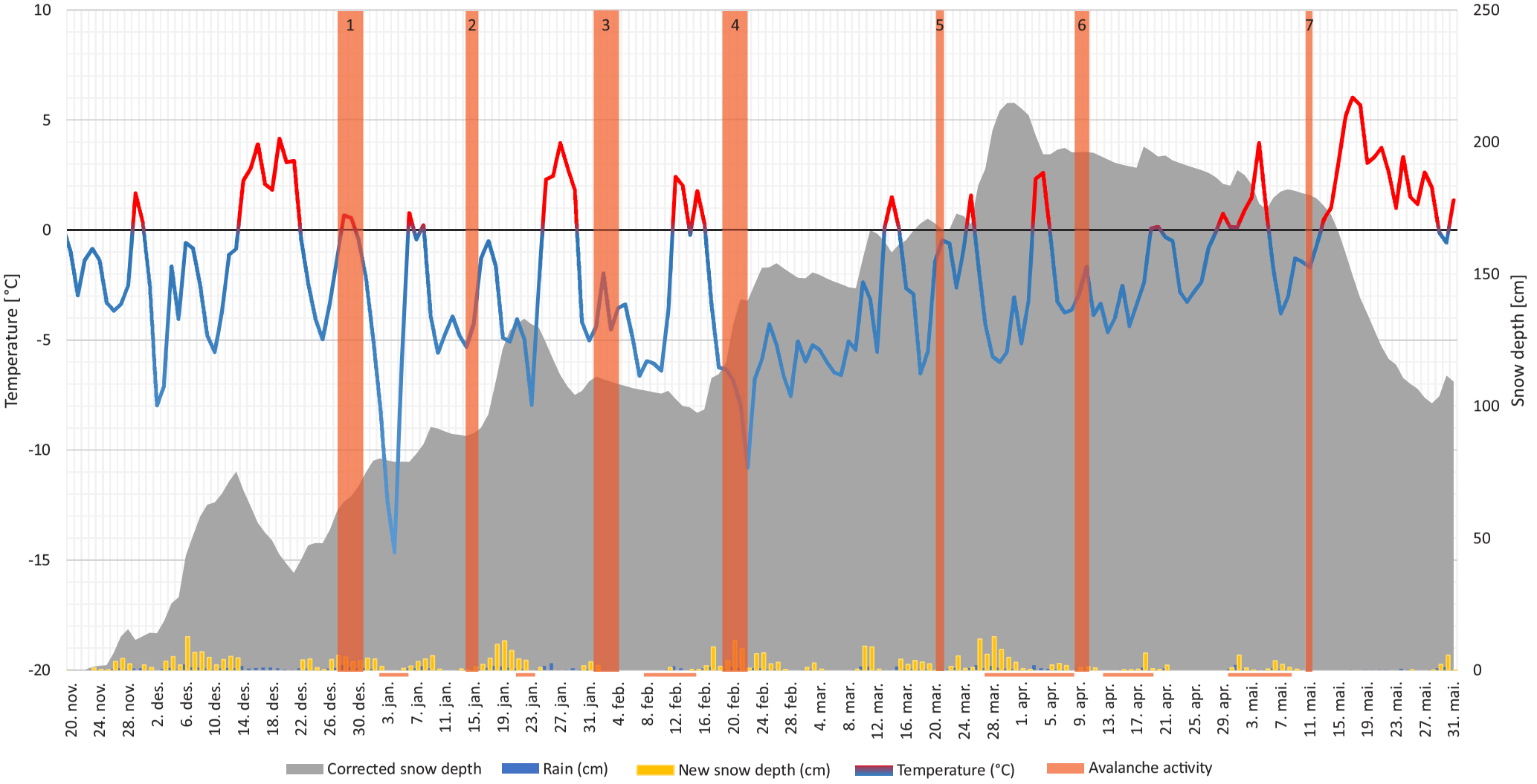

Figure 6.1: Summary of temperature, snow and rain precipitation, snow depth, avalanche cycles (vertical bars) and minor avalanche activity (horizontal bars) in the winter season 2016–2017. The data are averaged from SShi, FFhi, SSlo and FFlo, and the snow depths are corrected from average values obtained from snow pits and stake measurements. Depths from the FFlo stake were excluded from the calculations.

is shown, emphasizing what was the prevailing weak layer and driving force for the avalanche cycle. The dates for each avalanche cycle are given in the subsection title. The avalanche cycles are visualized in Figure 6.1, where the vertical bars represent the major cycle, while the horizontal bars represent minor avalanche activity.

The avalanche data from the 2017 winter season are based on observations by synthetic aperture radar (SAR) satellites and are provided by Markus Eckerstorfer. The avalanche data did not distinguish between different regions in and around Tromsø, but presented a count and area of total avalanches. Thus, the SAR data did not allow further discrimination of avalanche activity into the forecasting regions Tromsø and Lyngen.

6.1.1 *Avalanche cycles 1 to 7*

6.1.1.1 *Avalanche cycle 1 and 2 (Dec 27–30 and Jan 14–15)*

After a record-late snow season start (Resvoll & Johansen, 2016), the first snow of the persisting snowpack in the Tromsø area fell on November 26. Snow pits at Fagerfjellet and Steinskarfjellet December 12 and 13, respectively, exhibited dry snowpacks with depth hoar and facets. Between December 14 and 21, 41 mm of rain fell while the air temperature was 2.9°C on average, destroying the developed faceted crystals in the entire snowpack. Thus, after refreezing December 21, a snowpack comprising rounded polycrystals (MFpc) between 10 and 60 cm thick was the basis for the rest of the winter.

In the period between December 22 and the turn of the year, the air temperature stayed more or less below 0°C. Precipitation as snow occurred every day in the period. According to xgeo, in average 35 cm of snow fell between December 22 and December 31 at both Steinskarfjellet and Fagerfjellet. Between December 27 and 29, air temperatures were slightly above 0°C. No snow profiles nor ECTs were acquired in the period due to vacation time.

According to the SAR data, a great number of avalanches occurred in the period with higher air temperatures between December 27 and 29. Precipitation had persisted continuously since the rainfall on December 19. A gradual shift from precipitation as rain to snow suggests that snow temperature gradients were weak between December 22 and 27. Thus, the new snow may have formed storm or wind slabs that released during the warmer temperatures on December 27–29. An avalanche danger level of 3 was given in both Tromsø and Lyngen forecasting regions with storm slabs as the sole avalanche problem.

The coldest day of the year was on January 4 with around -15°C. On January 6, it was raining with an air temperature around 1°C, resulting in a temperature increase of 16°C over two days. Some avalanche activity was observed in SAR data in the period from January 3 to 5. After cooling to negative air temperatures, precipitation persisted

through January 9 until it stopped. In snow profiles on January 10 at Steinskarfjellet, temperature gradients between 2 and 3 °C/m were observed in 30 cm of graupels on top of MFpc with ECTN14-results within the graupels. ECTN19 was observed at the MFpc graupel interface. Similar temperature gradients were observed at Fagerfjellet on January 10, here only in ordinary precipitation particles, and with ECTX-results.

Between January 11 and 15, no more precipitation occurred. On January 15 and 16, the air temperature increased between 2°C and 5°C, which may have caused bonds to weaken in slabs from four days earlier, which eventually resulted in avalanche cycle 2. The avalanche danger remained at level 2 until intense snowfall on January 18 and 19 raised it to level 3 in both forecasting regions Tromsø and Lyngen.

6.1.1.2 *Avalanche cycle 3 (Feb 1–3)*

On January 17 at FFhi, the snowpack included 45 cm of refrozen rounded polycrystals (MFpc) in the lowest part. Above, the snow that fell after December 22 included both dry rounded crystals (RG), but also crusts of rounded polycrystals which had passed through a melt-freeze process. Facets were observed in conjunction with the crusts. At SShi on January 18 a similar structure was observed except that faceted crystals around crusts were not observed. Instead, graupels were observed both in snow from January 17 and 18, and in snow from late December.

The intense snowfall persisted until January 22, when a significant air temperature increase brougth the air temperature in all the study plots above 0°C through January 29 before cooling fast on January 30. As the precipitation persisted through the temperature decrease, more new snow fell around the turn of the month. The rain on January 29 turned decomposing and rounded particles into wet rounded polycrystals, and moistened the snow all the way down to the December 19 MFpc. Thus, there were no temperature gradients below the MFpc from January 25–29. New dry snow precipitating together with falling temperatures on January 31 mostly caused strong temperature gradients *above* the January 25–29 MFpc crust. Temperature gradients at FFhi were as high as 3.3°C/m in the uppermost part of the snowcover on January 31. ECT-results were between N22 and N29 at FFhi on January 31 and between N19 and N21 at SSlo on February 1 — all below 10–20 cm of refrozen MFpc after the January 25–29 rain. The avalanche danger was considered to be at level 1 on January 31 at Fagerfjellet and at level 2 on February 1 at Steinskarfjellet.

Avalanche cycle 3 occurred around a 3°C air temperature increase between February 1 and 3. Strong winds hindered me from reaching SShi on February 1. Rain and air temperatures oscillating above and below 0°C through January turned big portions of the snow cover to refrozen and stable crystals. Thus, with basis in the strong winds

observed at SShi February 1, fast formation and loading of wind slabs are considered being the reason for avalanche cycle 3.

6.1.1.3 *Avalanche cycle 4 (Feb 19–21)*

Between February 2 and February 11, the modeled snow depth showed compaction with no additional precipitation. Contradictory, snow depth measurements in snow pits at all the study plots except SShi were increasing. However, weather observations from both field and recreational trips showed clear skies and sun. The snow depth increase measured in the field Februray 7 and 8 was probably due to the snowfall that occurred on February 1. Surface hoar was observed at the snow surface at all the study plots except from SShi. Below the surface hoar, facets were developing due to strong temperature gradients. From observations in the field at Fagerfjellet on February 7 (ECTX) and Steinskarfjellet on February 8, the snow cover seemed stable. At SShi on February 8, a 40 cm thick, 400 kg/m^3 dense, K–hard, MFpc layer requiring effortful digging was in the top of the snowpack, and made me decide not do an ECT. On February 12, air temperatures increased approximately 6°C combined with strong winds from southwest, resulting in snow melting and additional water added to the snow cover (see Figure 6.3, page 83). While the snowpack had completely melted at FFlo on February 14, 10 cm of dry-to-moist rounded snow was observed at FFhi between the January 25–29 MFpc and on February 12 K-hard ice layer with temperature gradients above $2°C/m^3$. The air temperature increased from below 0 °C on February 14 to above 0 °C on February 15. At the Steinskarfjellet study plots, no temperature gradients were observed in the snowpack on February 15. The uppermost snow in the snowpack was moist, comprising moist-to-wet clustered rounded grains and had densities above 400 kg/m^3.

In the region, intense snowfall from polar lows and air temperatures close to -10°C occurred on February 20. Avalanche cycle 4 occurred on February 20 and 21, most likely due to formation of storm slabs and wind slabs from the intense snowfall produced by the polar lows. The avalanche bulletin (The Norwegian Water Resources and Energy Directorate, 2017) forecasted danger level 3 from February 18 to February 28 at all the study plots.

6.1.1.4 *Avalanche cycle 5 (Mar 21)*

New snow fell between February 17 and 26, while there was no precipitation between February 27 and March 9. Snow profiles from the period indicate clear skies, strong temperature gradients in a soft snow surface with foot penetration gradually decreasing from 48 cm to 27 cm. Surface hoar was observed at the snow surface on almost all field days. Negative air temperatures were observed in the entire

period with the second coldest day of the year being observed on February 22 with around -11°C. In the field, -10°C was observed at Fagerfjellet that day, when strong temperature gradients — 2.4°C/m in the upper 50 cm at FFhi — turned the rounded grains between the January 25–29 and February 12 crusts into facets. A similar facet layer was *not* observed at Steinskarfjellet; instead a weak interface within DF snow with graupels was considered to be the weak layer at a very snowy February 23 (S5). ECTs in the period displayed mostly X-results at SShi, and N-results between 14 and 24 together with a P16 result in the facets below the February 12 crust at FFhi.

Fluctuating air temperatures with steady precipitation describes the period between March 10 and March 25. The snow depth was gradually increasing, except from March 13–14, March 20–22 and March 25 when sleet and air temperatures around 0°C at high altitudes caused melting. Thus, the snowpack consisted of large amounts of precipitation and decomposed and fragmented particles at different degrees of bonding due to local wind effects. At FFhi on March 16, surface hoar was observed below decomposed and fragmented snow at 4F- hardness 50 cm into the snow cover. In two ECTs on March 16, only one ECT initiated a fracture at tap 23, while the other got an X-result.

On March 20, an air temperature increase of above 4°C occurred and significantly more avalanches were registered in the SAR-data, which has been classified as avalanche cycle 5. From the preliminary snow profiles, two possible scenarios for increased avalanche activity exist: As with avalanche cycle 1, 2, 3 and 4, wind creating and loading wind slabs that experienced decreased bonding due to the temperature increase on March 20 may have been the reason for avalanche cycle 5. The surface hoar observed on March 16 may also have been the most important weak layer, and hence the failing layer when increasing temperatures reduced bonding in the snow above on March 20. Wind slabs due to strong winds from south were the most important avalanche problems in the forecast in both Tromsø and Lyngen forecasting regions on March 20.

6.1.1.5 *Avalanche cycle 6 (Apr 9–10)*

A heavy snowfall occurred between March 26 and March 31 causing the deepest snowpack registration from xgeo during the winter. On March 28, a snow depth of 240 cm was registered in a snow pit and 215 at the stake at FFhi, and on March 29, a snow depth of 310 cm was registered in a snow pit at SShi. Both the low study plots had pit snow depths above 1 meter; SSlo had a similar reading on the stake while the canopy at the tree at FFlo gave a stake snow depth reading of 53 cm. At FFhi, a thin crust had formed on March 25 where a column at an ECT on March 28 initiated at tap 13 with 30 cm of 4F–1F hardness snow above. No similar thin crust was found at SShi on March 29.

Here, the main avalanche problem was F-hard precipitation particles 60 cm below F-to-1F progressively harder snow. A similar structure was also registered at SSlo the same day with ECT results of N16 and N19 at approximately 32 cm depth. On March 25, xgeo displayed positive 0.3°C at SShi and *warmer* at FFhi with 1.0°C. The new snow that fell between March 26 and 30 was graupels at both Steinskarfjellet and Fagerfjellet. On March 28, avalanche danger level 4 was forecasted in Lyngen forecasting region , while danger level 3 was forecasted in Tromsø forecasting region on March 29. The respective days and locations, danger level 3 was observed. There were mostly clear skies in the whole Troms county around March 31 to April 2, hence also most likely strong temperature gradients.

On April 2, the air temperature increased, culminating on April 3 and 4 with air temperatures above 0°C at all the study plots. Precipitation of rain occurred, resulting in snow melting. An air temperature decrease occurred on April 5, resulting in more snowfall. The rain on April 3 and 4 moistened the snow — also at the high altitude study plots — resulting in dry snow falling on moist snow on April 5 and 6. On April 5 and 6, ECTX was registered at both the high altitude study plots, while columns at FFlo and SSlo had a N21 and N19-result within MFpc layers, respectively. From April 5 until April 18, air temperatures stayed well below 0°C — around -6°C — and only small amounts of precipitation occurred. At FFhi on April 10, one ECTP27 result was obtained on a weak layer of rounding facets below what I believe was the March 25 crust 49 cm into the snowpack. Possibly strong temperature gradients around April 1 may have been the cause for allowing constructive metamorphism around the March 25 crust. In the period from April 2 to April 10, only danger level 2 was observed at all the study plots, while danger level 3 was forecasted at Fagerfjellet on April 5.

Avalanche cycle 6 occurred around April 9 and 10, simultaneously with an air temperature increasing from around -3°C to -1.5°C that was displayed in the xgeo temperature data. Since the avalanche activity data from Eckerstorfer did not distinguish different regions around Tromsø, they do not provide an answer if inland locations with Fagerfjellet as a representative experienced avalanche cycle 6 stronger than the coastal locations represented by Steinskarfjellet. Steinskarfjellet was not visited neither April 9 nor 10. However — the thin layer of rounding facets at FFhi could have been the important weak layer where well sintered and refrozen slabs from late March experienced weakened bonds due to the described temperature increase. Thus, avalanche cycle 6 may have been more intense at the inland locations. Both Tromsø and Lyngen forecasting regions had danger level 2 forecasted with wind slabs as the most important avalanche problem. Deep persistent weak layers were an avalanche problem only in the Lyngen

forecasting region, having low probabilities for avalanche propagation and requiring large additional loads to release.

6.1.1.6 *Avalanche cycle 7 (May 10–11)*

On April 18, a snowfall occurred at all the study plots, preventing a scheduled visit at SShi. Graupels were registered at SSlo that day, and strong temperature gradients — cold at 22 cm depth, warm at the snow surface — were registered. From April 18 to April 24, air temperatures above 0°C caused melting at low altitudes while high altitudes remained cold with dry snow surfaces. Clear skies dominated between April 18 and 24. A slight increase in snow depth occurred at SShi and FFhi on April 21. An avalanche danger level 2 was forecasted in both avalanche forecasting regions through the period. On April 24, a 7 cm thick layer of facets was observed 5 cm below the snow surface at FFhi combined with ECTX-results. On April 28, temperature gradients of up to 3.5 °C/m were observed at SShi with faceted crystals developed above MFpc crystals 30 cm below the surface, and with surface hoar on the snow surface. On April 29, air temperatures were above 0°C at the high altitude study plots, and on May 1, precipitation fell as snow. The high air temperatures probably caused a formation of a crust above the faceted crystals from April 28 at SShi. Thus, the new snow from May 1 sintered, and an ECTP21 and 17-result was obtained at SShi on May 3. The avalanche danger was forecasted to be level 3 on May 1 at Steinskarfjellet and Fagerfjellet and level 3 at Fagerfjellet on May 2. On May 4, the air temperatures increased even further, resulting in snow melting at all the study plots. On May 3, the avalanche danger was forecasted to be level 2, but level 3 was observed at SShi and level 1 at SSlo. An increase — but still less than a third of the least intense avalanche cycle — in avalanche activity was observed in the SAR data around May 1.

On May 4, the air temperatures dropped and new snow fell at all the study plots. Dry graupels above rounding facets were observed on May 8 at FFhi, and normal precipitation particles were observed on May 9 at SShi. Two ECTP-results (P23 and P26) were obtained on facets on a crust 40 cm below the snow surface at SShi on May 9. A snow surface temperature of -6.6°C was observed in the field where snow temperatures were at 0°C 10 cm below the surface. This may have been a measurement error, hence stronger temperature gradients further down may have caused constructive metamorphism above the crust where the ECT column propagated. The May 7 to May 9 precipitation also occurred under air temperatures around -5°C according to xgeo, hence stronger temperature gradients may have been present in the snow cover some days prior to May 10 and 11.

On May 10 and 11, the seventh and last avalanche cycle took place in the winter season 2016–2017. Strong snow temperature gradients allowing crystal growth around crusts at 0°C acting as energy barriers

between May 7 and 9 may have created a weak layer where slabs that experienced weakened bonding on May 9 could come loose on May 10.

END OF FIELD SEASON From interpolated air temperature data obtained from xgeo, May 2017 was the second coldest since 1957. Air temperatures was below 0°C between May 19 and May 31 causing precipitation as snow on May 29 and 30 at SShi, FFhi, and SSlo. On May 31, lightly moist decomposed and fragmented snow was registered at FFhi. The layer with facets developed on February 12 was still recognizable, but had turned into rounded polycrystals. When May, the field season of this project, and the avalanche forecast for the winter season 2016–2017 ended, interpolated snow depths at the high altitude locations were between 157 cm and 178 cm.

6.1.2 *Monthly rain events and weak layer position*

Figure 5.13 on page 58 shows that the weak layer seldom appears in the lower third of the snowpack. Precipitation at temperatures above 0°C — i. e. rain and sleet — occurred every month during the winter. Rain on snow first causes destructive metamorphism and reduced bonding between the snow crystals, before the snow pack can refreeze at lower temperatures. The strength of such a layer with MFpc crystals is lower in a wet state, but high in a frozen state where multiple *melt-freeze cycles* increase the strength of a layer with MFpc crystals (Fierz et al., 2009). Thus, the snow pack at all locations was stabilized by refreezing after rain every month through the snow season. The high strength of the refrozen MFpc crystals prevented weak layer formation any further down, which may explain the seldom occurrence of weak layer in the lower third of the snow pack. The weakest layer was registered in the bottom third, only at Steinskarfjellet. Depth hoar was observed prior to December 14 to 21 rain once, and facets were evolving at the top of the December 19 MFpc twice.

FFlo had the lowest average snow depth of all the study plots, hence was more susceptible to influence by air temperatures and precipitation. This is also displayed in the way that the location of the weakest layer is more distributed between the middle and the upper third of the snow pack, 57% and 42%, respectively. Every time the weakest layer was in the middle third, faceted grains were the cause, while loose wet was the most occurring avalanche problem in the upper third. The snow pack at FFlo completely melted after the February 12 rain event. Thus, the snow pack at FFlo did not have the effect of the refrozen, strong and dense MFpc layer preventing constructive metamorphism within the snowpack.

6.2 DIFFERENCES BETWEEN SITES

This section tries to answer the question of how Steinskarfjellet and Fagerfjellet differs from each other, and if this is correlated to their respective distance from open sea. When choosing study plots prior to the field period, one theory was that Fagerfjellet itself was closer to a large mass of water (Ramfjorden) and therefore would show more characteristics of a maritime snow climate and avalanche regime than Steinskarfjellet. If not, why is Fagerfjellet more inland? And furthermore, is Fagerfjellet representative for locations much further inland e. g. southern Lyngen Alps or the Tamok valley, close to the Swedish border?

6.2.1 *Study plot locality and local wind conditions*

Differences in topography on very small scales — e. g. less than 1 m to 100 m — affects if wind deposits or erodes snow at different wind directions (Mott, Schirmer, Bavay, Grünewald, & Lehning, 2010), and affects the amount of insolation in a pit. At SShi, all wind directions registered were either south or north, which is expected in the ravine at SShi. At larger scales, e. g. kilometer scale, surrounding mountains, valleys and fjords control wind directions (McClung & Schaerer, 2006). For example as noticed during the field work at SShi, storm-scale winds from southeast, east and northeast, all resulted in wind directions from the *south at* the SShi study plot. This might have been air masses pushed into Steinskarbotn, the cirque south of the study plot in Figure 4.2, using the SShi ravine as an escape route. An average snow stake depth at SShi 85% deeper than the modeled snow depth may support the impression that SShi was exposed to wind deposited snow. Compared to SShi, FFhi had a more wind exposed locality since Fagerfjellet has a convex face towards southwest and west. During the field work, wind directions on Fagerfjellet were often from the south, suggesting that wind was guided by Lavangsdalen, the valley leading south from Fagerfjellet.

Greater wind exposure at FFhi than SShi can be shown from the snow depth data in Figure 5.7, where FFhi in average had a 69% deeper snow depth at the stake than modeled compared to 85% for SShi.

Differences in a plot's susceptibility to snow eroding or depositing affect how fast precipitation particles decompose to rounded crystals and sinter after settling (McClung & Schaerer, 2006; Fierz et al., 2009). Figure 5.8a displays that while SShi had more precipitation particles, SShi had less than half the amount of decomposed and fragmented particles compared to FFhi (3.1% vs 7.8%) but had similar amounts of rounded grains (23.1% vs 24.1%, respectively). Along with impressions from the field, this suggests that precipitation particles decomposed to

rounded grains *faster* at SShi than at FFhi. Slightly more precipitation particles and graupels were also observed at SShi, suggesting that they had a higher tendency to deposit than erode, given similar snow amounts at the two locations.

The difference between FFlo and SSlo supports the argument that the relative amounts of PP, DF and RG represent wind conditions. FFlo was well sheltered compared to SSlo (Figure 4.3, page 32 and Figure 4.6 and page 36) and exhibited less RG and more DF and PP in profiles than SSlo. Thus, relative amounts of precipitation particles, decomposing and fragmented particles, and rounded grains may be more dependent on less-than-hundred-meter-scale wind conditions than distance to open sea.

6.2.2 *Graupels and distance to open sea*

The relative amount of graupels differed significantly between Steinskarfjellet and Fagerfjellet. Graupels are formed by riming on ice particles by supercooled water droplets at convective uplifts of cold fronts in the atmosphere (McClung & Schaerer, 2006) and typically precipitate downwind of relatively warm seas, e. g. the warm seas from the Norway Current. Air masses experience the fastest orographic lifting — hence the most intense precipitation — when they hit a mountain perpendicular to their direction of travel (McClung & Schaerer, 2006). Thus, cold fronts hitting Kvaløya from approximately north-west will give the most intense snowfalls. As Kvaløya is exposed to open sea in the north-west, more graupels can be expected here than further inland, which is reflected in the results.

Graupels are considered a weak layer in the snow pack due their bearing form that may cause a slab to «roll» on it. Graupels may also roll on surfaces where they do not bond to, i. e. crusts. According to Tremper (2008), graupels stabilize one or two days after deposition, hence they are *not* considered a persistent weak layer. Graupels were in the initiating or propagating layer in 5 of 18 (28%) ECTs at SShi compared to 1 of 18 (6%) at FFhi. Twenty-one ice layers were observed in the snowpack at FFhi compared to nine at SShi. At the surface, none were observed at SShi, while two were observed at FFhi. Thus, for the winter season 2016–2017, a possible higher avalanche danger due to more graupels at SShi seemed to have been canceled out by the minor presence of ice layers at the surface. Or, turned the other way around, the higher frequency of ice layers at Fagerfjellet seemed to increase the avalanche danger if graupels precipitated. For instance, in a situation of persisting polar lows, convective lifting of air masses above water masses may happen also in fjords further inland causing precipitation of graupels on potential ice covered inland mountains.

Graupels have a higher density than stellar and dendritic particles (Judson & Doesken, 2000). Thus, local wind conditions may subject

the new snow particle composition to sorting, i. e. removal of the low density particles, leaving graupels behind. This *winnowing effect* would in this case cause a higher relative fraction of graupels at the wind exposed FFhi and a lower relative fraction of of graupels at SShi. As this is *not* the case, I find it reasonable to argue that snow precipitation as graupels occur more often at Kvaløya than further inland. *This will support the argument of Fagerfjellet being less maritime than Steinskarfjellet*.

6.2.3 *Rainfall and ice layers*

More than twice as many ice layers were observed at FFhi than at SShi during the winter, 21 vs nine, respectively. Crusts are persistent *layers* that may alter the energy transfer in the snow pack or act as a bed layer for avalanches, thus acting as a weak *interface* (McClung & Schaerer, 2006). They are not considered as weak layers as the may distribute added weight of a skier or a snowfall over a large area, hence lowering the stresses on potential weak layers. Ice layers alter energy transport through the snow pack and may cause strong temperature and vapor pressure gradients favoring constructive metamorphism of snow crystals (Jamieson, 2006).

During the snow season, i. e. between November 26 and May 31, Fagerfjellet received nearly three times more rain (64 mm vs 23 mm). Also, Fagerfjellet had 150% more rainy days (15 vs 6) and 133% more occurrences of ice crusts (21 vs 9) during the winter season than Steinskarfjellet. Thus, one can argue that the number of rainy days favored ice crust formation in the snow pack at Fagerfjellet.

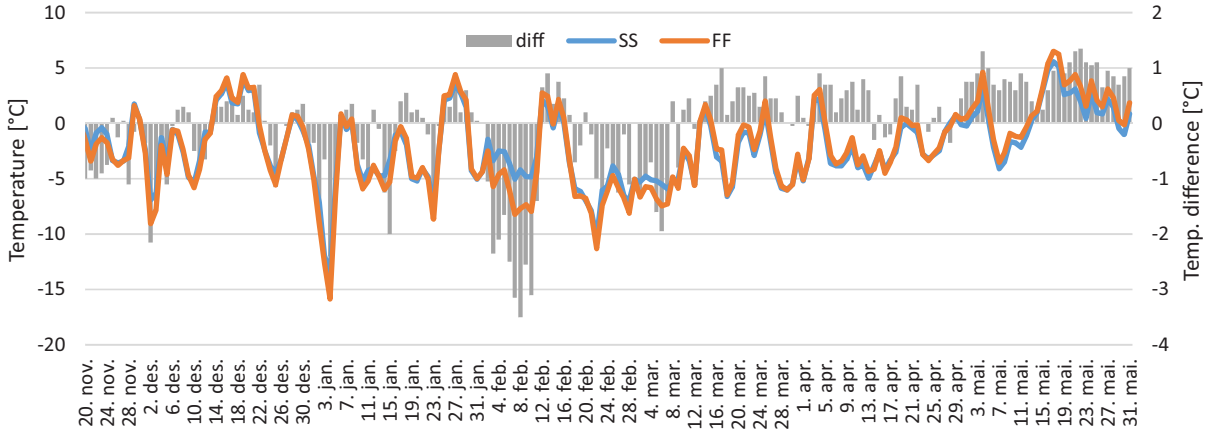

Figure 6.2: Air temperature differences between Steinskarfjellet (SS) and Fagerfjellet (FF). The bars represent the air temperature differences from SS's perspective.

The greater number of observations of faceted grains at Fagerefjellet may be explained by the greater number of ice layers found, hence also the greater number of days with rain. Persistent slabs as the main

avalanche problem — facets on crusts seven of nine times — were also observed more often at Fagerfjellet than at Steinskarfjellet. Figure 6.2 shows a larger air temperature span at FFhi than SShi resulting in *faster* air temperature changes. Thus, the larger air temperature span creates a positive feedback mechanism for facet creation in the snow cover by *increasing* the number of days with rain, hence *increasing* the number of ice crusts in the snowpack, resulting in *stronger* snow temperature gradients around crusts at large air temperature variations. This in turn, favors constructive metamorphism of crystals around crusts in the snowpack.

6.3 SNOW CLIMATE AND WINTER AVALANCHE REGIME

6.3.1 *Historical snow climate classification*

Table 6.1, page 82 shows snow climate classifications for the 60 winter seasons from 1957–1958 to 2016–2017. Table 6.2 shows a summary of Table 6.1 counting numbers of the different classifications and classification levels. The most apparent difference is between the low and high altitudes, where the low altitudes are classified maritime more than twice as often than its respective high altitude location. Warmer and wetter, or more maritime-like snow conditions at low altitudes rather than high altitudes are as expected from theory of lapse rates and will not be discussed any further.

Steinskarfjellet is classified maritime more often mostly due to higher average air temperatures (decision level 2) than Fagerfjellet (Table 6.3) . Overall, years with relatively lower mean air temperatures had *larger* temperature differences between the more inland Fagerfjellet and the more coastal Steinskarfjellet similar to the case example in Figure 6.3. This may show that mean average air temperatures are high in large portions of the Tromsø region during years with frequent high temperature storms from south-west and west. Contrasting, in years with fewer warm fronts, a west-east spatial air temperature gradient may be present between the border areas and the coastal areas resulting in larger differences between e. g. Steinskarfjellet and Fagerfjellet with their respective adjacent mountains.

Snow temperature gradients around the threshold of 10°C/m were the reason why most of the years Fagerfjellet was classified as continental in decision level 3 and Steinskarfjellet was not. These years seemed average with respect to air temperatures and snowfall. Thus, it may seem to be an oscillating air temperature gradient between the relatively high temperatures from the Norwegian Current in the ocean and relatively low temperatures from the continental plateaus in Sweden, Finland and Russia. Both Steinskarfjellet and Fagerfjellet are classified into the same snow climate class in years with particularly high or low air temperatures. In intermediate years, Steinskarfjellet

	SShi	FFhi	SSlo	FFlo
57/58	3	3	3	3
58/59	3	3	1	1
59/60	3	3	3	3
60/61	3	3	2	1
61/62	3	3	3	3
62/63	6	6	3	3
63/64	4	4	1	1
64/65	4	7	3	4
65/66	3	3	3	3
66/67	3	3	3	3
67/68	3	3	3	3
68/69	7	3	1	3
69/70	7	7	4	7
70/71	7	7	4	3
71/72	4	4	1	2
72/73	2	4	1	1
73/74	4	3	2	3
74/75	1	1	1	1
75/76	3	3	3	3
76/77	3	3	3	3
77/78	3	3	7	3
78/79	3	3	3	3
79/80	7	3	4	7
80/81	6	3	7	7
81/82	3	3	3	3
82/83	3	3	2	3
83/84	7	7	4	7
84/85	3	3	3	3
85/86	3	3	3	3
86/87	3	3	3	3
87/88	7	3	4	3
88/89	4	4	2	2
89/90	3	3	1	1
90/91	4	4	1	2
91/92	1	1	1	1
92/93	2	4	2	2
93/94	3	3	3	3
94/95	4	4	2	2
95/96	4	7	4	4
96/97	3	3	3	3
97/98	7	7	4	3
98/99	3	3	2	3
99/00	3	3	2	3
00/01	1	1	1	1
01/02	7	3	1	1
02/03	3	3	1	1
03/04	3	3	1	1
04/05	2	4	2	2
05/06	3	3	1	3
06/07	3	3	1	1
07/08	2	3	1	1
08/09	3	3	2	2
09/10	3	3	3	3
10/11	3	3	3	3
11/12	3	3	2	2
12/13	3	3	3	3
13/14	2	4	2	1
14/15	3	3	1	2
15/16	4	4	2	2
16/17	4	3	1	1
Average	3	3	3	3

Table 6.1: Historical snow climates. Numbers represent decision level in the classification table (Figure 2.2) classifying winters into maritime (dark shading), transitional (intermediate shading) and continental (light shading) climates. The average row is based on average meteorological data from 1957–2017.

	SShi	FFhi	SSlo	FFlo
Maritime	18	13	38	27
Tran	8	6	2	4
Cont	34	41	20	29
1	3	3	18	15
2	5	0	13	10
3	32	40	20	29
4	10	10	7	2
5	0	0	0	0
6	2	1	0	0
7	8	6	2	4

Table 6.2: Summary of Table 6.1. The green cells show the count of each snow climate. The red cells show the count of each decision level. The tint of the cells represent the value of its respective number, where a stronger color represents a higher value.

may be classified maritime in decision level 2 or transitional in decision level 7, while Fagerfjellet is classified continental in level 3.

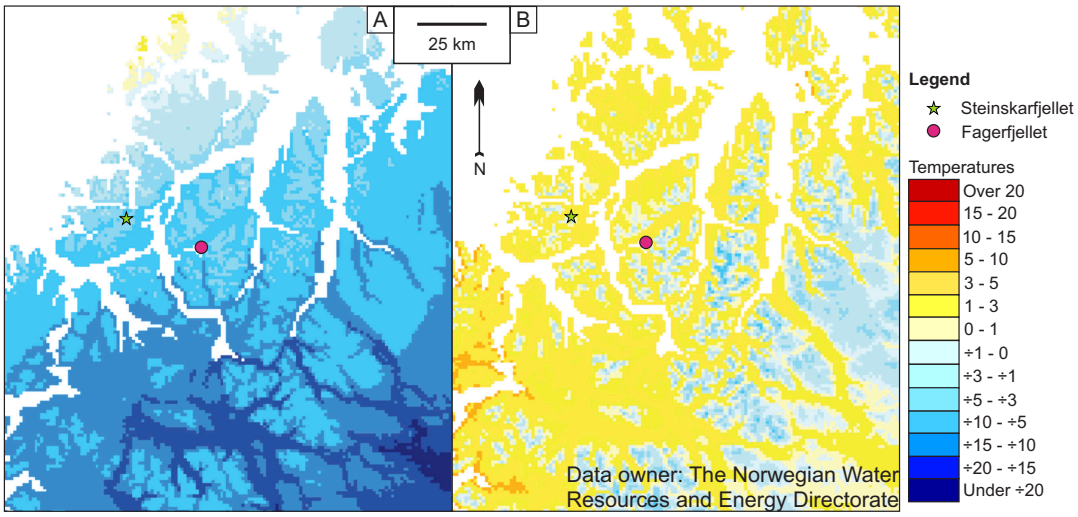

Figure 6.3: Case example of typical air temperatures during relatively cold (*A*) and warm (*B*) winter days in the Tromsø area. The maps are from www.xgeo.no. *A:* February 11, 2017. Cold, continental type weather. *B:* February 12, 2017. Warm, maritime type weather.

From average meteorological data in Table 6.3 , all study plots are classified as continental from decision level 3. Whether precipitation falls as snow or rain in the transition period between fall and winter is highly affecting December snow temperature gradients. Shallow snow depths favor strong snow temperature gradients. Simultaneously, shallow snow depths are highly susceptible to both constructive and destructive metamorphism, making e. g. rain events after snowfall essential information of the general winter avalanche regime. Rain and melting after first snowfall were key events for the 2016–2017 snow season in different ways; it destroyed early-season facets at the bottom of the snowpack, and it made ice layers acting as energy barriers in the

snowpack favoring constructive metamorphism. The reason for faceted crystals being observed more often at Fagerfjellet in the 2016–2017 season was not a cold December with little precipitation; it was highly oscillating air temperatures creating crusts and ice layers were facets could grow. Despite being more prone to strong snow temperature gradients, Fagerfjellet was closer to a maritime classification from decision level 1 with more precipitation as rain during the 2016–2017 winter season. This supports the argument of Hägeli and McClung (2007) that the existing snow climate classes have limits in capturing important weather events important for the snow stability.

Table 6.3: Mean meteorological data from the 60 winter seasons 1957–1958 to 2016–2017 at the study plots.

Location	*Rain [mm]*	*Temperature [°C]*	*December TG [°C/m]*	*New snow density [kg/m^3]*	*Snowfall [cm]*
SShi	28	-5.1	14	99	347
FFhi	25	-5.8	19	95	311
SSlo	61	-3.6	38	107	299
FFlo	54	-4.4	49	101	268

6.3.2 *The winter season 2016–2017: persistent weak layers in a maritime snow climate*

6.3.2.1 *Snow climate*

Mock and Birkeland (2000) utilize December–March as months for his snow climate flow chart shown in Figure 2.2, page 8. The *sum* of values are used in step 1 and 5, resulting in a bias towards these steps if number of compared months were increased. Thus, even if the snow season 2016–2017 in Tromsø lasted from mid-November to late June, data in from December through March is used in this subsection unless otherwise written.

Comparing rain data from the study plots reveal that SShi experienced 18.8 mm rain, FFhi 45.8 mm, SSlo 161.3 and FFlo 135.3 mm rain. Thus, both the low study plots had above 80 mm of rain and will be classified as having a maritime snow climate. The high altitude study plots received less rain and will therefore move to the mean air temperature test in the flow chart.

Average air temperatures for the study plots were -3.7°C at SShi, -4.0°C at FFhi, -2.2°C at SSlo and -2.6°C at Fflo. The low altitude study plots are already placed in a maritime snow climate class due to the rain data, but are included to shed a light over the differences. Both the

high altitude study plots had lower mean air temperatures than -3.5°C, but only by 0.2°C and 0.5°C. From the comparison of interpolated and weather station measured air temperatures in Section 3.2.1, the mean measured air temperature was 0.2°C lower than the mean interpolated air temperature. Nevertheless, the interpolated temperature may be obtained from a location close to the border in 1-x-1 km route in xgeo introducing an error that may be above 0.2°C. Thus, both SShi and FFhi are not classified into a maritime snow climate in step 2 in the flow chart. But, they could have been both above or below -3.5°C since they both were near the threshold value. Step 6 in the flow chart asks if the mean air temperature is below -7°C, hence does not apply to any of the study plots.

December air temperature gradients were 8.7°C/m at SShi, 11.9°C/m at FFhi, 12.6°C/m at SSlo and 21.4°C/m at FFlo. Thus, at FFhi, SSlo and FFlo the temperature gradients were strong enough to fall into a continental snow climate according to Mock and Birkeland's flow chart. Armstrong and Armstrong (1987) and Mock and Birkeland (2000) classified snow covers as continental if the December snow temperature gradients were stronger than 10°C/m, as depth hoar is growing under such conditions. But, heavy rainfalls will destroy depth hoar unless they are hidden under thick and solid, hence stabilizing ice layers in the snow pack. Thus, in a given snow pack that experienced strong temperature gradients in December information of possible subsequent rainfalls are important, as they may tell if the depth hoar still existed or not. This was the situation for the winter season 2016–2017; a heavy rainfall between December 14 and 21.

The mean new snow densities at the different study plots were all above 100 kg/m^3 with 109, 105, 114 and 109 at SShi, FFhi, SSlo and FFlo, respectively. Thus, all the study plots fall into a maritime snow climate. From Equation 3.1, page 26, new snow density is calculated from air temperatures, where higher air temperatures give higher new snow densities at temperatures above -18°C. Thus, the study plots would still be classified as maritime if the actual air temperatures were 0.2°C higher.

The total snowfall recorded was below the threshold value of 560 cm from Mock and Birkeland at all the study plots. The total snowfall at the different study plots were 501 cm, 470 cm, 329 cm and 315 cm at SShi, FFhi, SSlo and FFlo respectively. Thus, step 5 in the flow chart did not discriminate any of the study plots.

Summarized, both the low altitude study plots end up in a maritime snow climate. They experienced more than 8 cm of rain during December to March, and was discriminated in step 1 in Figure 2.2. SShi also ended up with a maritime snow climate since it displayed a mean new snow density above 100 kg/m^3 in step 4. FFhi had a December temperature gradient above 10°C/m and ended up with a continental snow climate. Step 2, 4 and 6 are all based on mean values. Since the

actual winter season lasted from November 26 until late June, many days of average values affecting the snow cover were not included when using the flow chart. Calculating mean air temperature values between November 1 and May 31 changed the outcome of the snow climate classification, with both SShi and FFhi experiencing a mean air temperature of -3°C. Average measured air temperatures from field days between December 1 and March 31 were -2.5°C and -3.9°C at SShi and FFhi, respectively. Still, the mean air temperatures in the whole area were close to the step 1 maritime snow climate threshold value of -3.5°C, making an argument for classifying all study plots in the maritime class reasonable.

6.3.2.2 *Winter avalanche regime*[1]

According to Figure 5.12, page 57, wet slabs were the avalanche problem that could differ Fagerfjellet from Steinskarfjellet. Wet slabs may occur when liquid water either from snow melts or rain percolates through the snow meeting an impermeable layer, such as an ice layer. The liquid water lubricates and lowers the friction on the ice bed layer, allowing a slab of the moistened snow to glide at once (McClung & Schaerer, 2006). The risk for wet slab avalanches is greater when a *dry* slab of rounded grains gets moistened for the first time than when a slab of rounded polycrystals that have been through a melt-freeze process gets moistened (The Norwegian Water Resources and Energy Directorate, n.d.). From Figure 6.2, one can see that the air temperature at Fagerfjellet varied *faster* and *more* than at Steinskarfjellet, suggesting that the snow cover at Fagerfjellet may experience rain on dry snow more often.

On the other hand, wet slabs do not *characterize* Fagerfjellet. Persistent slabs were the most occurring avalanche problem both at SShi, FFhi and FFlo, also despite the early season rain. Almost all the persistent weak layers considered as the main avalanche problem occurred in conjunction to ice crusts. Thus, Fagerfjellet should be more susceptible to snow crystal growth within the snowpack than Steinskarfjellet and can be characterized as «more» continental. Still, both locations are characterized with faceted crystals near crusts.

The early season rain was an important weather event for the snow season 2016–2017, as it prevented depth hoar to persist in the snow pack. Monthly rain events also stabilized the snowpack throughout the winter. Without the December 14 to 21 rain event — e. g. around 2°C lower air temperature — depth hoar could have been a defining characteristic weak layer for this snow season.

1 Hägeli and McClung, 2007.

6.3.2.3 *Snow climate and winter avalanche regime summary*

As altitudes above the treeline of approximately 400 m a.s.l. are regularly visited by mountain recreationists, the high altitude study plots are used for placing Steinskarfjellet and Fagerfjellet in winter avalanche regimes. Consequently, Steinskarfjellet in the winter season 2016–2017 exhibited a maritime snow climate and Fagerfjellet exhibited a continental snow climate. At the same time, both plots exhibited similar snow structures with persistent weak layers adjacent to crusts and melt-freeze layers. Hägeli and McClung (2007) separated his classes by number of persistent weaknesses and dominant persistent weak layers and named them after after their respective mountain area name: the Whistler area with several pure crust interfaces, the Central Selkirk Mountains with one facet–crust weak layer and several surface hoar weak layers, and the Columbia Icefield with one weak layer of potential depth hoar. Both Steinskarfjellet and Fagerfjellet in 2016-2017 *displayed similarities* to the more maritime characterized winter season of 1996–1997 in the Central Selkirks with a facet–crust combination as an active avalanche problem. Steinskarfjellet and Fagerfjellet *differed* from the Central Selkirks when it came to surface hoar. Thus, the winter avalanche regime in the Tromsø area for the winter season 2016–2017 seemed to fall between the maritime like Whistler area regime and transitional like Central Selkirk mountains regime from Hägeli and McClung (2007). By using regional names for the winter regimes, Hägeli and McClung acknowledge the large variations the exist at all scales of winter mountain climate. As classifying snow climates into abstract classes encompassing all possible variations *will miss important details*, a relative comparison setting typical regional or local snow cover properties in a context might be as relevant.

6.4 INTERNATIONAL CONTEXT

A greater amount of rain is associated with a more maritime snow climate. With respect to that, Fagerfjellet and adjacent mountains would have a more maritime snow climate than Steinskarfjellet. But, LaChapelle (1966), Armstrong and Armstrong (1987), Mock and Birkeland (2000), McClung and Schaerer (2006), Hägeli and McClung (2007) emphasized that avalanches in maritime climates usually take place *during* or *immediately after* snow fall events. Non-persistent weaknesses are the cause for snow avalanches in maritime snow climates. Contrary, *persistent weak layers* are often the cause for snow avalanches in continental snow climates. Since Fagerfjellet *more often* had persistent slabs as an avalanche problem, it can be argued that *Fagerfjellet was* more *inland with* more *continental characteristics*.

Ikeda et al. (2009) did a study of the snow climate in the Japanese Alps where they identified a new snow climate class named a «rainy continental snow climate» at one of their study plots. Such a snow

pack climate was characterized by a thin snowpack experiencing 75 mm of rainfall between December and March with an average air temperature of -6.6°C and a temperature gradient of 16.1°C/m. Both Steinskarfjellet and Fagerfjellet are similar when it comes to mean air temperature and December snow temperature gradient (Table 6.3), but has significantly less rain and also less snowfall.

Eckerstorfer and Christiansen (2011) conducted a 2-year investigation on snowpack characteristics for central part of Svalbard, where they found that despite its Arctic localization, Svalbard experience warm temperatures through large temperature fluctuations from ocean currents and storms arriving from the south. As a consequence of this, Eckerstorfer and Christiansen (2011, p. 20) identified a *High Arctic maritime snowpack* that is characterized by: "...a relatively thin and cold snowpack with a persistent structural weakness caused by depth hoar, as well as a significant amount of ice layering due to the overall meteorological maritime influence during the entire snow season."

According to LaChapelle (1966), Armstrong and Armstrong (1987), Mock and Birkeland (2000), rain is rare or extremely rare in the transitional and continental snow climates. Even in a «coastal transition zone» , defined by LaChapelle (1966, p. 354), "[w]inter rain is much rarer than in the coastal mountains". Thus, the snow climate in the Tromsø area fits better with the classes from Ikeda et al. and Eckerstorfer and Christiansen describing continental climates with strong maritime characters. Nevertheless, if imagining a transitional snow climate as either a maritime or continental snow climate with characteristics of the opposite climate as features in the original (Figure 2.4, page 13), Tromsø could have a transitional climate.

An ARCTIC TRANSITIONAL snow climate is therefore suggested as a term for describing the typical snow pack in the Tromsø area. *Transitional* describes a process changing from one state to another, which strictly speaking accounts for all processes in a snowpack. However, due the fact that the Tromsø area lies between the relatively warm ocean in the west and a relatively cold plateau in the east, *transitional* describes the conflicting property of the two weather processes affecting the snow cover reasonably accurate. The *Arctic* can be defined as the region north of the Arctic Circle which is where the polar night and midnight sun cause large annual variations in insolation (Grønnestad, 2016). During the polar night in Tromsø lasting from November 21 to January 21, there is no insolation. Insolation one month prior and after the polar night is low and only on south facing mountains. This allows strong snow temperature gradients during clear and cold days and nights at all aspects in significant time of the winter, favoring facet growth in the snow cover. Thus, the low-insolation *Arctic* component is important for the energy influencing the snow cover. *Arctic* describes a snowpack without insolation, hence with strong temperature gradients. *Transitional* describes a snowpack

situated in between a high temperature ocean and a low temperature arctic plateau.

6.4.1 *Persistent weak layers in an Arctic transitional snow climate.*

Weak layer observations from this thesis are shown in an updated Table 6.4 (prior, Table 2.2, page page 10), forming the idea that *all* weak layers can occur in *all* meteorological data based snow climates. Thus, the idea of Hägeli and McClung (2007) that an understanding of the processes behind the potential weak layers aids the division of different avalanche danger in an area. That is also why I got at length discussing the seasonal development of the snowpack and its producing weather conditions in Section 6.1 in the discussion. This thesis has made a modest suggestion on how mean air temperatures vary spatially in especially warm and especially cold winters in the Tromsø area exemplified in Figure 6.3. This rises the question of the controlling forces for winter season storm scale wind directions around Tromsø. A winter with frequent storms from ocean areas will probably lead to a winter with spatially homogenous air temperatures and many rain events that cause extensive ice crust formation in continental areas where facets may grow at strong air temperature gradients. A calmer winter with less rain will cause a stronger influence by cold air temperatures from continental Sweden, Finland and Russia which allows depth hoar to be present, especially further away from the coast. In this way, synoptic scale weather or ocean scale circulation observations prior to a winter season may say something about resulting weak layers months ahead (Birkeland, Mock, & Shinker, 2001; Keylock, 2003; Castebrunet et al., 2012; McClung, 2013).

Scaling down from synoptic weather systems and ocean circulation, Tromsø based winter mountain recreationists still face their everyday choices. Whether to go east or west from the city, north or south from the road, the sunny or shady slope, climb steep or walk the gentle way around are the questions we ask ourselves hoping to meet our expectations for a trip. From this thesis, it may seem that going west towards the ocean is the safer choice for snow recreation in Tromsø — at least for the 2016–2017 winter season. Still, probably the most important question to ask yourself for the crossroads you will meet is: *what do you want to experience*?

Table 6.4: An updated compilation of snow climate weak layers including those found in this thesis. The weak layers mentioned are active unless *inactive* is stated.

	Weak layer characteristics		
Author	*Maritime*	*Transitional*	*Continental*
LaChapelle (1966)	CR	—	DH
Armstrong and Armstrong (1987)	—	—	DH, SH
Mock and Birkeland (2000)	—	—	DH
Hägeli and McClung (2003)	—	FC/CR and SH	DH
Hägeli and McClung (2007)	FC, CR, inactive SH	FC, SH, inactive CR	FC (DH)
Eckerstorfer and Christiansen (2011)	—	—	FC, DH
Velsand (2017): this thesis	FC/CR	FC/CR, FC, SH	FC/CR, FC, SH, DH

CR = pure crusts, FC = faceted grains, FC/CR = facet-crust combinations, SH = surface hoar, and DH = depth hoar. ( ) = potentially.

7 CONCLUSIONS

- Heavy rainfall early in the snow season was a significant weather event for the winter season 2016–2017 in the Tromsø area. The rainfall destroyed growing facets and depth hoar in the snow cover, leaving a solid and dense base of frozen rounded poly-crystals.
- A coast proximate (c. 20 km away from open sea) and more coast distal (c. 45 km away from open sea) study plot, respectively Steinskarfjellet and Fagerfjellet experienced a relatively warm winter with small differences in air temperature in 2016–2017. The air temperatures at Fagerfjellet varied within a greater air temperature span, allowing *more* rainy days favoring a greater amount of crusts.
- Contradictory to classical snow climate classifications, more rain increased the frequency of persistent weak snow crystals around crusts at the more inland Fagerfjellet, indicating that processes leading to persistent weak layers can occur in all snow climates.
- From historical weather and snow data from xgeo, relatively warm winters seemed to display comparable air temperatures at Steinskarfjellet and Fagerfjellet, while the air temperatures seemed to diverge more during relatively colder winters.
- *Arctic transitional* is suggested as a term describing the snow climate and winter avalanche regime around Tromsø. Months with low insolation both before and after the month-long polar night combined with the conflicting forces of a relatively warm ocean in the west and relatively cold continental areas in the east are represented in the term.

A

APPENDIX

A.1 STEINSKARFJELLET HIGH SNOW PROFILES

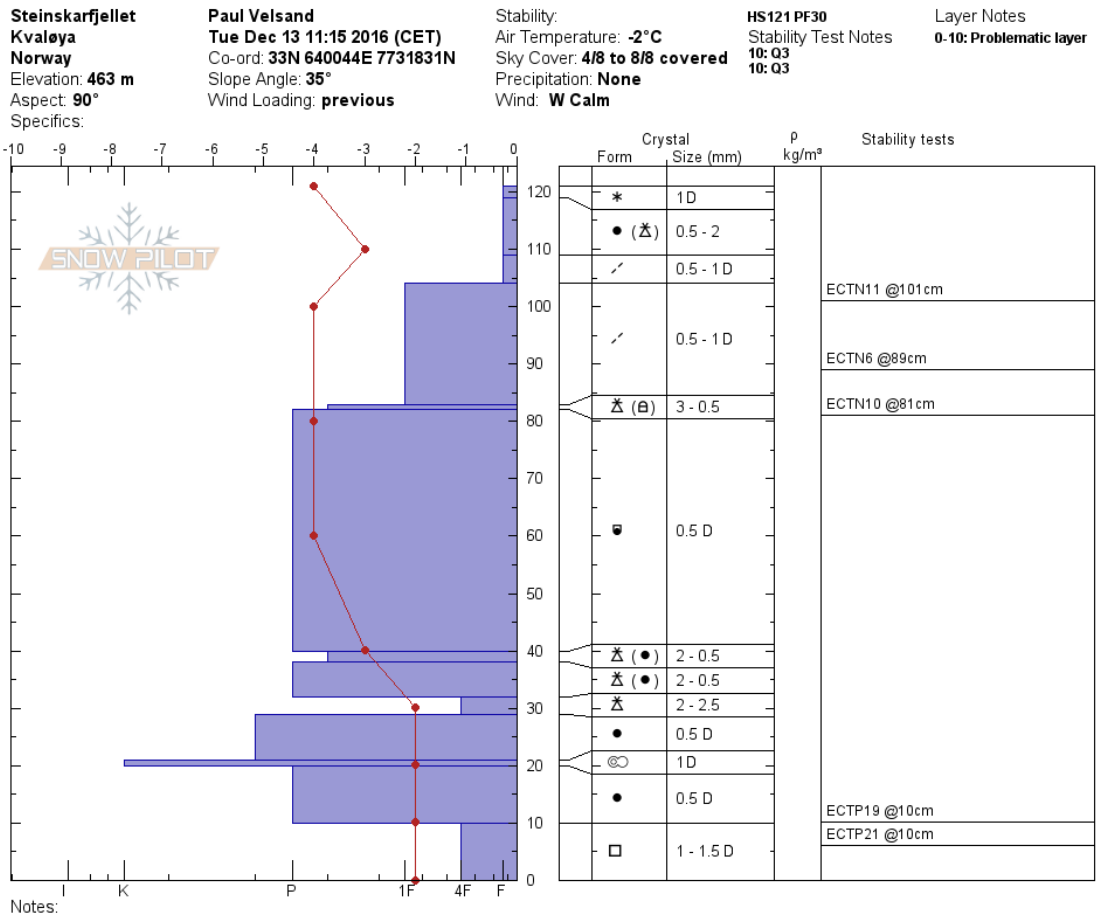

Figure A.1: Snowprofile from Steinskarfjellet high, December 13 2016.

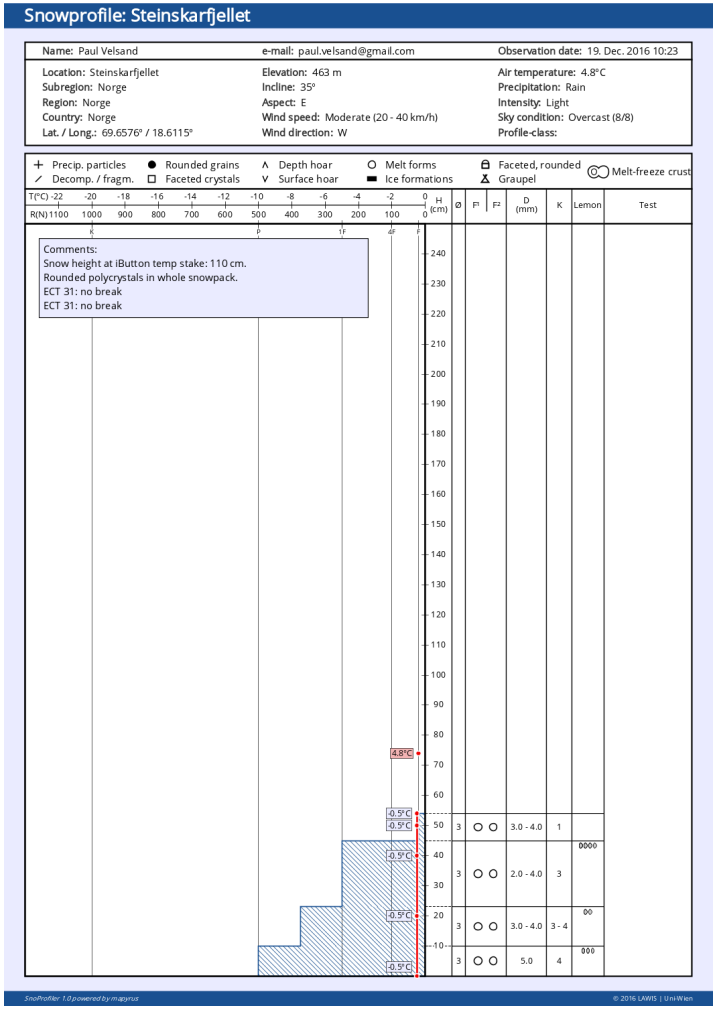

(a) December 19, 2016.

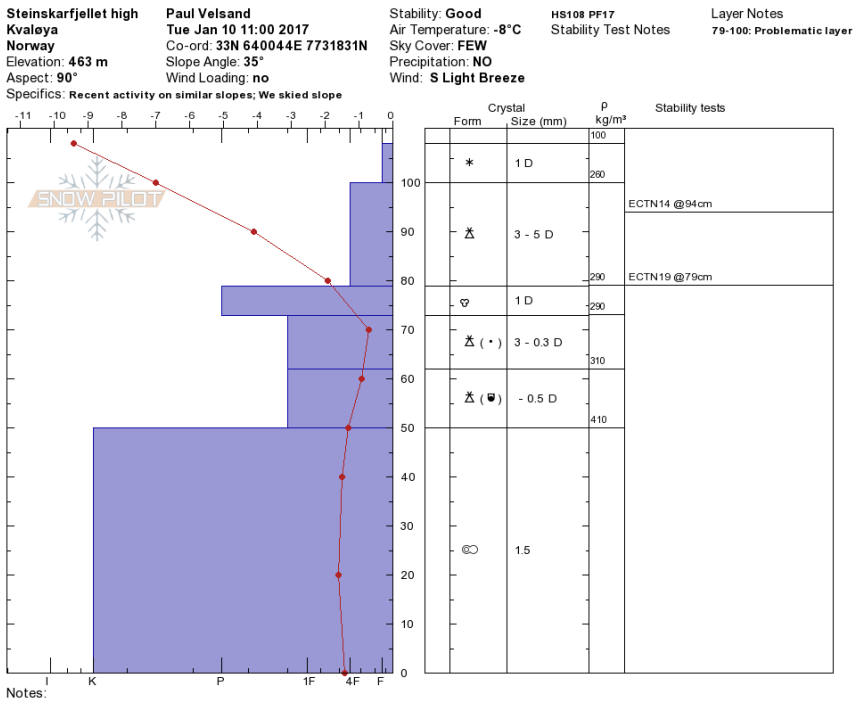

(b) January 10, 2017.

Figure A.2: Snow profiles SShi, December 2016 and January 2017.

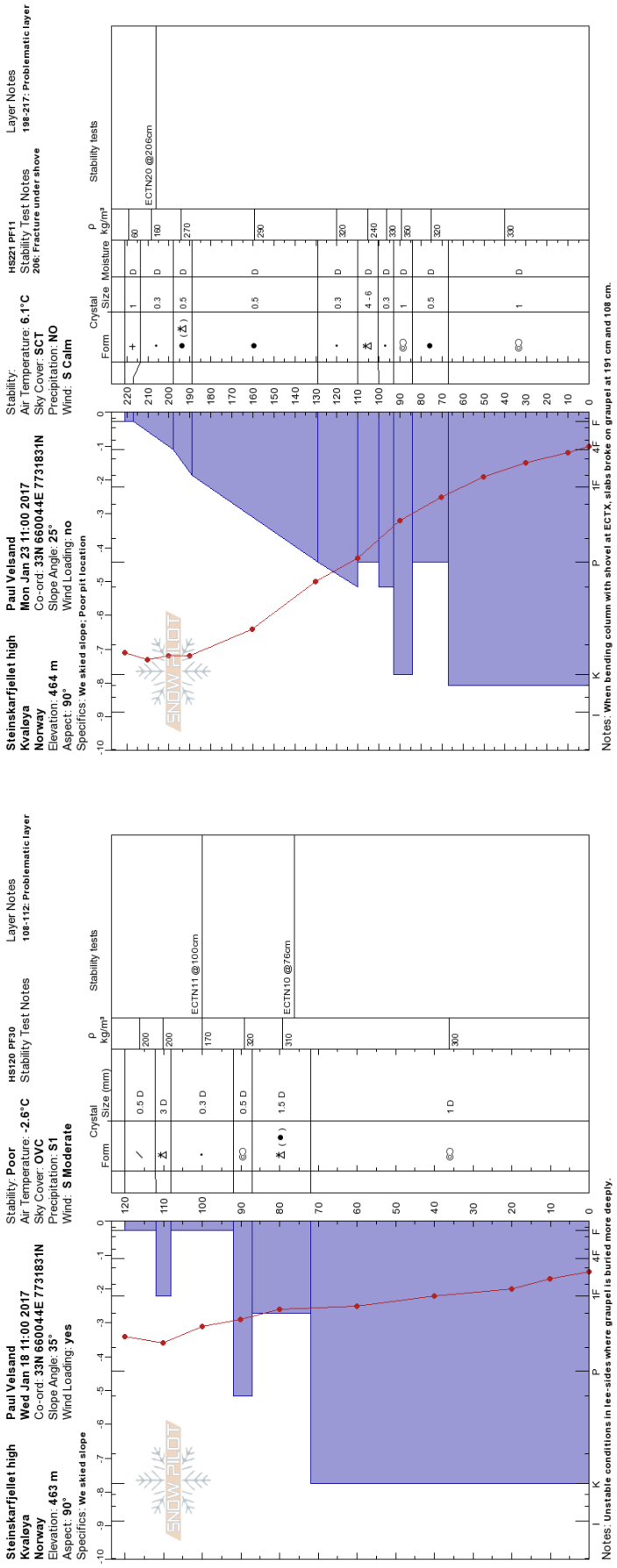

(a) January 18, 2017.

(b) January 23, 2017.

Figure A.3: Snow profiles SShi, January 2017.

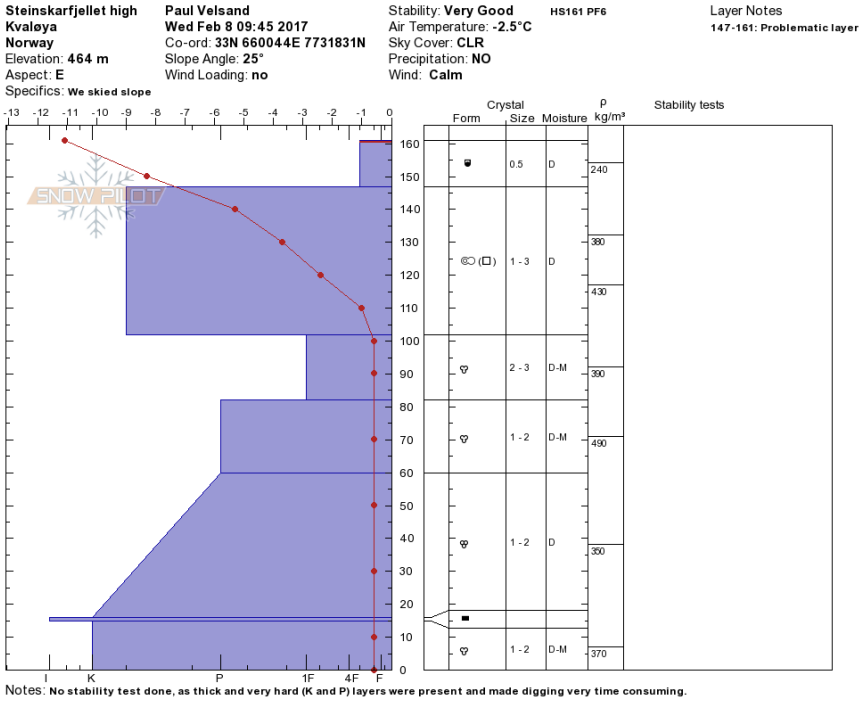

(a) February 8, 2017.

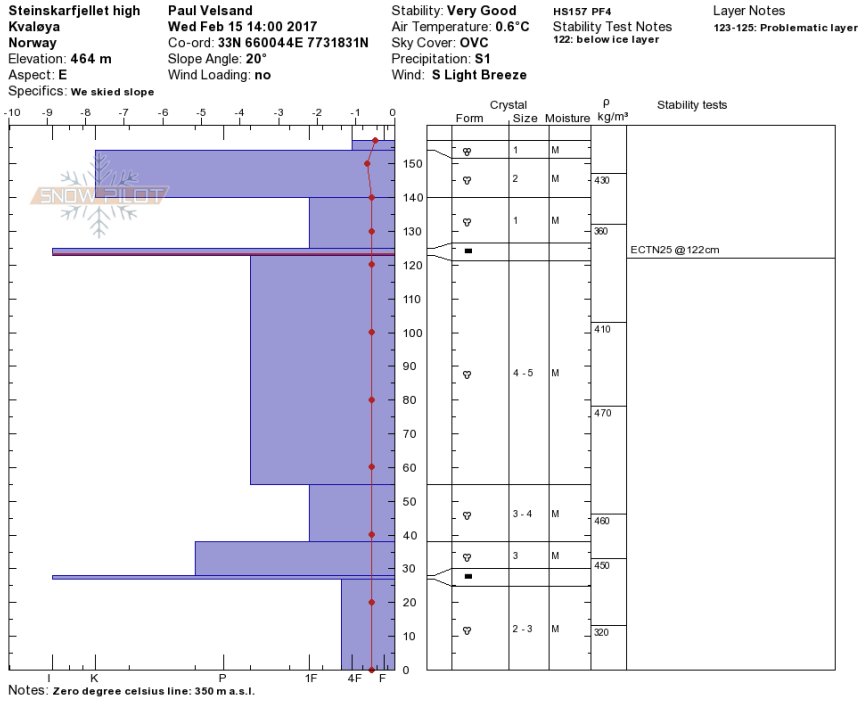

(b) February 15, 2017.

Figure A.4: Snow profiles SShi, February 2017.

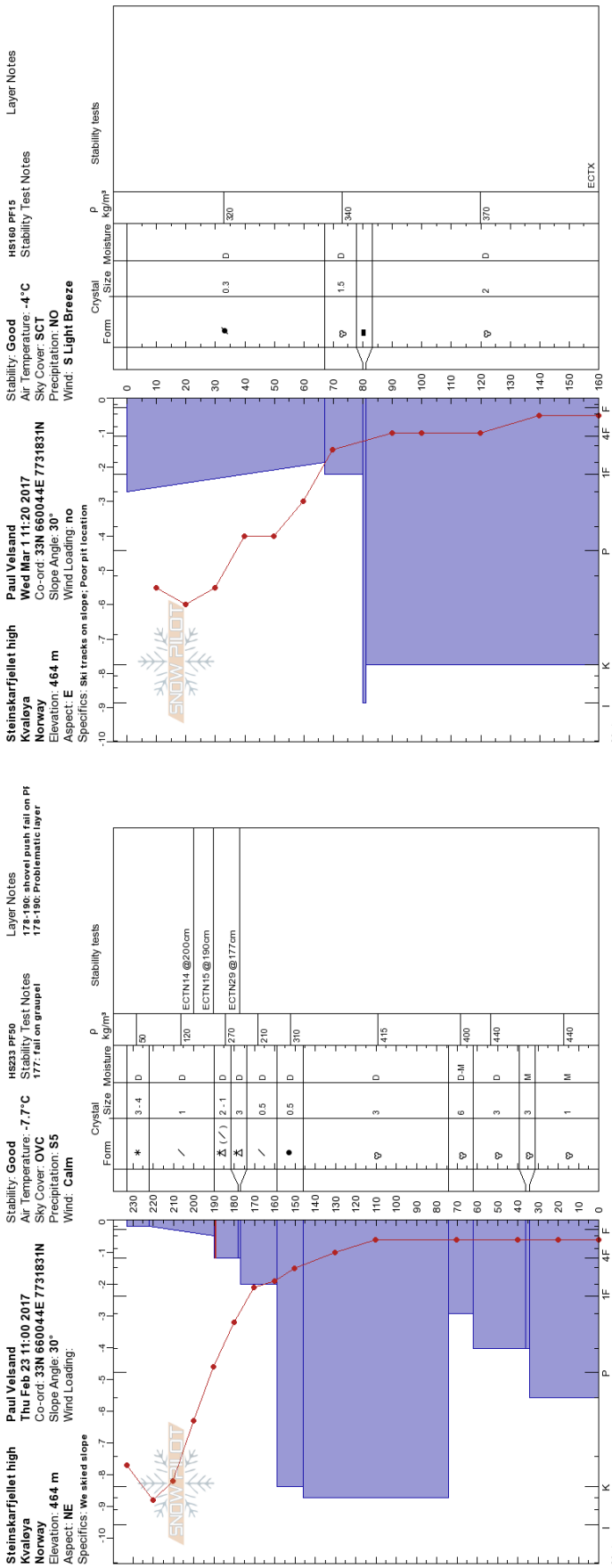

(a) February 23, 2017.

(b) March 1, 2017.

Figure A.5: Snow profiles SShi, February and March 2017.

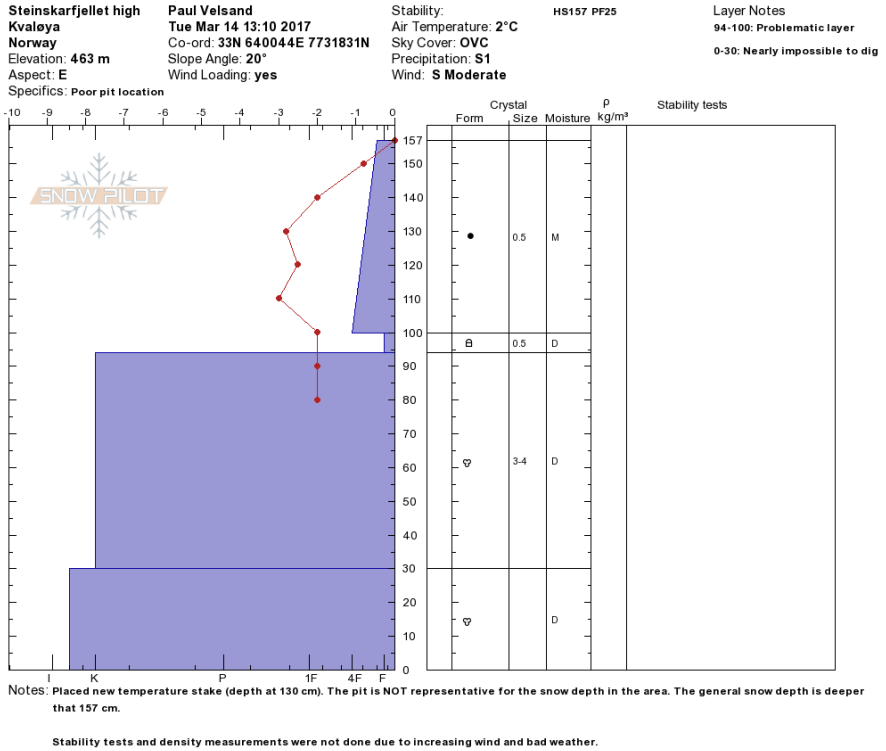

(a) March 13, 2017.

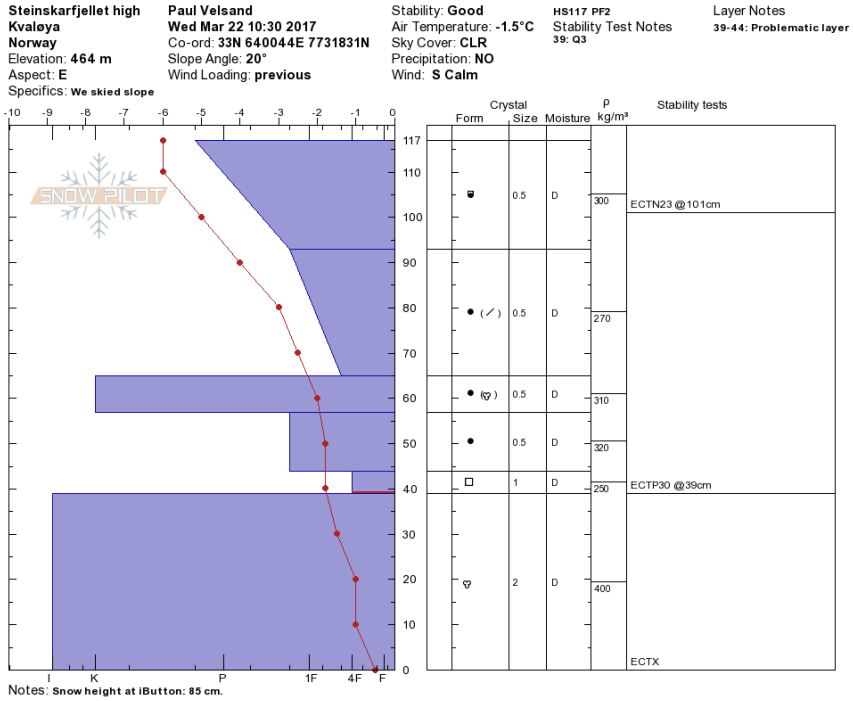

(b) March 22, 2017.

Figure A.6: Snow profiles SShi, March 2017.

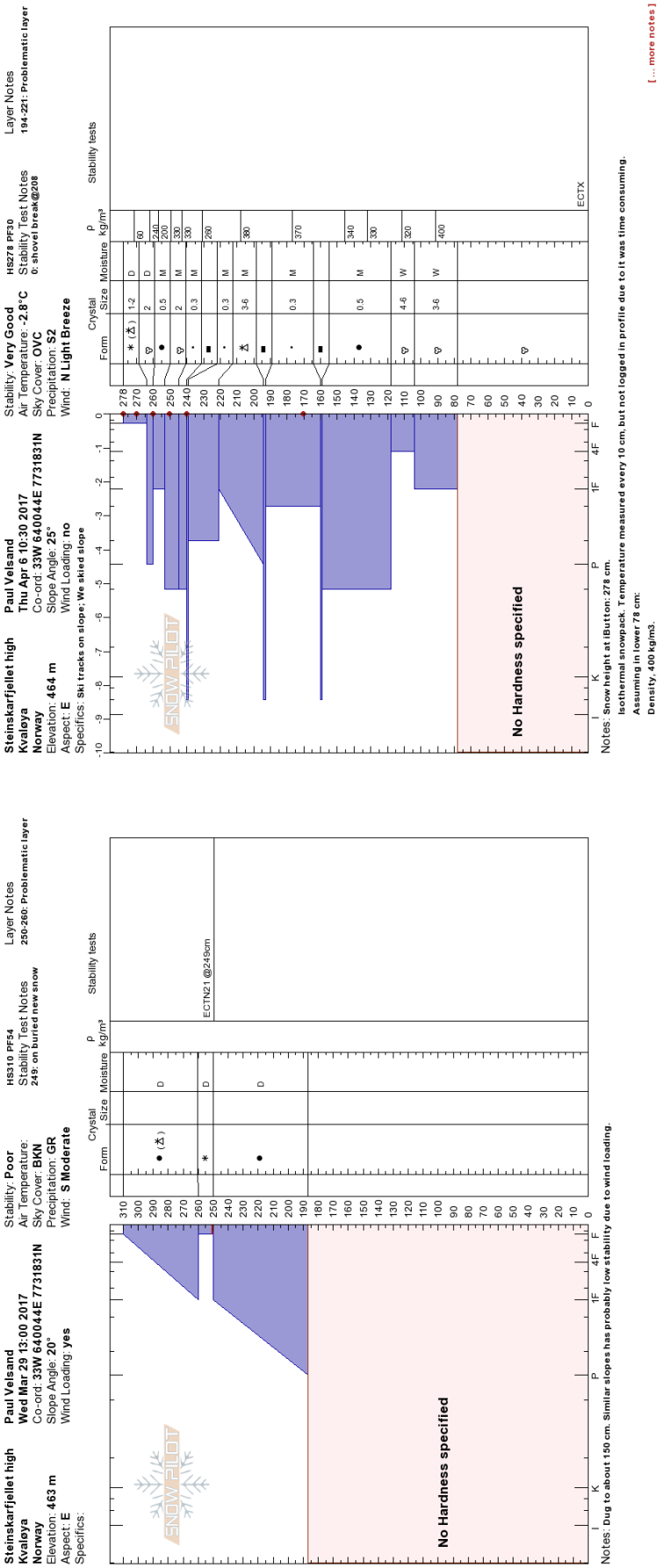

(a) March 29, 2017.

(b) April 06, 2017.

Figure A.7: Snow profiles SShi, March and April 2017.

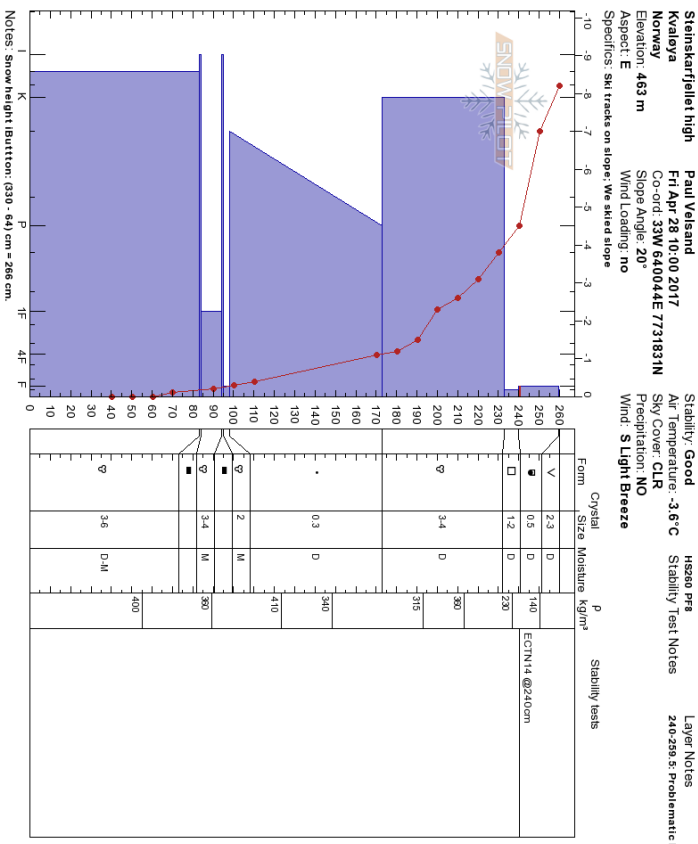

(a) April 29, 2017.

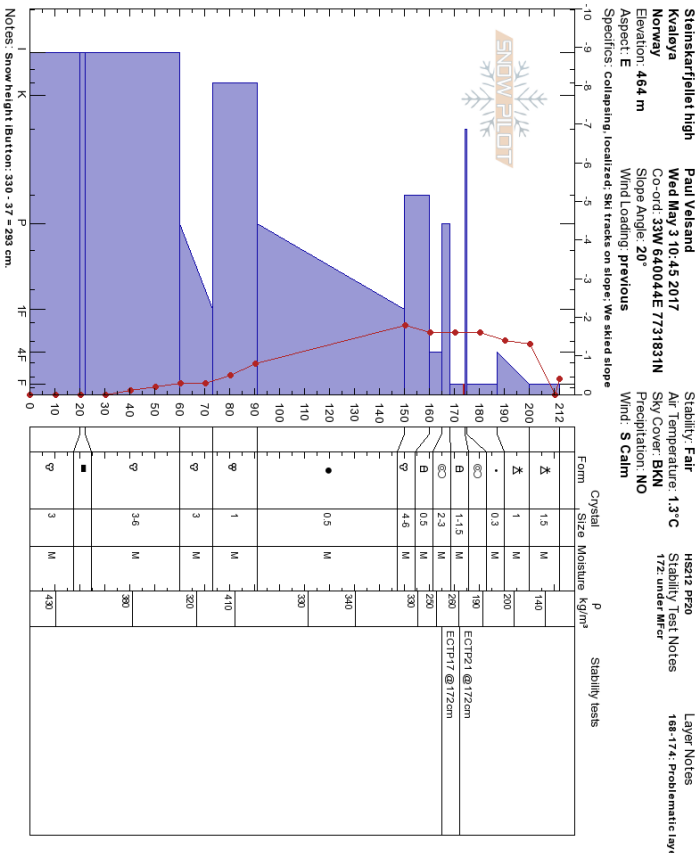

(b) May 3, 2017.

Figure A.8: Snow profiles SShi, April and May 2017.

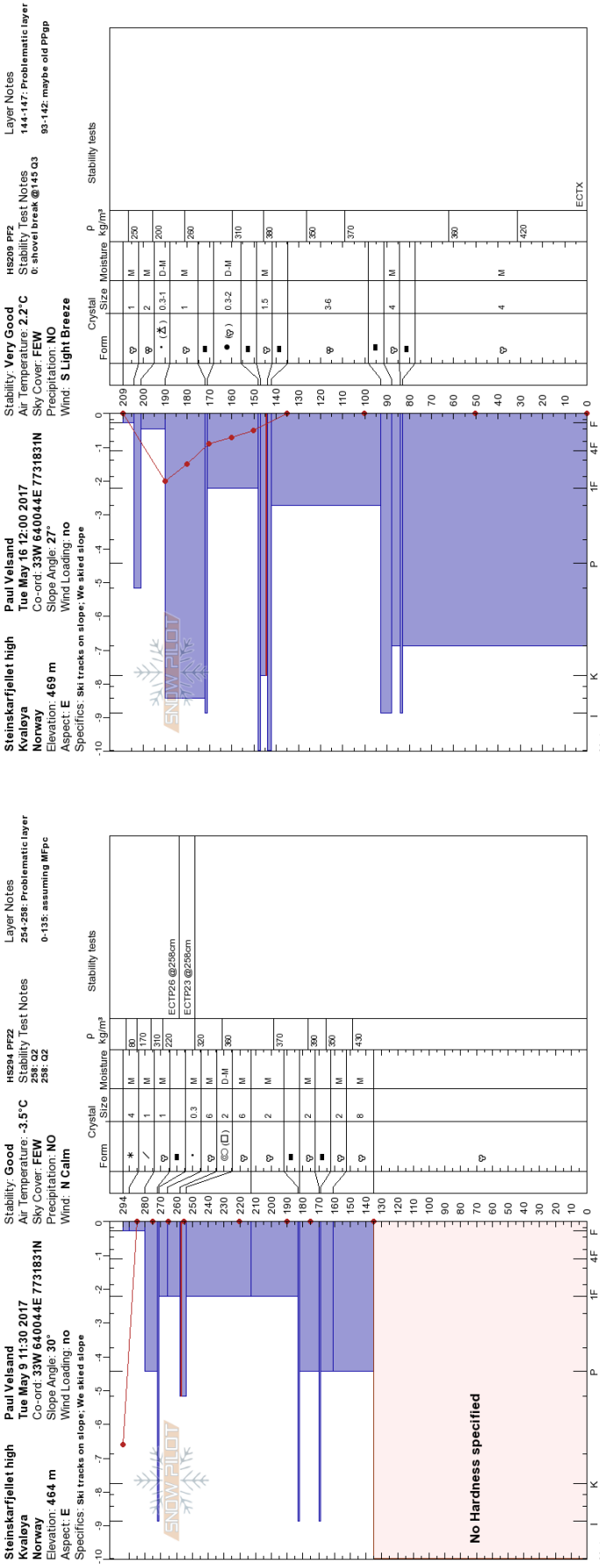

(a) May 9, 2017.

(b) May 16, 2017.

Figure A.9: Snow profiles SShi, May 2017.

A.2 STEINSKARFJELLET LOW SNOW PROFILES

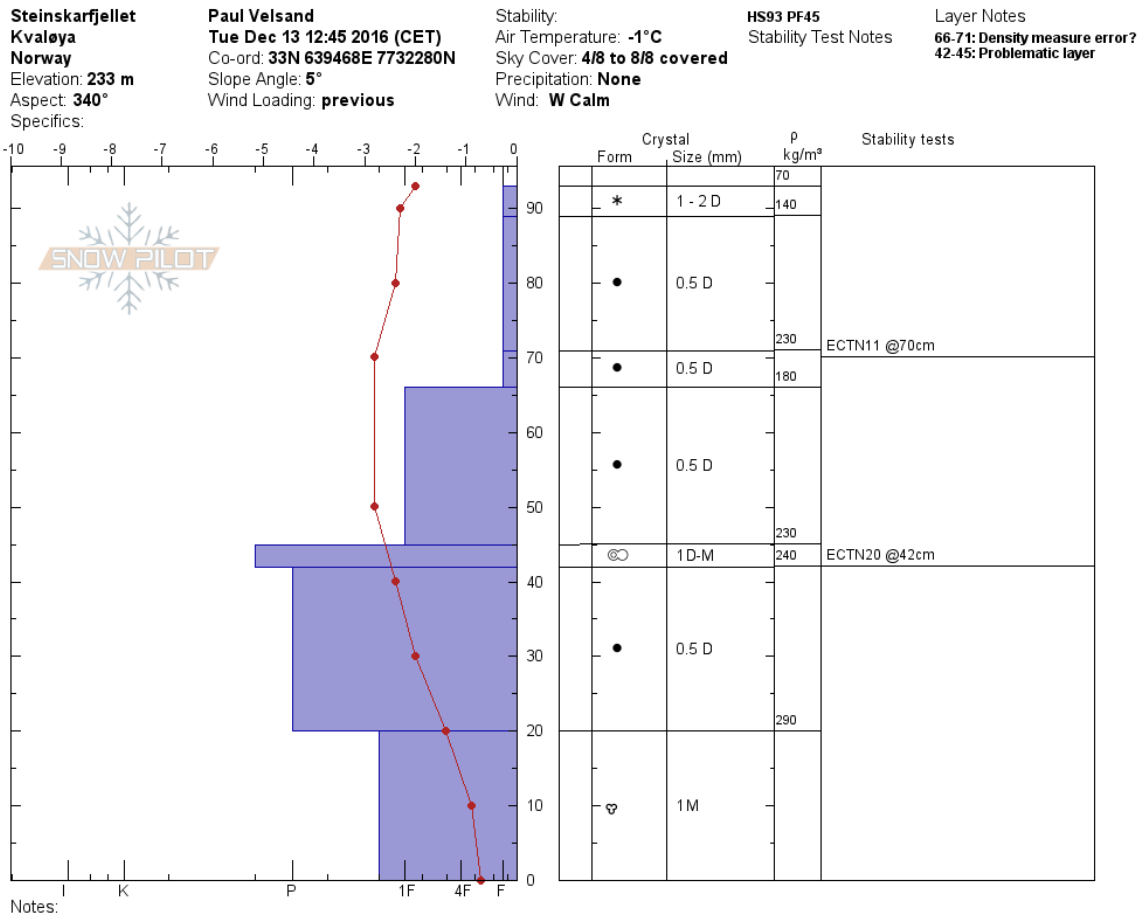

Figure A.10: Snowprofile from Steinskarfjellet low, December 13 2016.

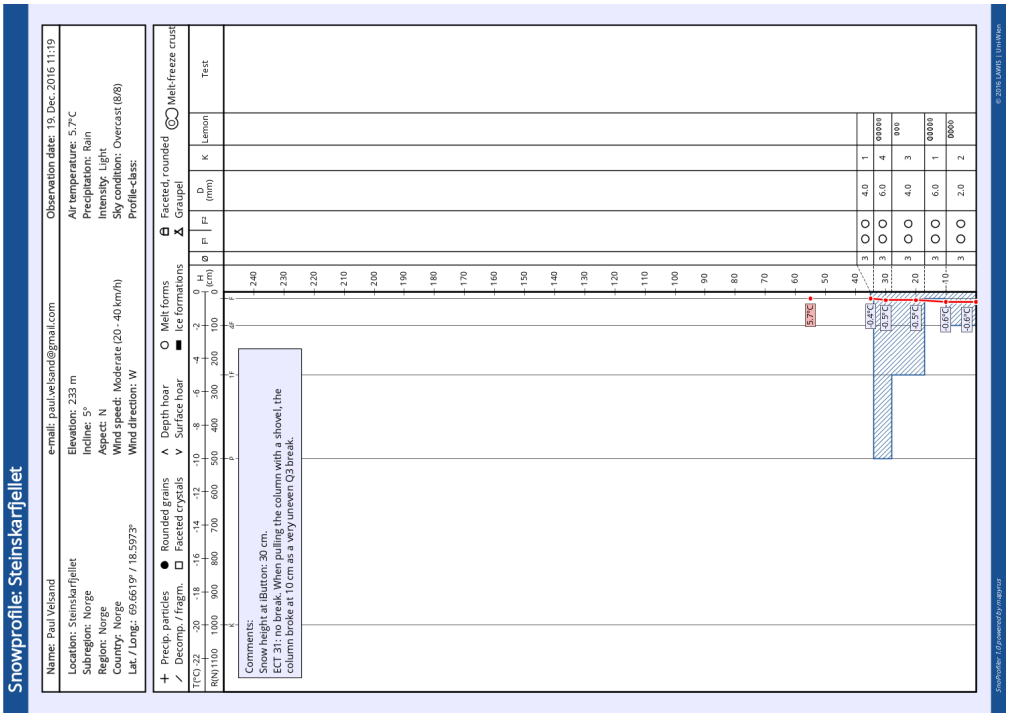

(a) December 19, 2016.

(b) January 10, 2017.

Figure A.11: Snow profiles SSlo, December 2016 and January 2017.

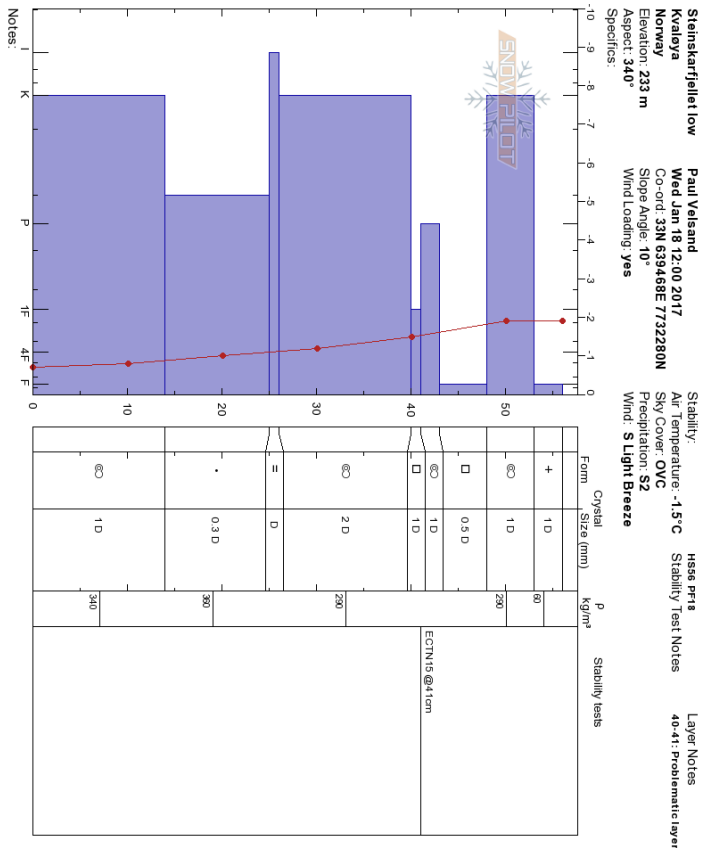

(a) January 18, 2017.

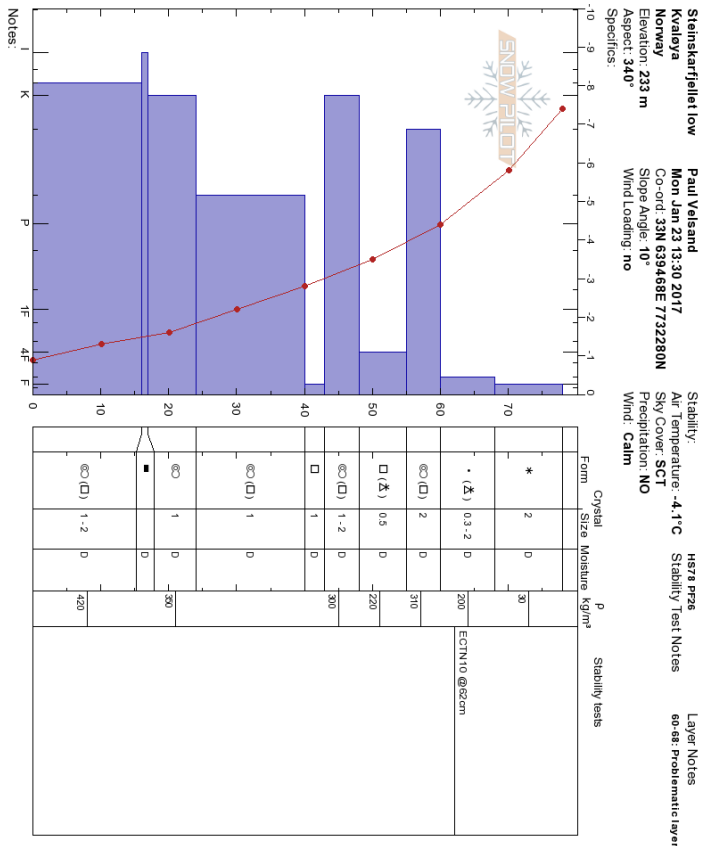

(b) January 23, 2017.

Figure A.12: Snow profiles SSlo, January 2017.

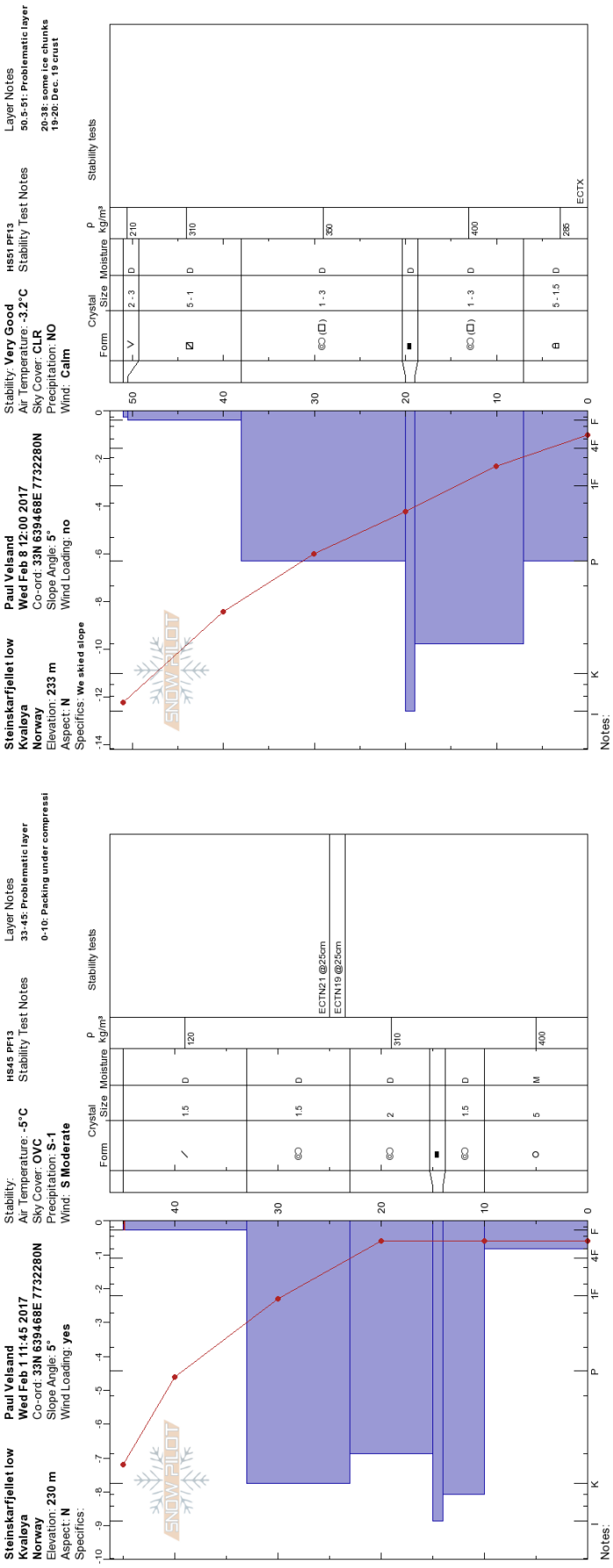

(a) February 1, 2017.

(b) February 8, 2017.

Figure A.13: Snow profiles SSlo, February 2017.

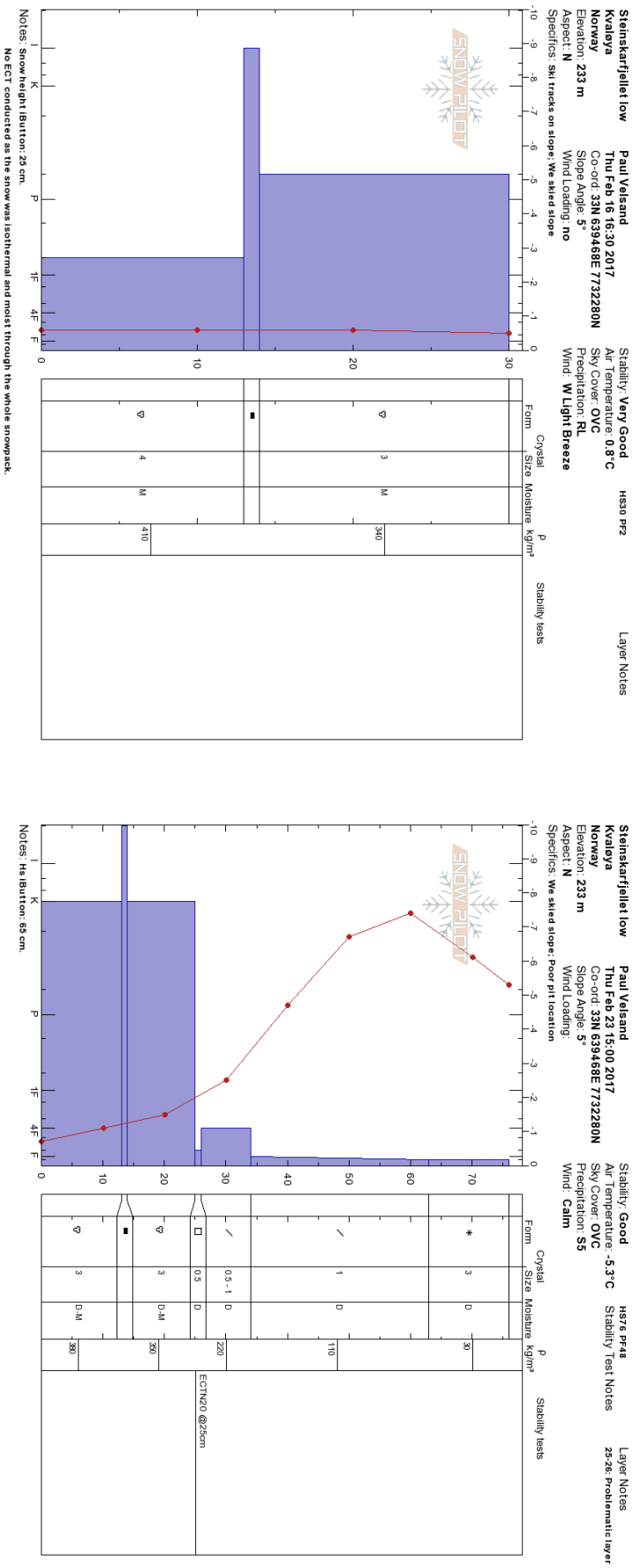

(a) February 15, 2017.

(b) February 23, 2017.

Figure A.14: Snow profiles SSlo, February 2017.

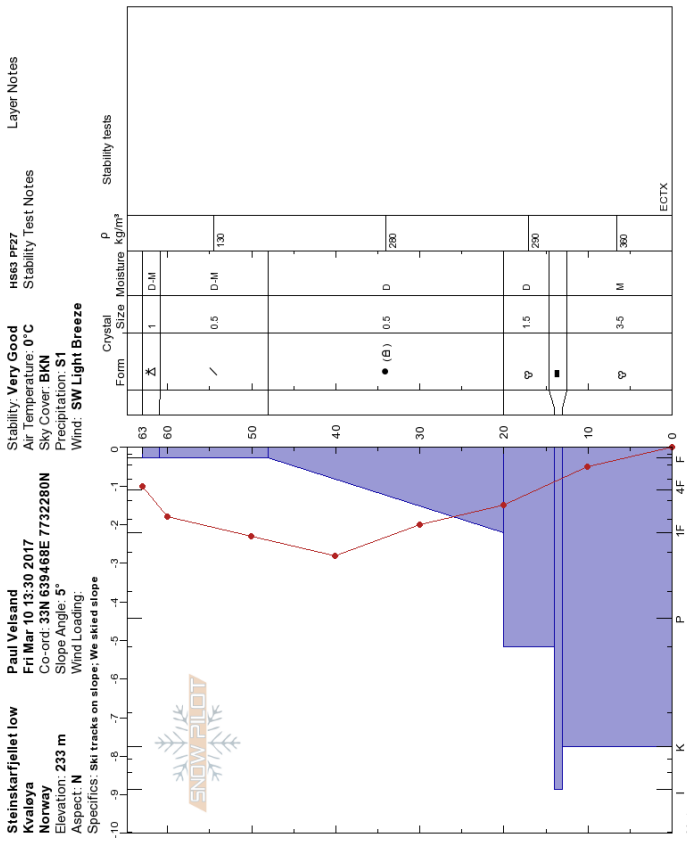

(a) March 3, 2017.

(b) March 10, 2017.

Figure A.15: Snow profiles SSlo, March 2017.

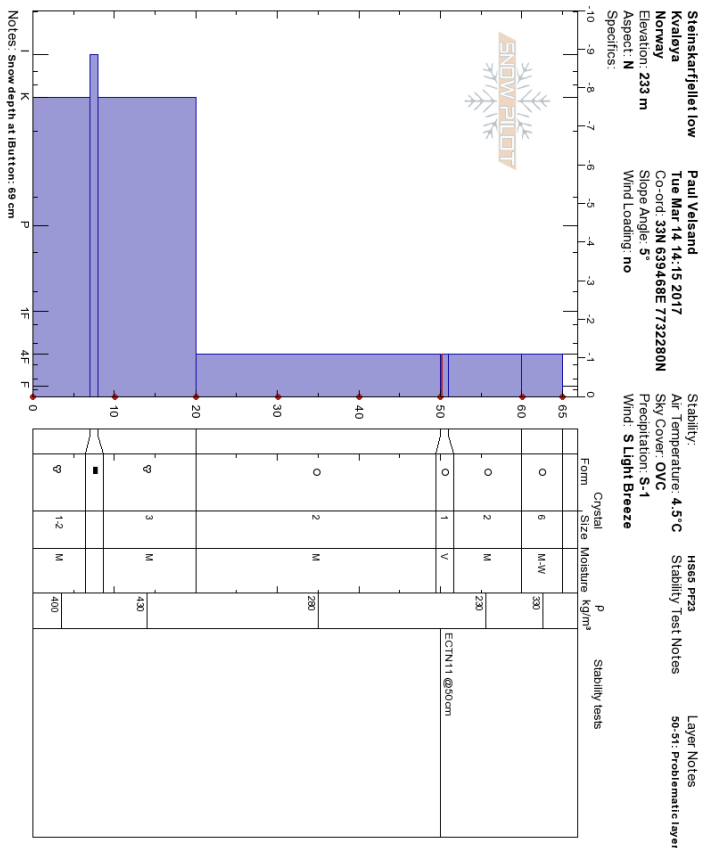

(a) March 14, 2017.

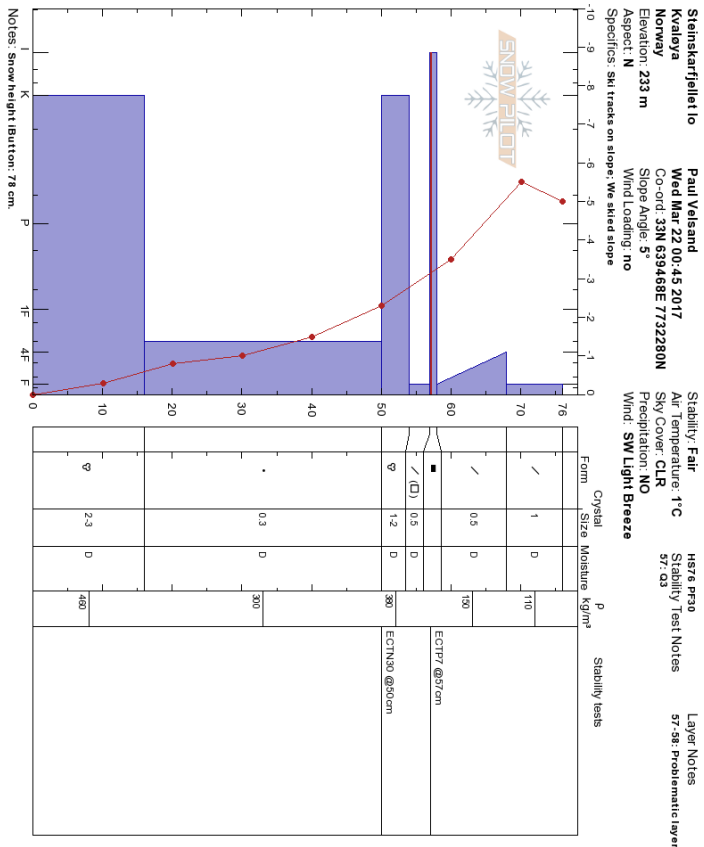

(b) March 22, 2017.

Figure A.16: Snow profiles SSlo, March 2017.

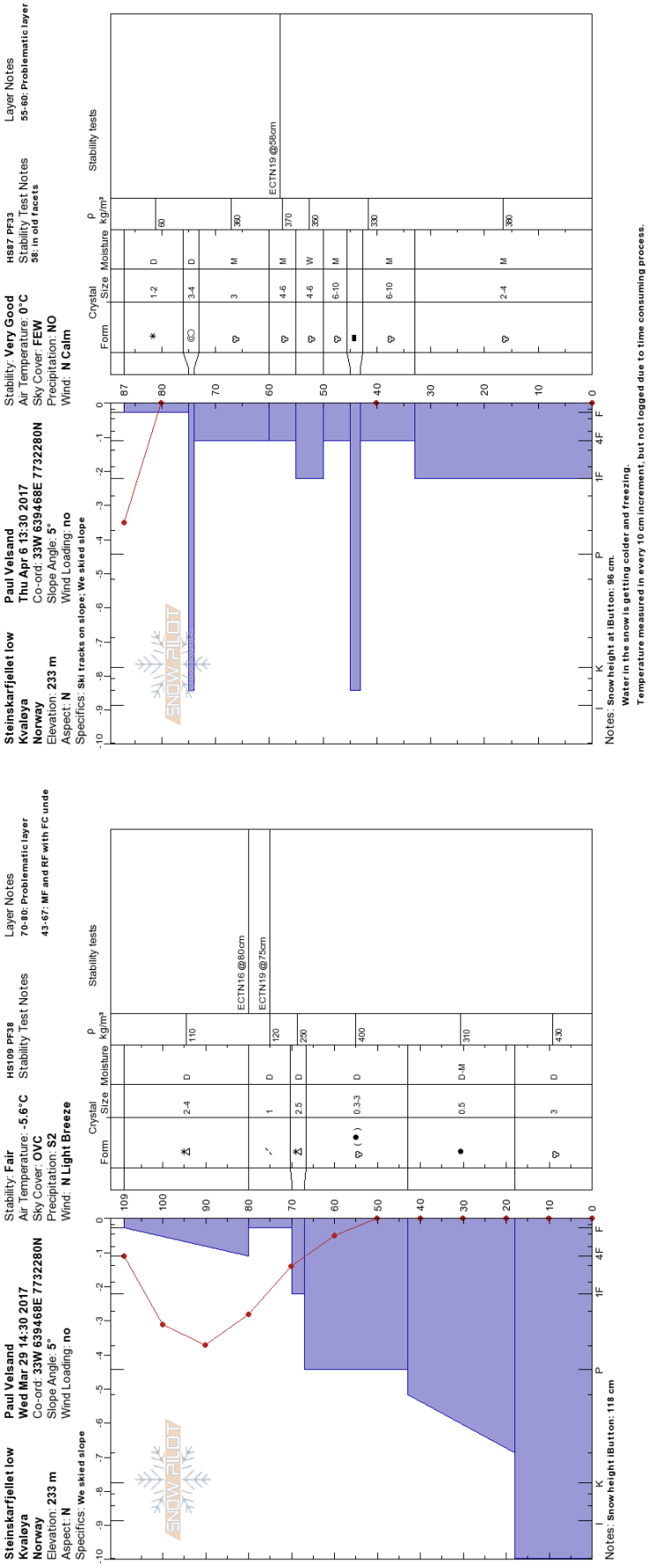

(a) March 29, 2017.

(b) April 6, 2017.

Figure A.17: Snow profiles SSlo, March and April 2017.

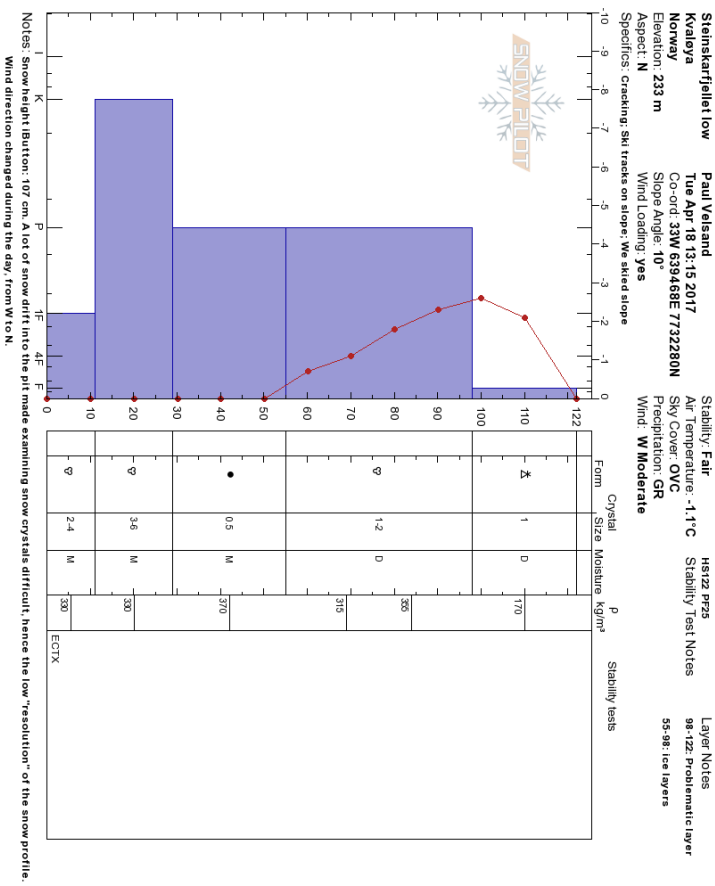

(a) April 18, 2017.

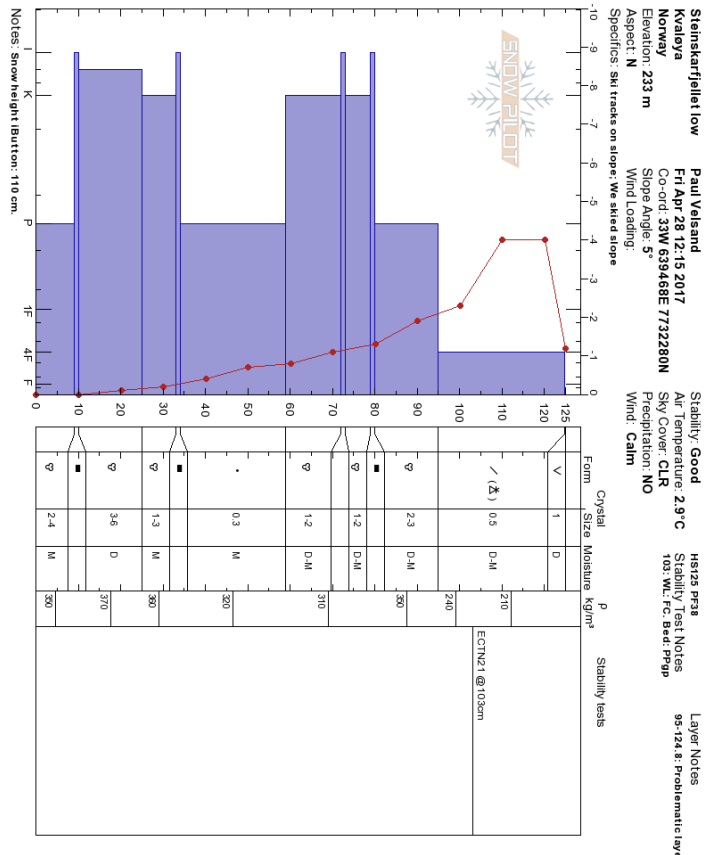

(b) April 28, 2017.

Figure A.18: Snow profiles SSlo, April 2017.

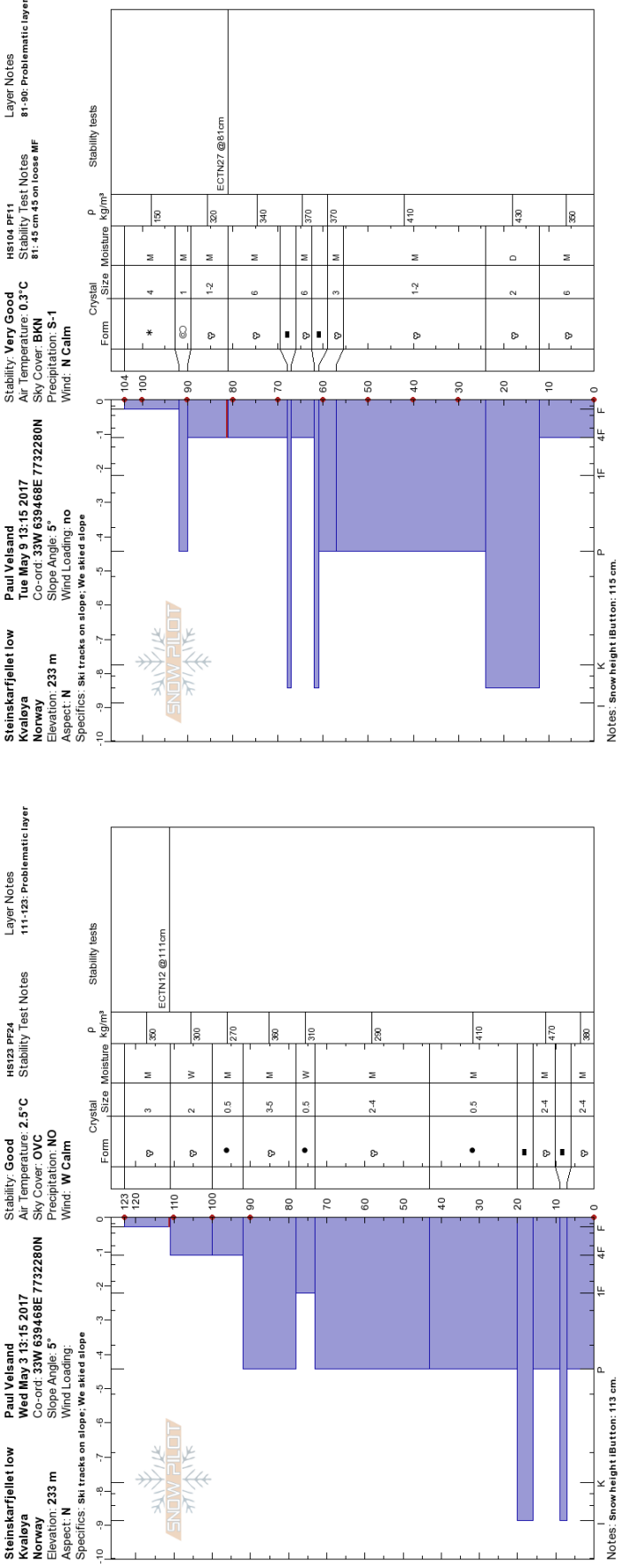

(a) May 3, 2017.

(b) May 9, 2017.

Figure A.19: Snow profiles SSlo, May 2017.

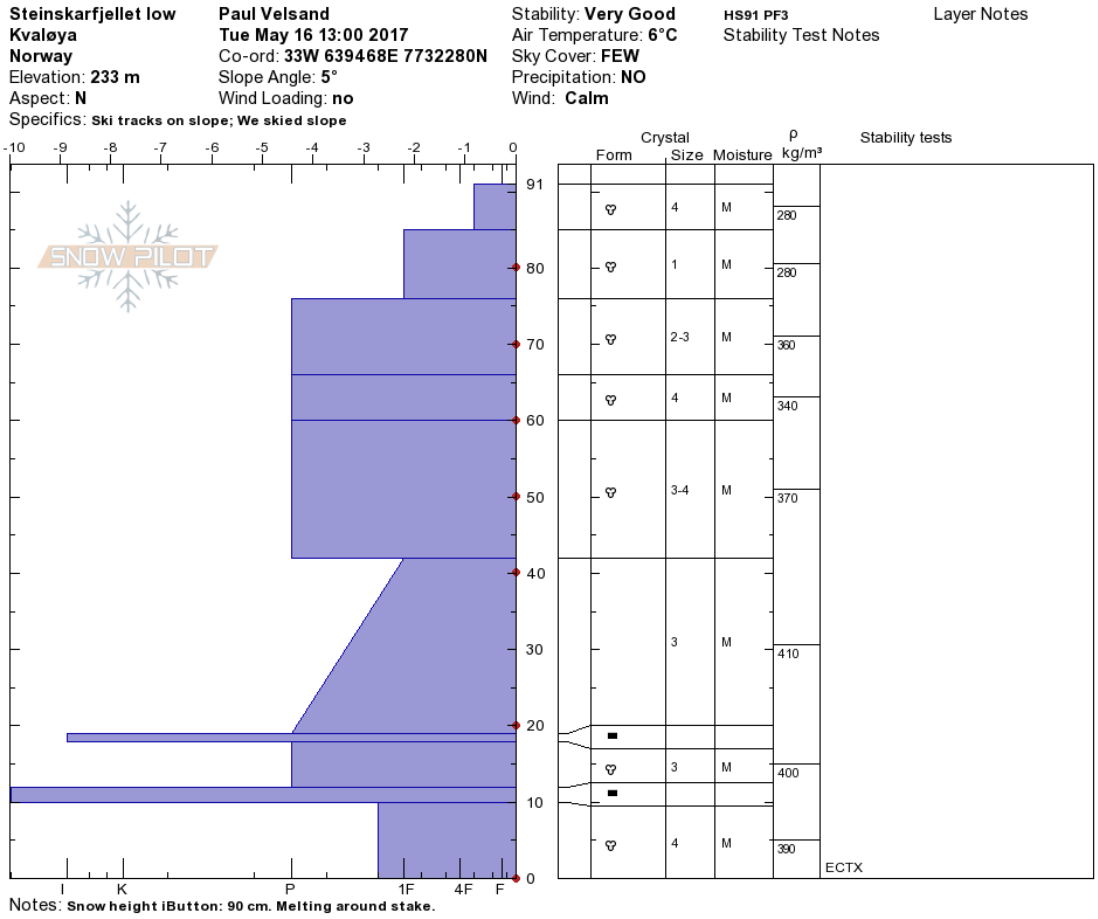

Figure A.20: Snowprofile from Steinskarfjellet low, May 16 2017.

A.3 FAGERFJELLET HIGH SNOW PROFILES

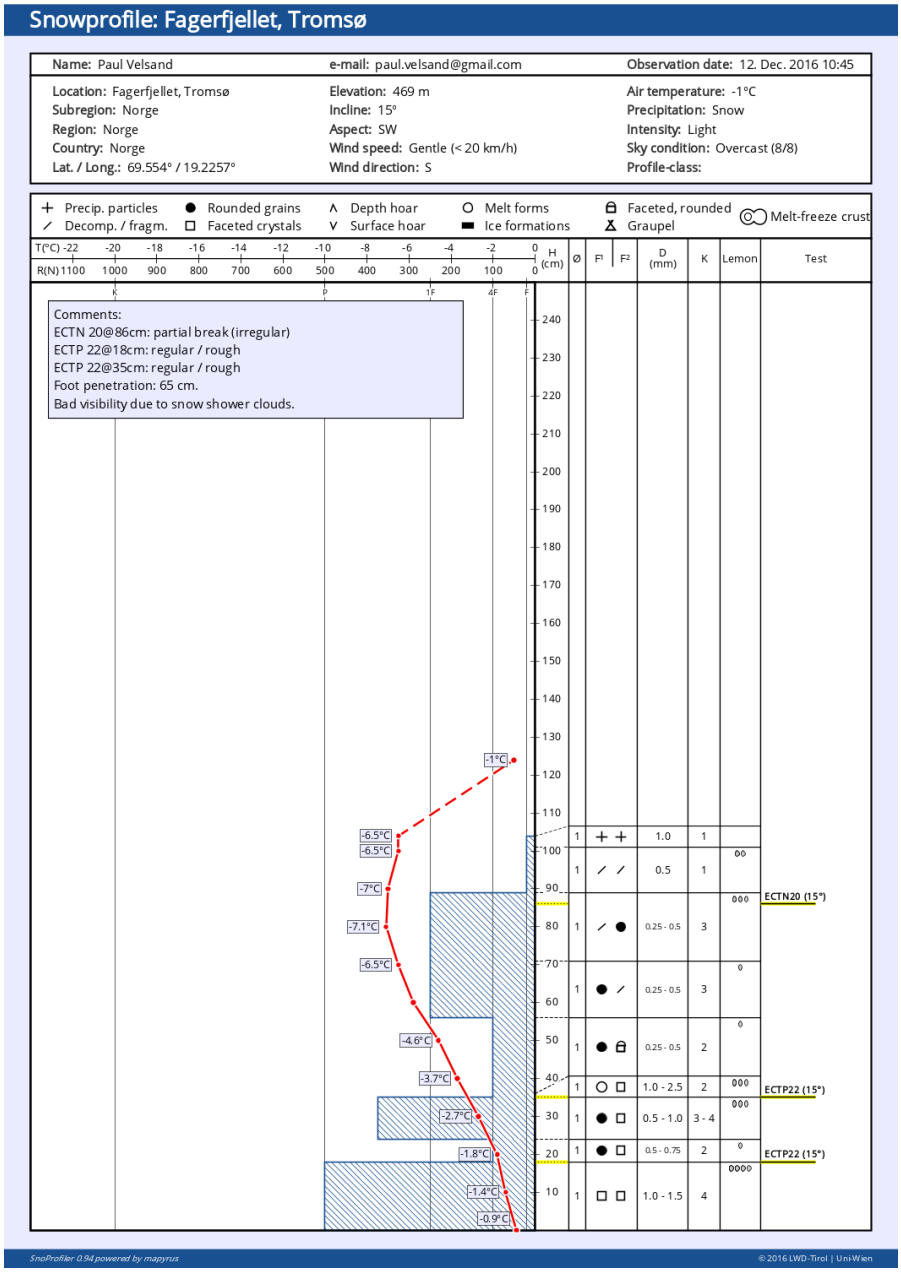

Figure A.21: Snowprofile from Fagerfjellet high, December 12 2016.

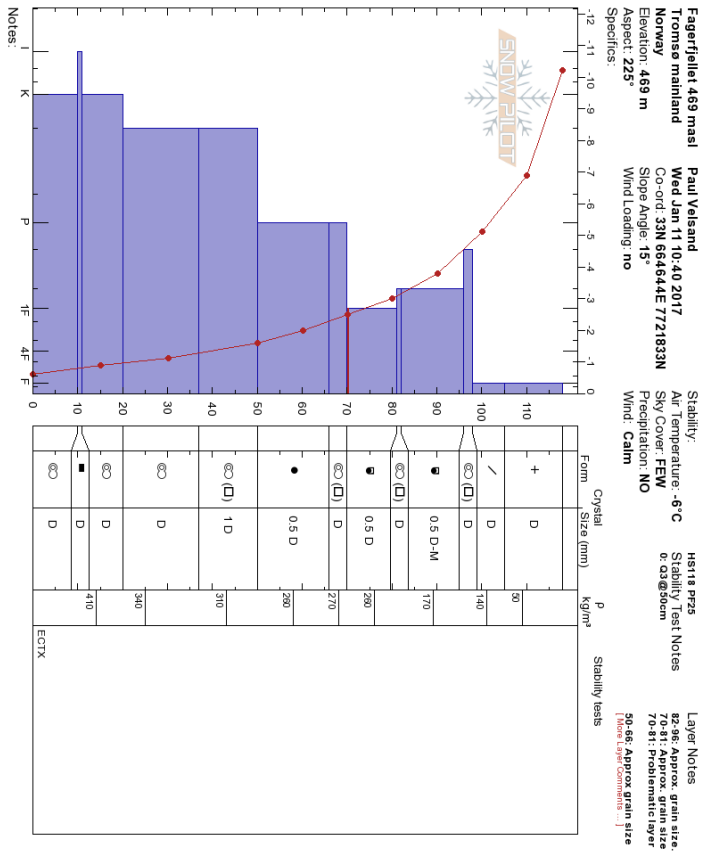

(a) January 11, 2017.

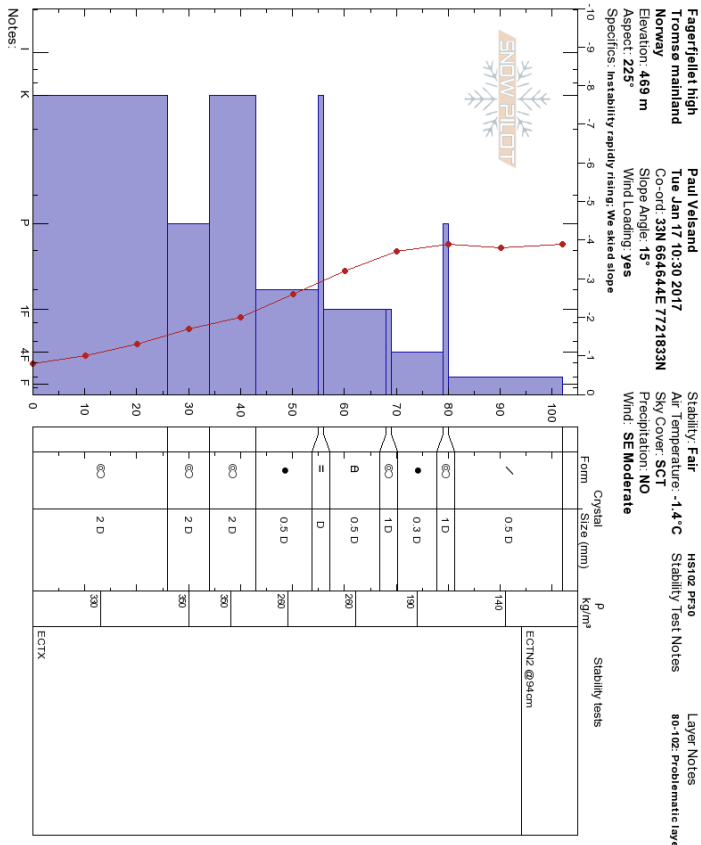

(b) January 17, 2017.

Figure A.22: Snow profiles FFhi, January 2017.

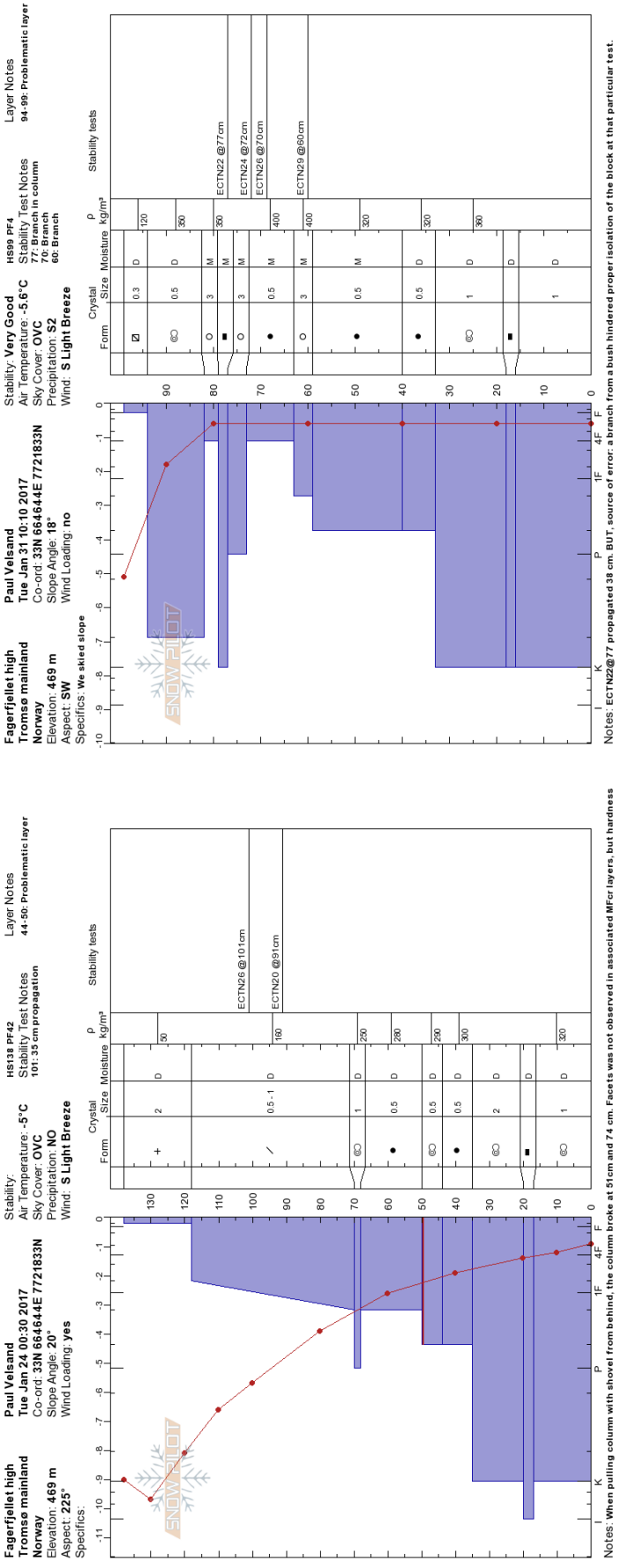

(a) January 24, 2017.

(b) January 31, 2017.

Figure A.23: Snow profiles FFhi, January 2017.

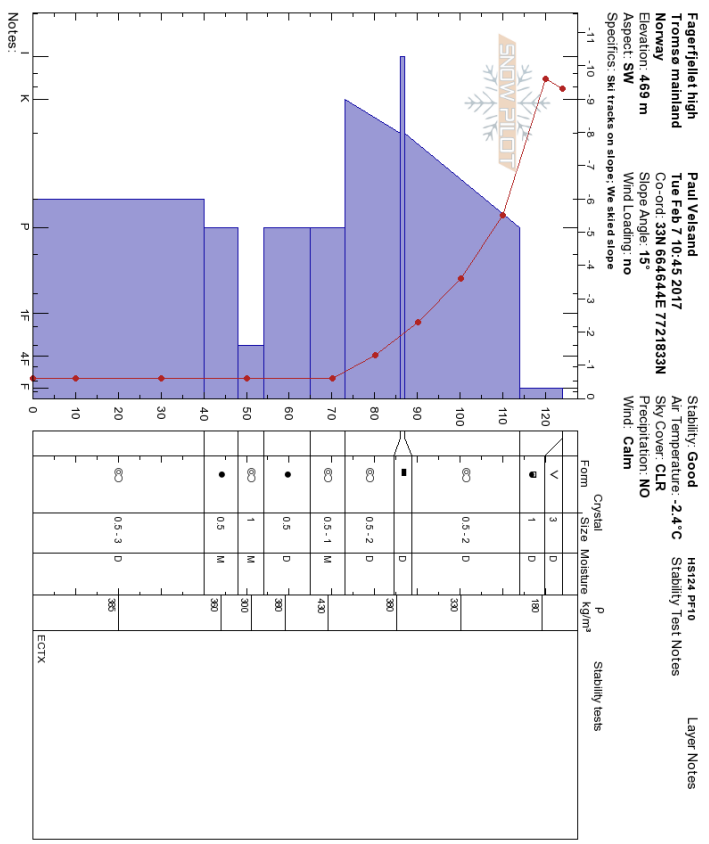

(a) February 7, 2017.

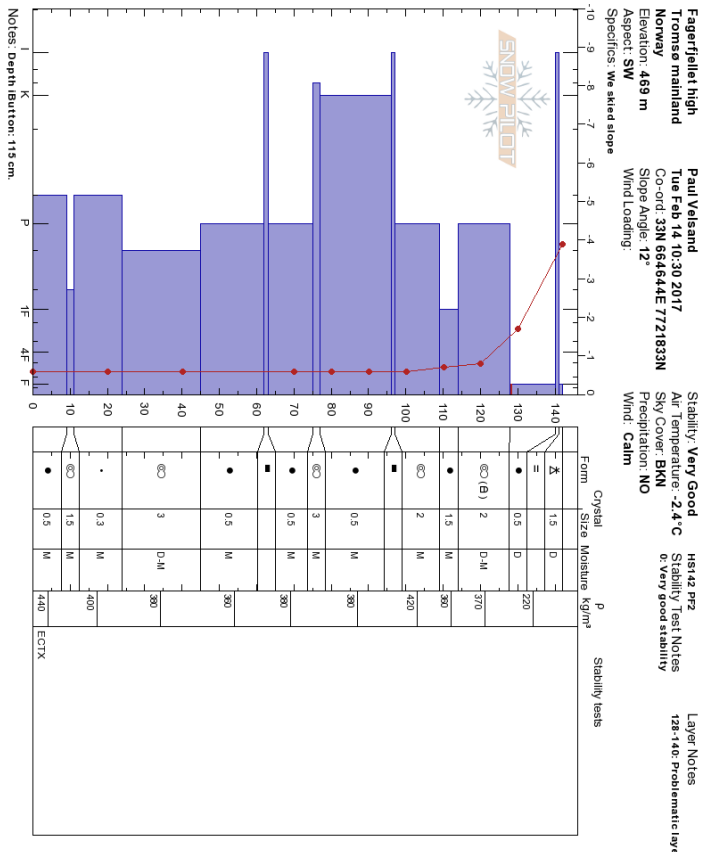

(b) February 14, 2017.

Figure A.24: Snow profiles FFhi, February 2017.

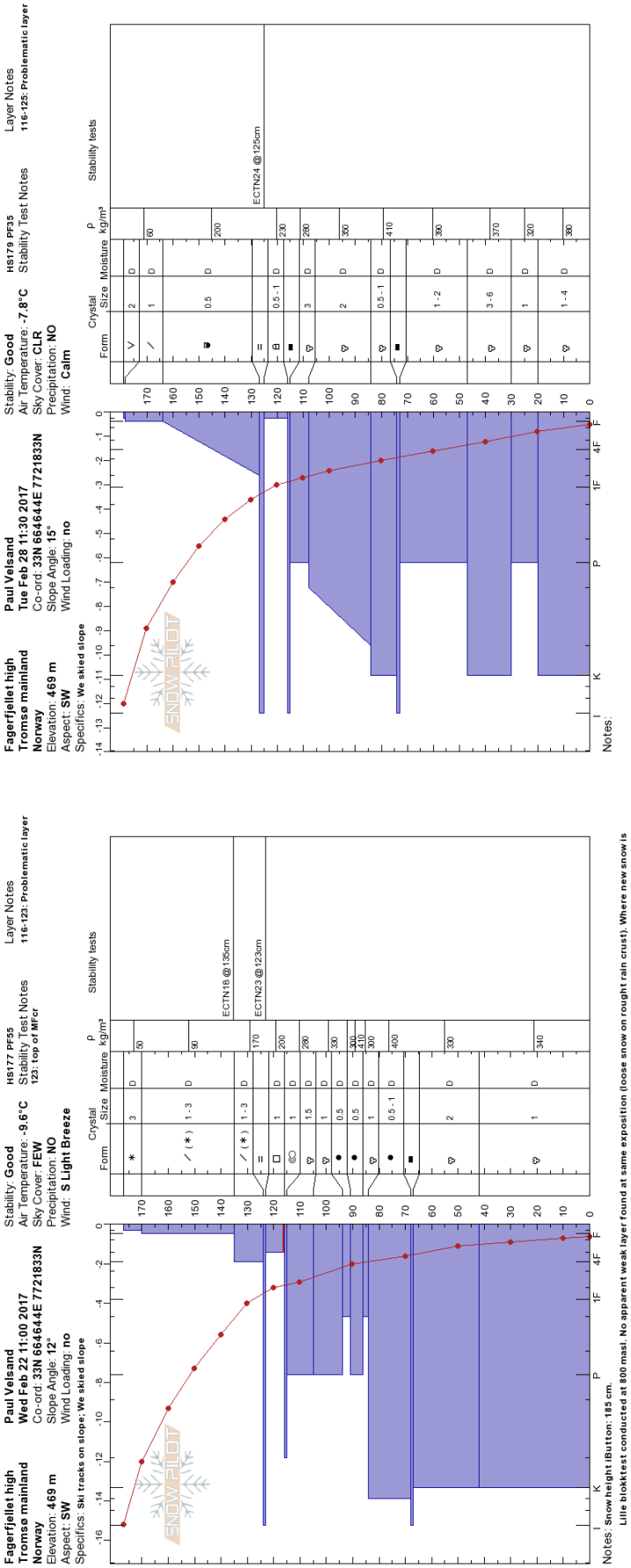

(a) February 22, 2017.

(b) February 28, 2017.

Figure A.25: Snow profiles FFhi, February 2017.

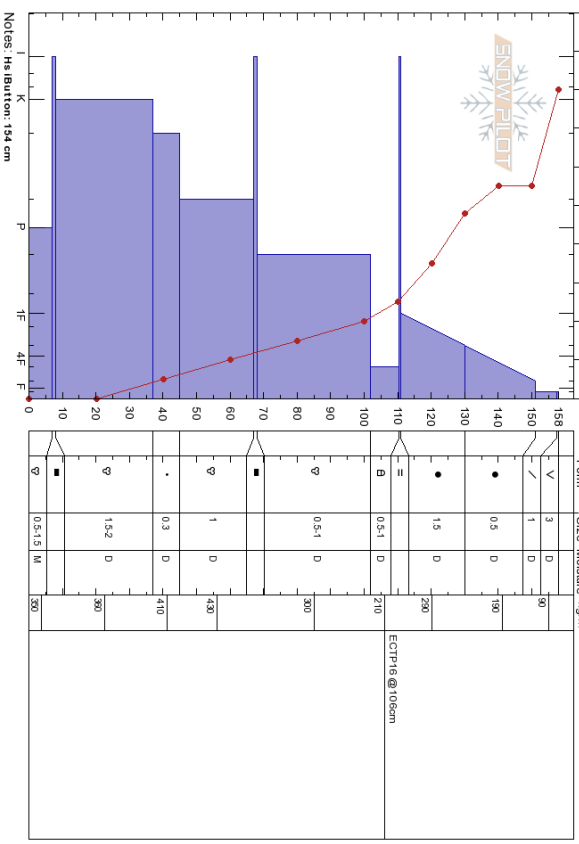

(a) March 7, 2017.

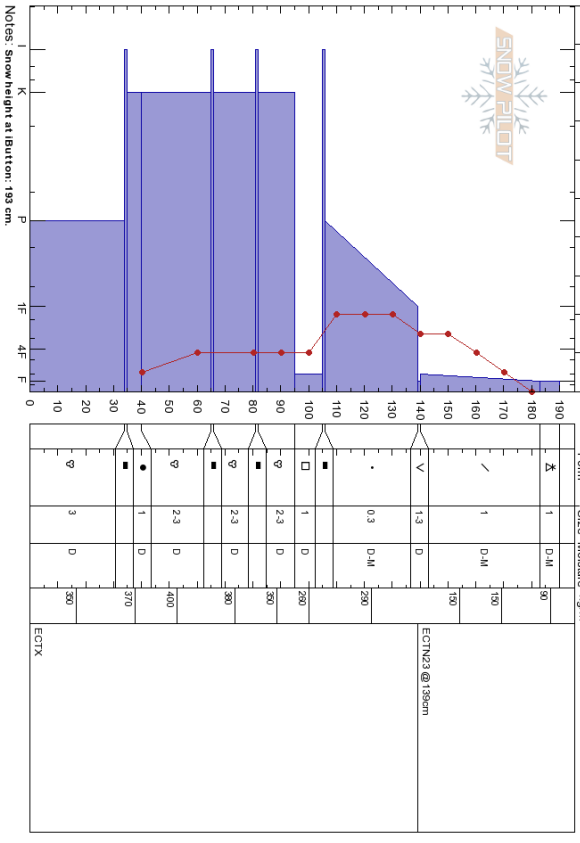

(b) March 16, 2017.

Figure A.26: Snow profiles FFhi, March 2017.

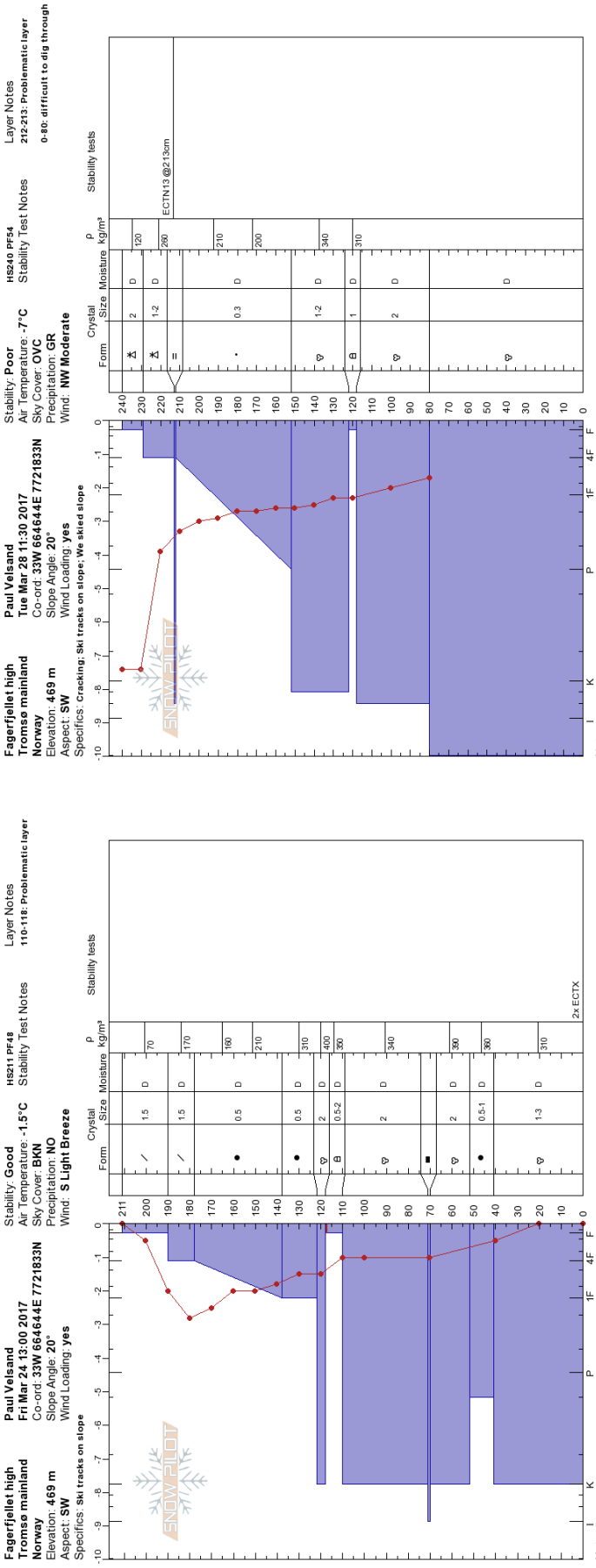

(a) March 24, 2017.

(b) March 28, 2017.

Figure A.27: Snow profiles FFhi, March 2017.

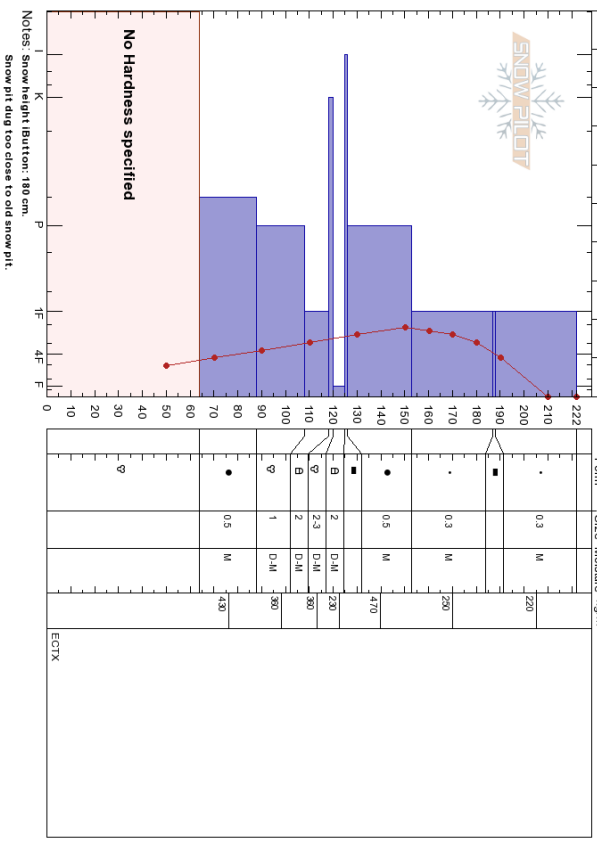

(a) April 5, 2017.

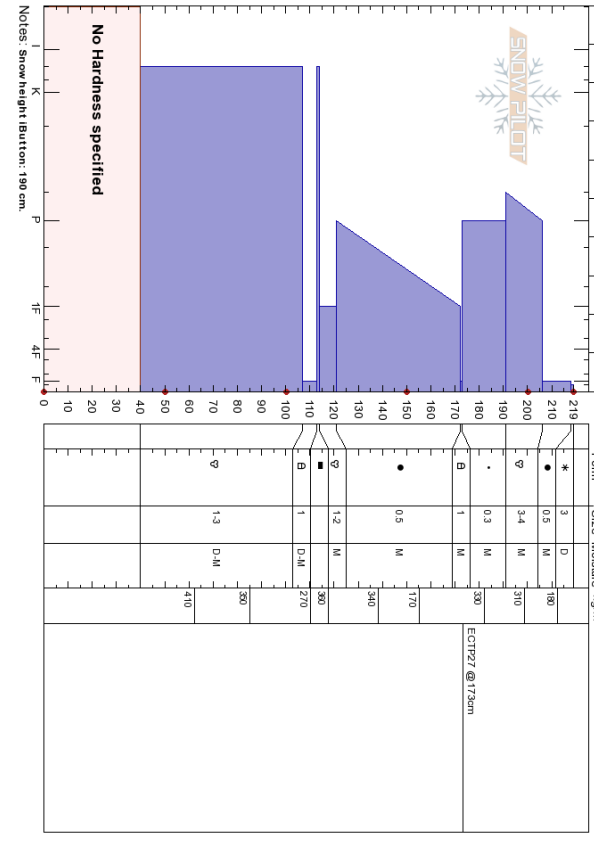

(b) April 10, 2017.

Figure A.28: Snow profiles FFhi, April 2017.

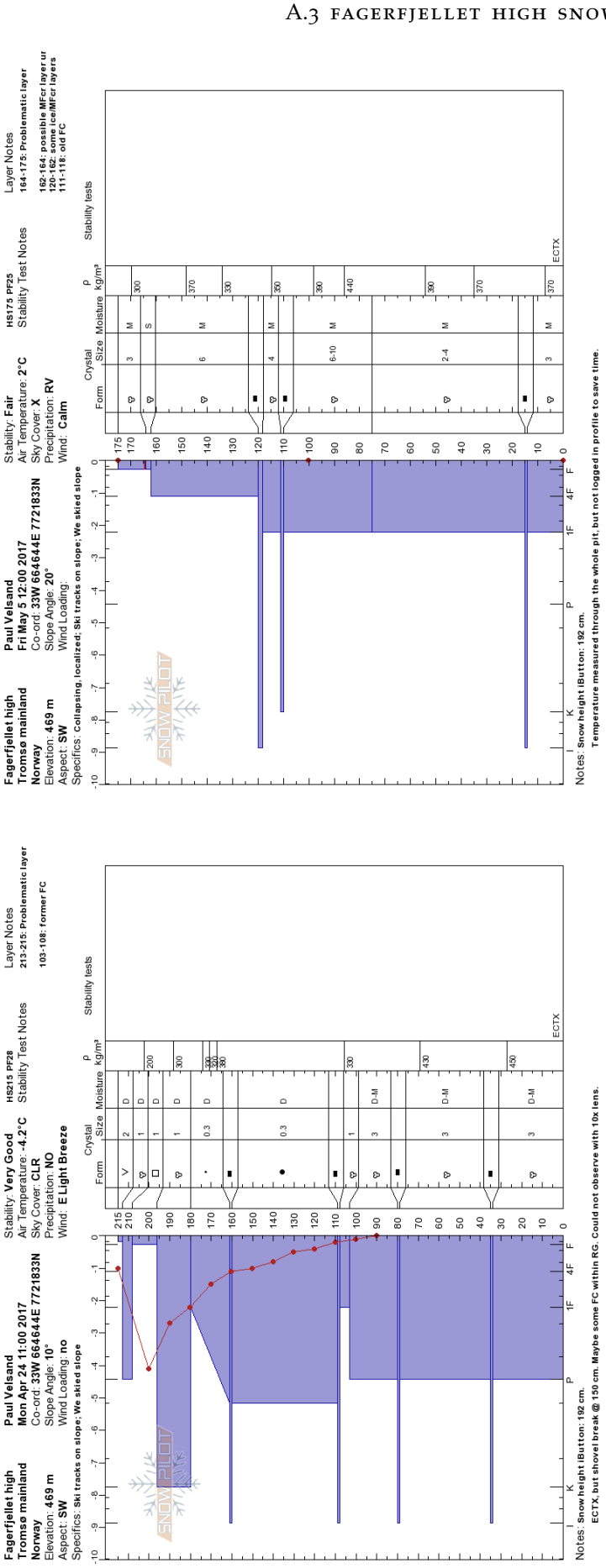

(a) April 25, 2017.

(b) May 5, 2017.

Figure A.29: Snow profiles FFhi, April and May 2017.

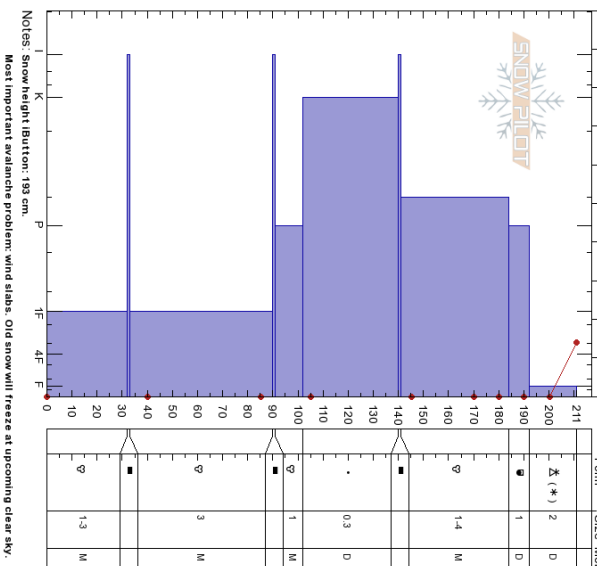

(a) May 8, 2017.

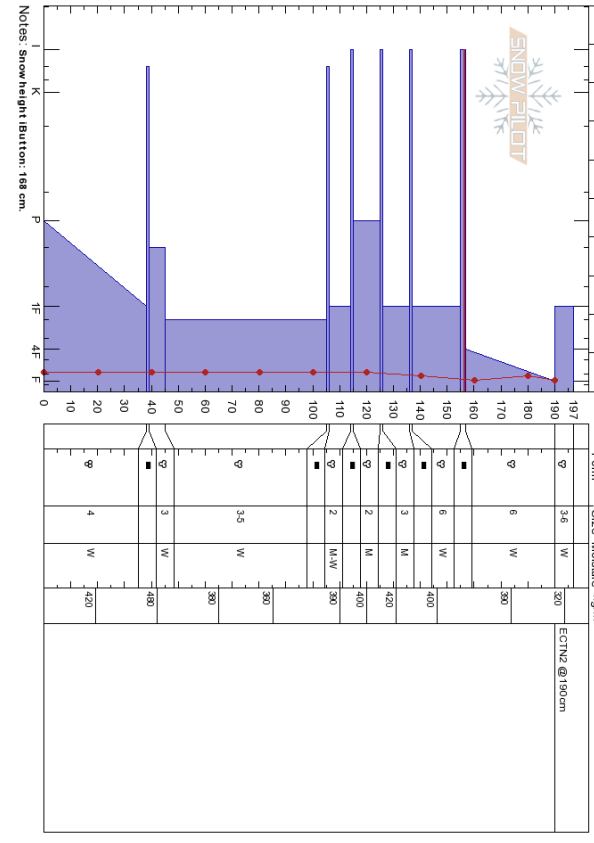

(b) May 19, 2017.

Figure A.30: Snow profiles FFhi, May 2017.

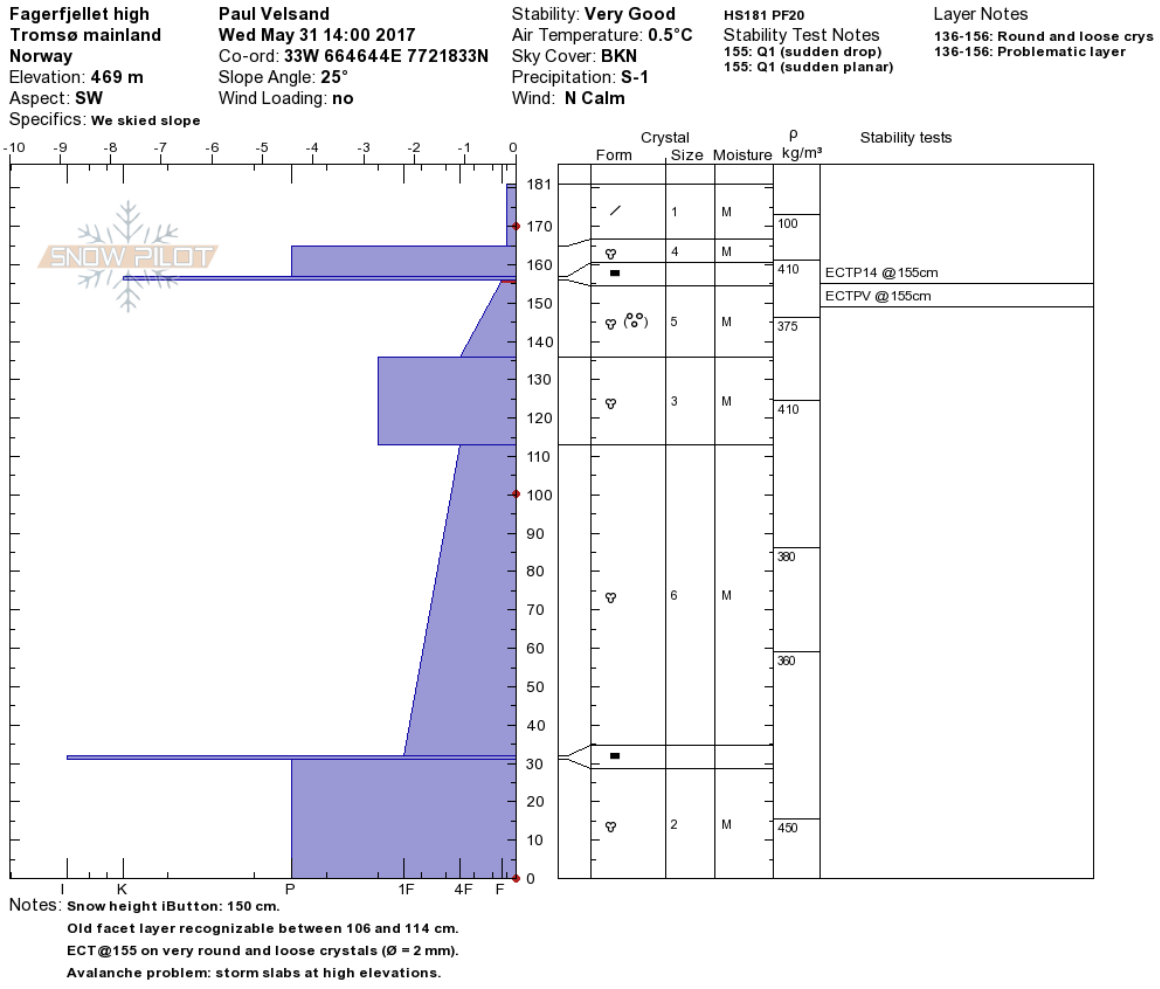

Figure A.31: Snowprofile from Fagerfjellet high, May 31 2017.

A.4 FAGERFJELLET LOW SNOW PROFILES

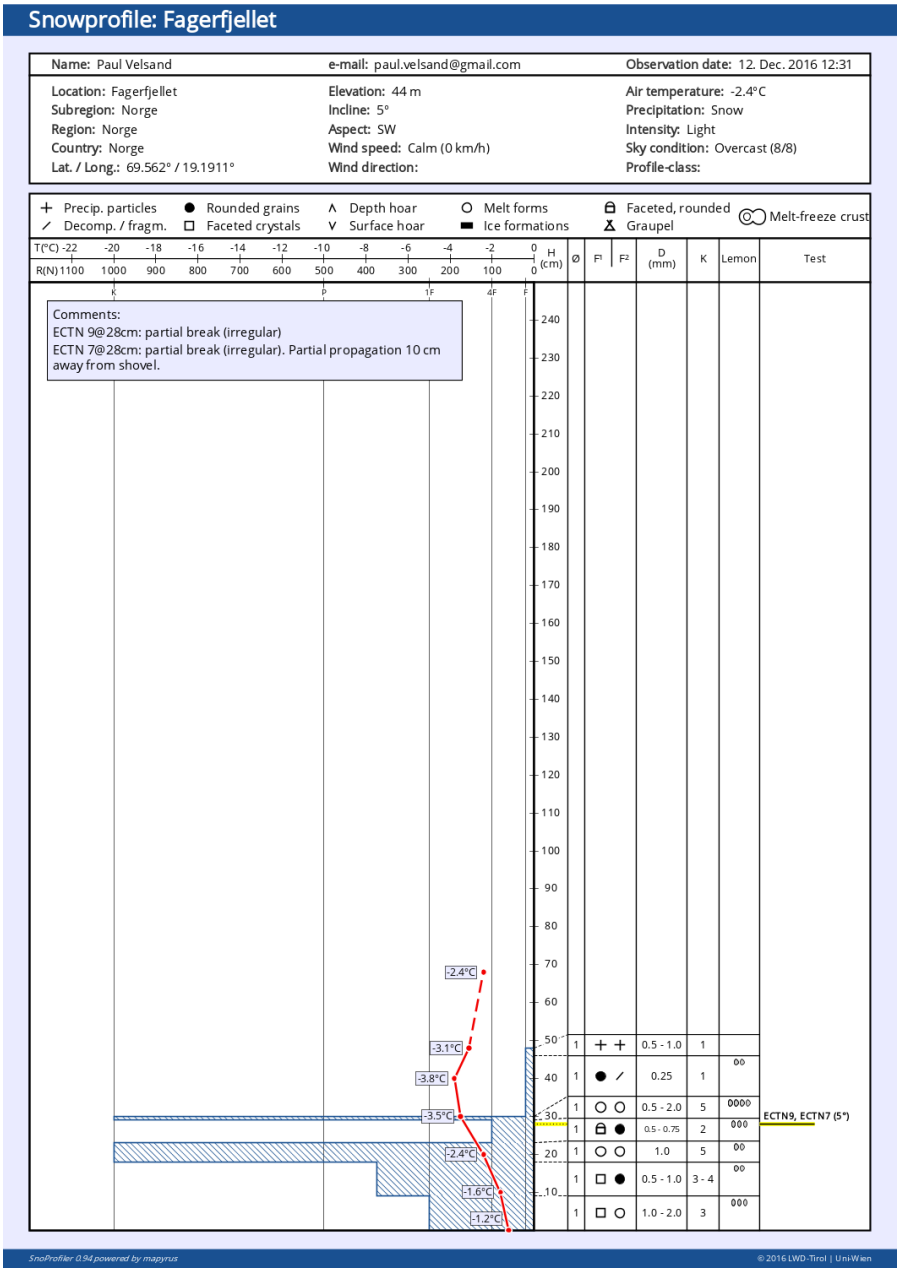

Figure A.32: Snowprofile from Fagerfjellet low, December 12 2016.

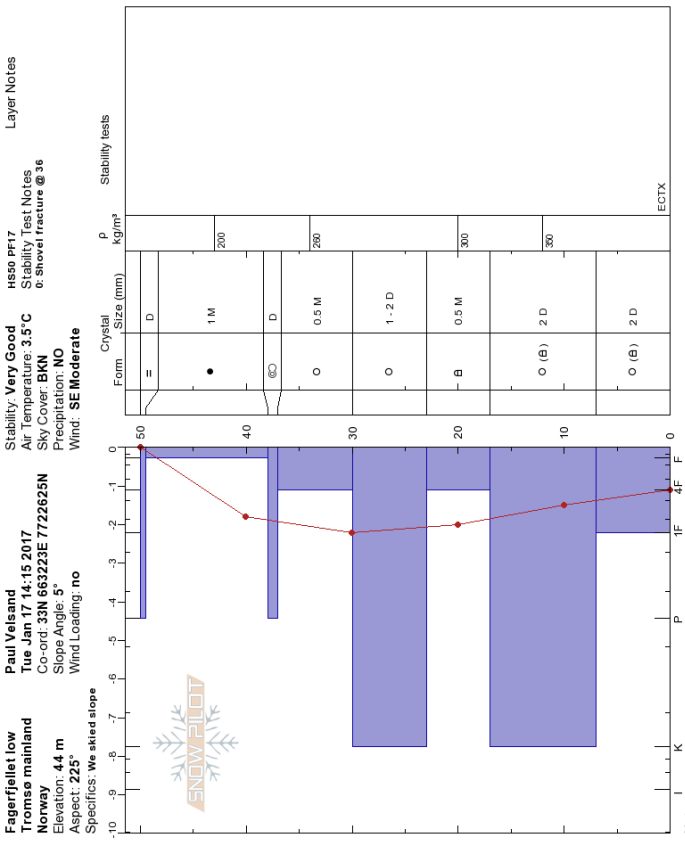

(b) January 17, 2017.

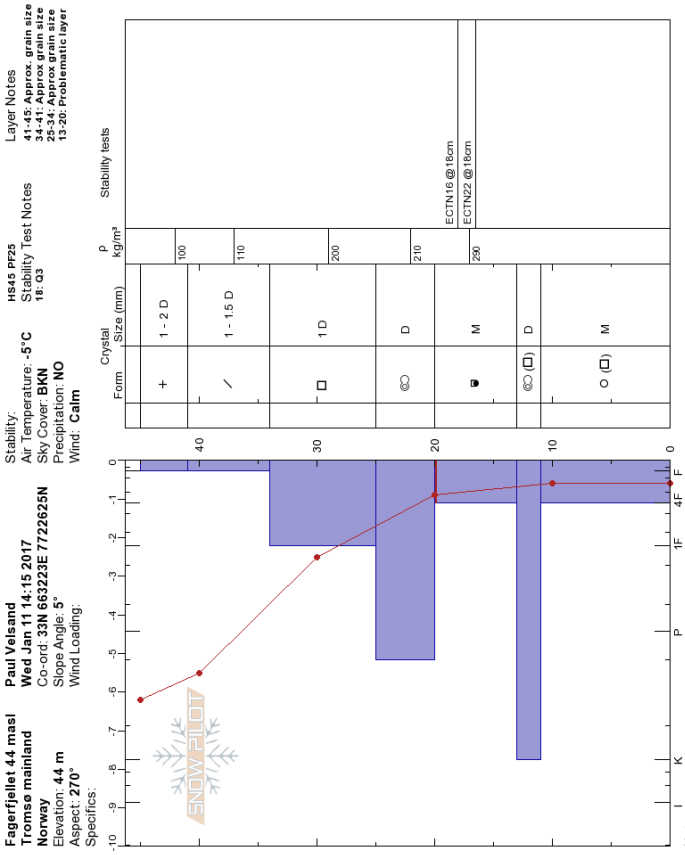

(a) January 11, 2017.

Figure A.33: Snow profiles FFlo, January 2017.

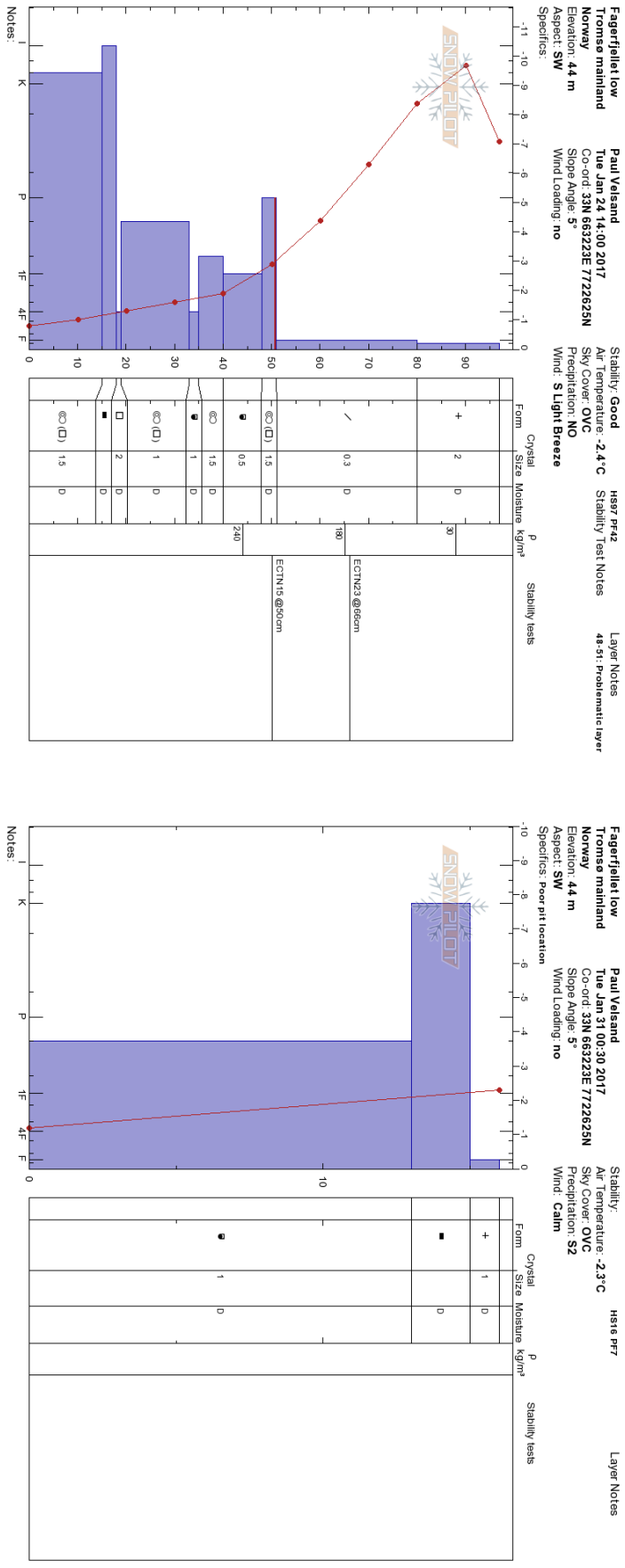

(a) January 24, 2017.

(b) January 31, 2017.

Figure A.34: Snow profiles FFlo, January 2017.

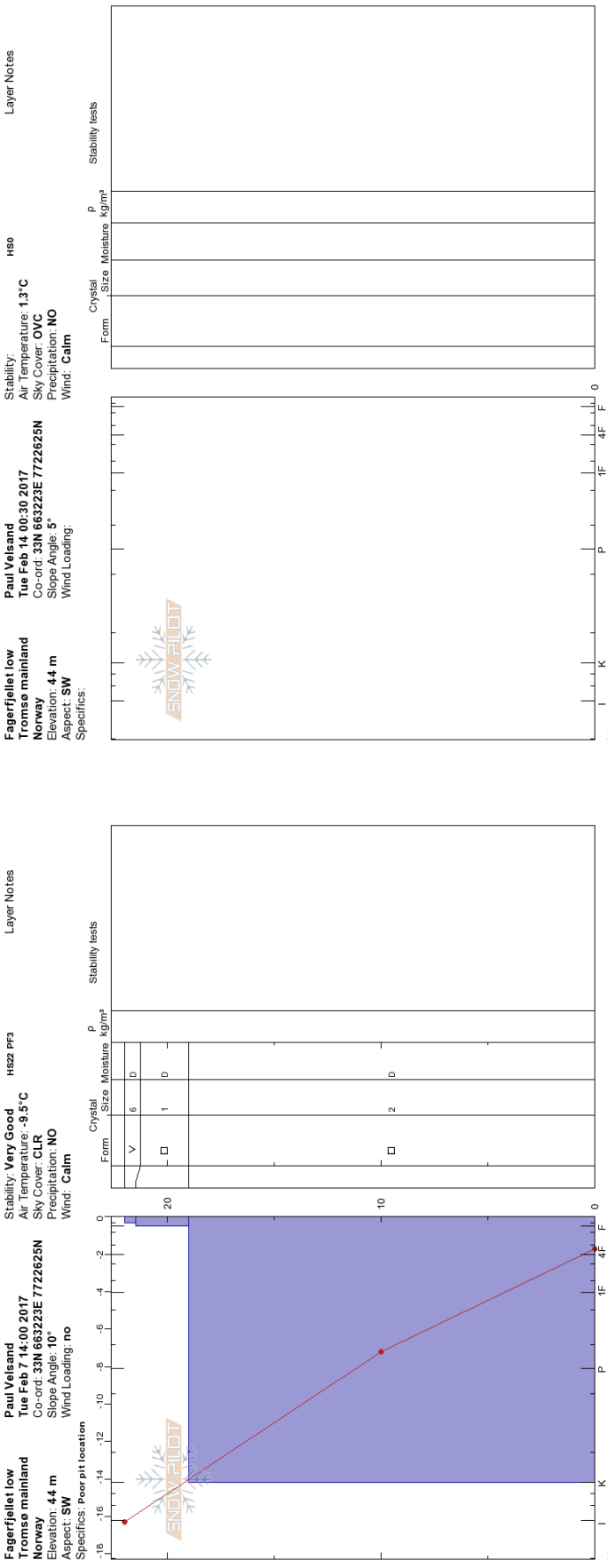

(a) February 7, 2017.

(b) February 14, 2017.

Figure A.35: Snow profiles FF1o, February 2017.

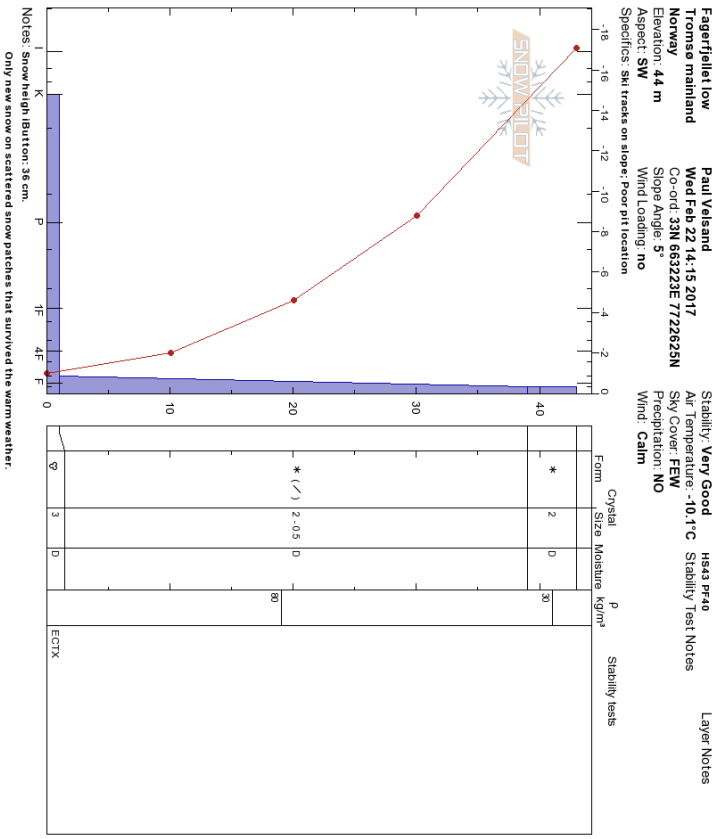

(a) February 22, 2017.

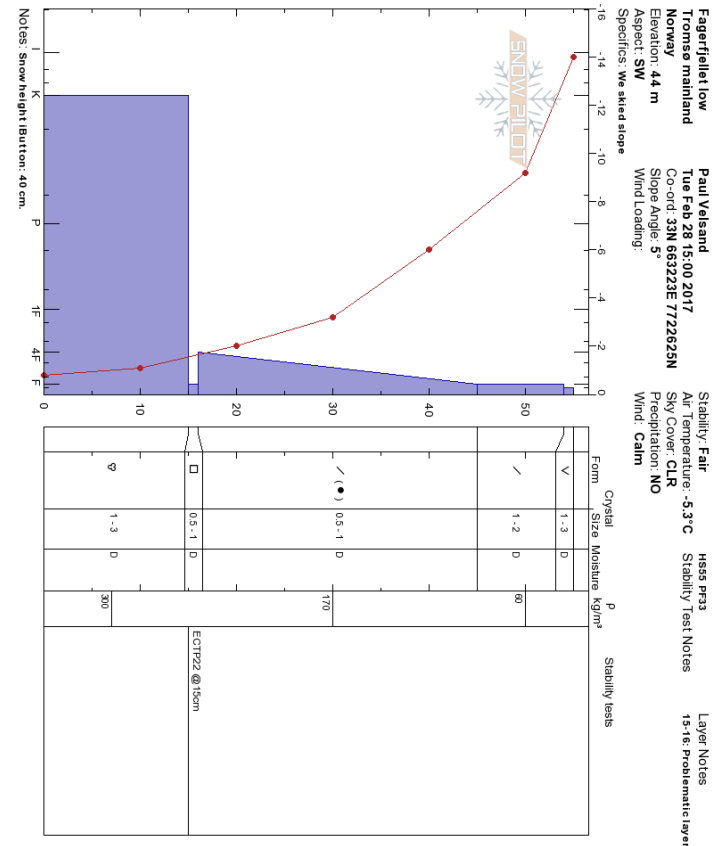

(b) February 28, 2017.

Figure A.36: Snow profiles FFlo, February 2017.

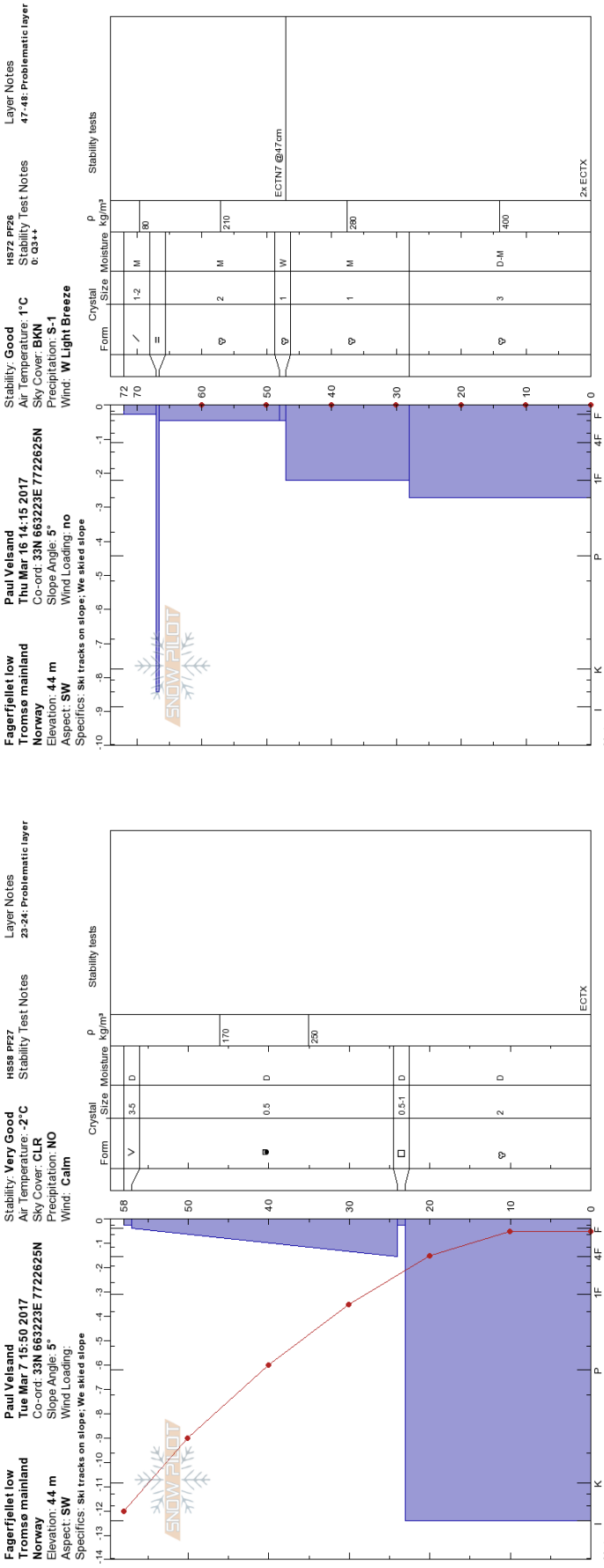

(a) March 7, 2017.

(b) March 16, 2017.

Figure A.37: Snow profiles FFlo, March 2017.

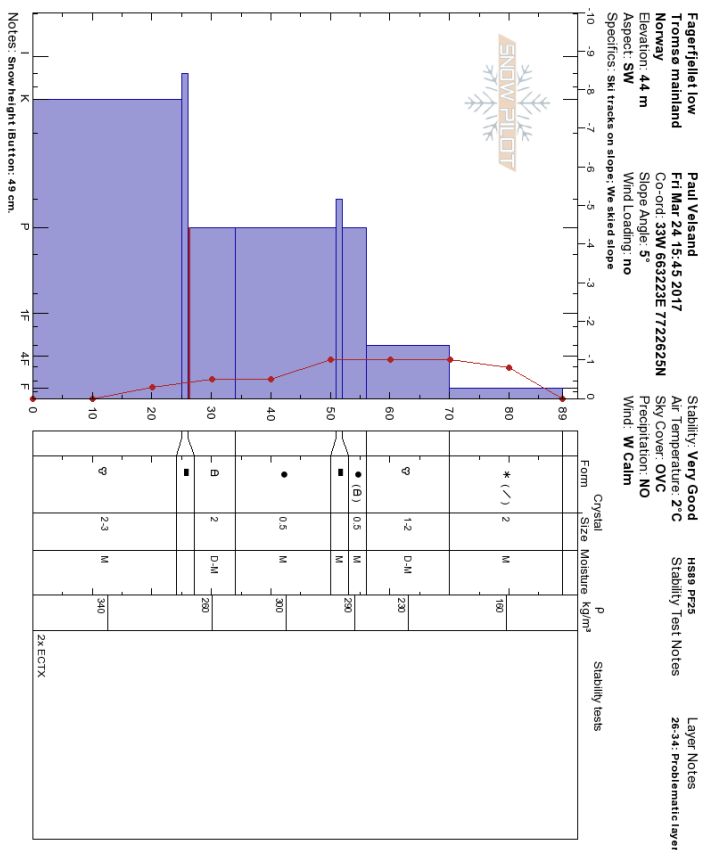

(a) March 24, 2017.

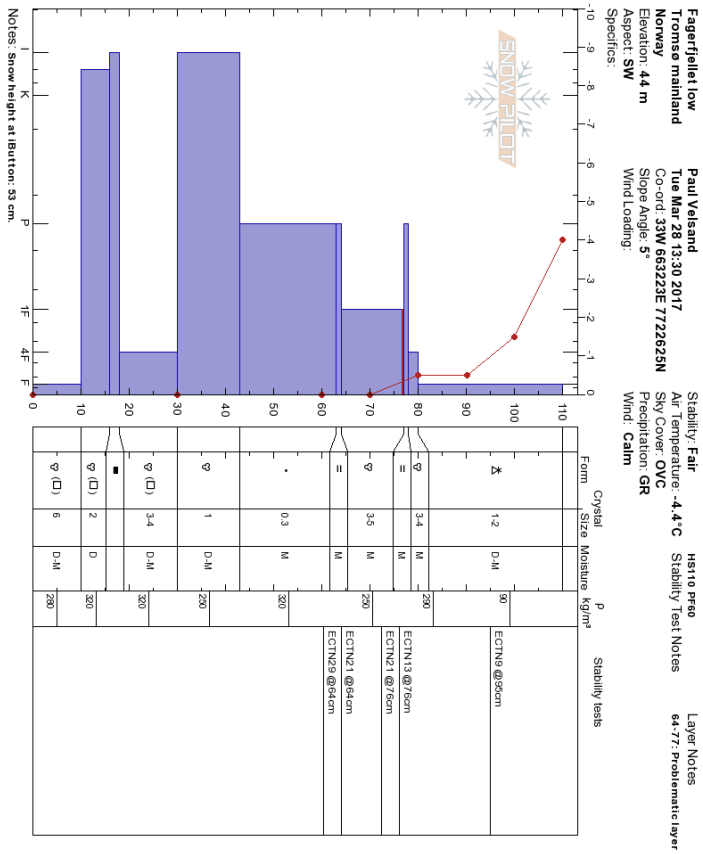

(b) March 28, 2017.

Figure A.38: Snow profiles FFlo, March 2017.

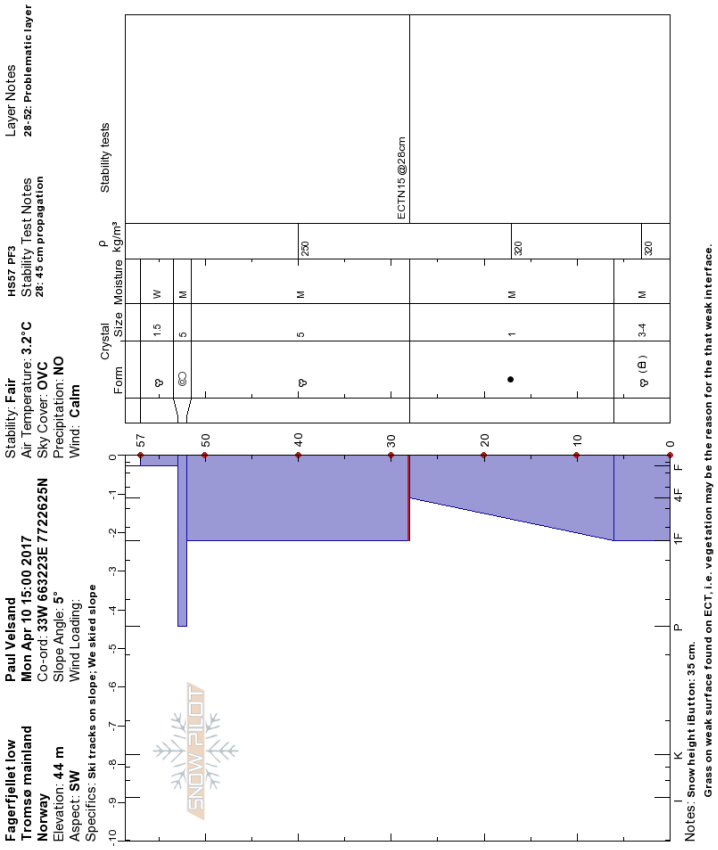

(b) April 10, 2017.

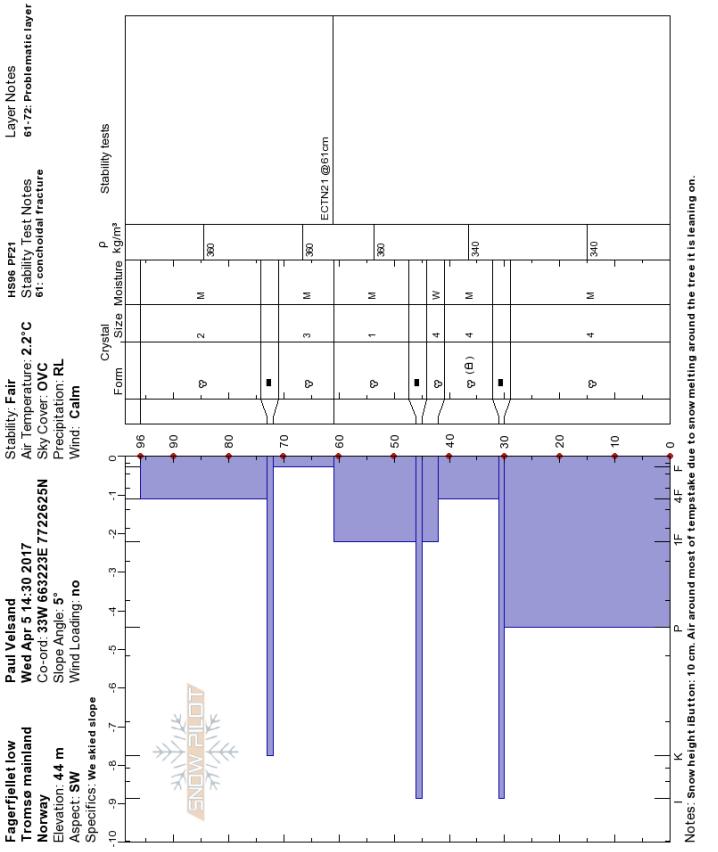

(a) April 5, 2017.

Figure A.39: Snow profiles FF10, April 2017.

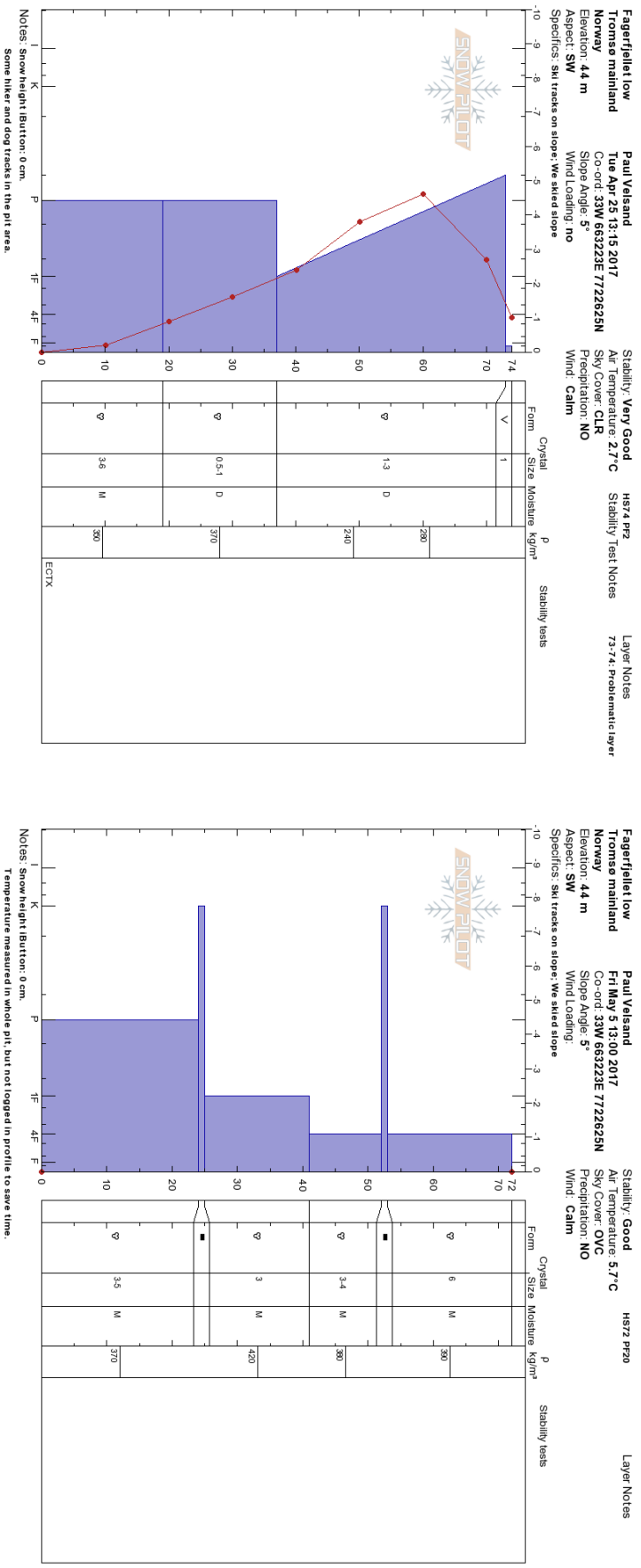

(a) April 25, 2017.

(b) May 5, 2017.

Figure A.40: Snow profiles FFlo, April and May 2017.

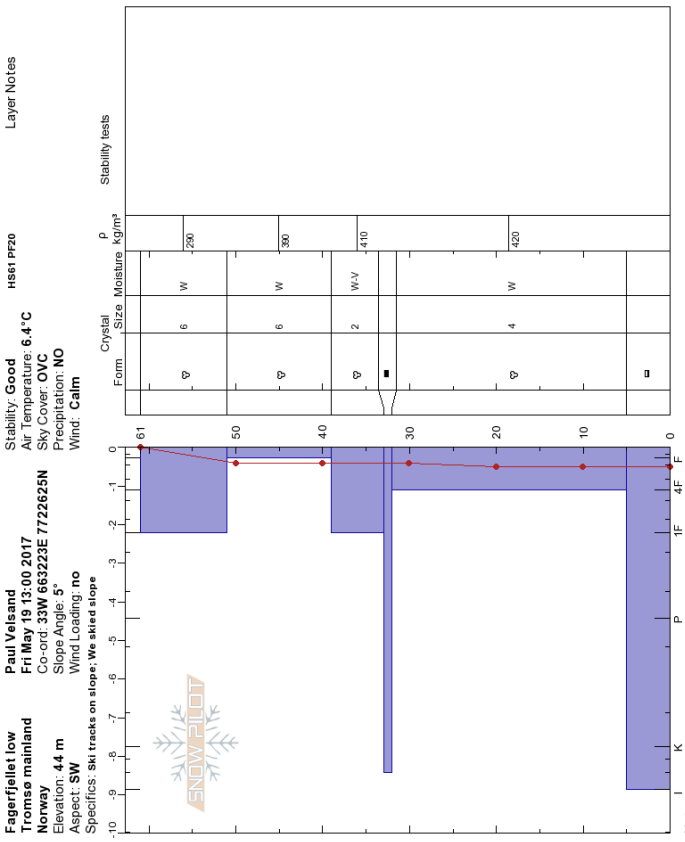

(b) May 19, 2017.

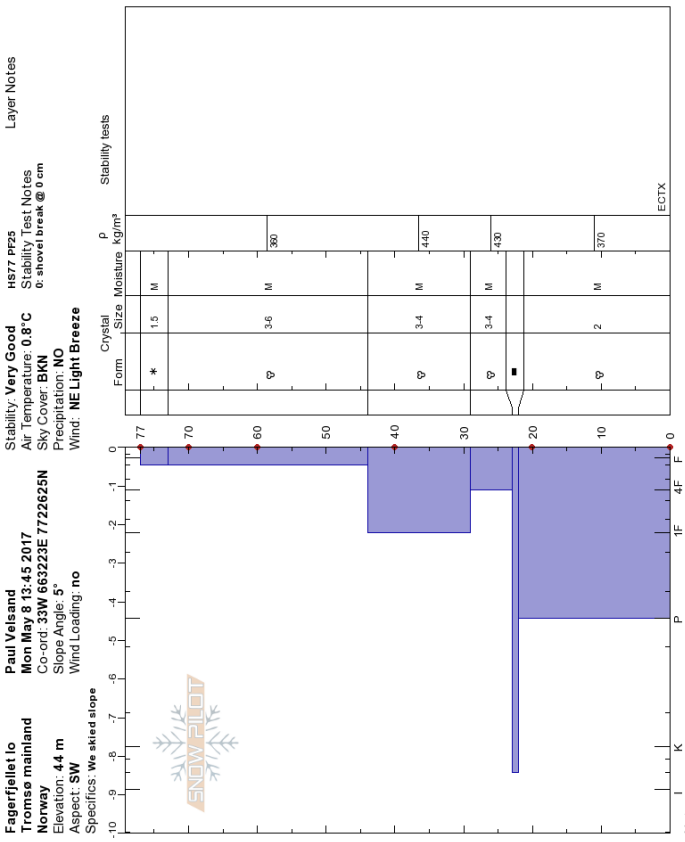

(a) May 8, 2017.

Figure A.41: Snow profiles FFlo, May 2017.

BIBLIOGRAPHY

About xgeo.no. (n.d.). Retrieved July 10, 2017, from http://www.xgeo.no/aboutXgeo.html?show=on

Armstrong, R. L. & Armstrong, B. (1987). Snow and Avalanche Climates of the Western United States: A comparison of Maritime, Intermountain and Continental Conditions. *Proceedings of the Davos Symposium, IAHS Publ. 162*, 281–294.

Aronsen, I. B. & Benjaminsen, T. (2016). Vinterturismen har skutt i været -itromso.no. Retrieved January 26, 2017, from http://www.itromso.no/nyheter/2016/06/14/Vinterturismen-har-skutt-i-v%7B%C3%A6%7Dret-12891412.ece

Beniston, M., Keller, F., & Goyette, S. (2003). Snow pack in the Swiss Alps under changing climatic conditions: An empirical approach for climate impacts studies. *Theoretical and Applied Climatology*, *74*(1-2), 19–31. doi:10.1007/s00704-002-0709-1

Birkeland, K. W. (1998). Terminology and predominant processes associated with the formation of weak layers of near-surface faceted crystals in the mountain snowpack. *Arctic and Alpine Research*, *30*(2), 193–199. doi:10.2307/1552134

Birkeland, K. W., Mock, C. J., & Shinker, J. J. (2001). Avalanche extremes and atmospheric circulation patterns. *Annals of Glaciology*, *32*, 135–140. doi:10.3189/172756401781819030

Birkeland, K. W., Simenhois, R., & Heierli, J. (2010). The effect of changing slope angle on extended column test results: Can we dig pits in safer locations? *Proceedings ISSW 2010*, 55–60.

Castebrunet, H., Eckert, N., & Giraud, G. (2012). Snow and weather climatic control on snow avalanche occurrence fluctuations over 50 yr in the French Alps. *Climate of the Past*, *8*(2), 855–875. doi:10.5194/cp-8-855-2012

de Quervain, M. R. (1950). Die Festigkeitseigenschaften der Schneedecke und ihre Messung. *Geofisica Pura e Applicata*, *18*(1), 179–191. doi:10.1007/BF02000325

Eckerstorfer, M. & Christiansen, H. H. (2011). The "High Arctic Maritime Snow Climate" in Central Svalbard. *Arctic, Antarctic, and Alpine Research*, *43*(1), 11–21. doi:10.1657/1938-4246-43.1.11

Ekker, R., Kværne, K., Os, A., & Humstad, T. (2013). regObs - public database for submitting and sharing observations. *International Snow Science Workshop*.

Emberland, T., Medby, A., & Pedersen, J. N. (2015). Snøskred i Tromsø. Retrieved November 10, 2016, from http://www.nordlys.no/snoskred-i-tromso/s/5-34-149653

Engeset, R. V. (2013). National Avalanche Warning Service for Norway – established 2013. *International Snow Science Workshop*, (January), 301–310.

European Avalanche Warning Services. (2017). The European Avalanche Danger Scale. Retrieved September 16, 2017, from http://www.avalanches.org/eaws/en/main%7B%5C_%7Dlayer.php?layer=basics%7B%5C&%7Did=2

Fierz, C., Armstrong, R. L., Durand, Y., Etchevers, P., Greene, E., McClung, D. M., … Sokratov, S. (2009). The International Classification for Seasonal Snow on the Ground. *IHP-VII Technical Documents in Hydrology*, *83*(1), 90.

Fitzharris, B. (1987). A Climatology of Major Avalanche Winters in Western Canada. *Atmosphere-Ocean*, *25*(2), 115–136. doi:10.1080/07055900.1987.9649267

Fitzharris, B. & Bakkehøi, S. (1986). A synoptic climatology of major avalanche winters in Norway. *Journal of Climatology*, *6*, 431–446.

Greene, E., Birkeland, K. W., Elder, K., Landry, C., Lazar, B., McCammon, I., … Williams, K. (2010). *Snow, Weather and Avalanches: Observation Guidelines for Avalanche Programs in the United States*. Pagosa Springs, CO: American Avalanche Association.

Grønnestad, K. S. (2016). What Is the Arctic? Retrieved September 30, 2017, from https://www.barentswatch.no/en/articles/Hva-er-Arktis/

Hägeli, P. & McClung, D. M. (2003). Avalanche characteristics of a transitional snow climate - Columbia Mountains, British Columbia, Canada. *Cold Regions Science and Technology*, *37*(3), 255–276. doi:10.1016/S0165-232X(03)00069-7

Hägeli, P. & McClung, D. M. (2007). Expanding the snow-climate classification with avalanche-relevant information: Initial description of avalanche winter regimes for southwestern Canada. *Journal of Glaciology*, *53*, 266–275. doi:10.3189/172756507782202801

Hansen, J. A. (2015). Tar hånd om skiturismen i nord. Retrieved January 26, 2017, from http://www.framtidinord.no/nyheter/2015/11/07/Tar-h%C3%A5nd-om-skiturismen-i-nord-11782339.ece

Höller, P. (2009). Avalanche cycles in Austria: An analysis of the major events in the last 50 years. *Natural Hazards*, *48*(3), 399–424. doi:10.1007/s11069-008-9271-1

Ikeda, S., Wakabayashi, R., Izumi, K., & Kawashima, K. (2009). Study of snow climate in the Japanese Alps: Comparison to snow climate in North America. *Cold Regions Science and Technology*, *59*(2-3), 119–125. doi:10.1016/j.coldregions.2009.09.004

Jamieson, B. (1995). *Avalanche prediction for persistent snow slabs* (Doctoral dissertation, University of Calgary).

Jamieson, B. (2006). Formation of refrozen snowpack layers and their role in slab avalanche release. *Reviews of Geophysics*, *44*(2), 1–15. doi:10.1029/2005RG000176

Jamieson, B. & Johnston, C. D. (1992). Snowpack characteristics associated with avalanche accidents. *Canadian Geotechnical Journal*, *29*(5), 862–866. doi:10.1139/t92-093

Jewell, E. J. & Abate, F. (2010). *The New Oxford American Dictionary* (3rd ed.) (A. Stevenson & C. A. Lindberg, Eds.). Oxford, England: Oxford University Press.

Judson, A. & Doesken, N. (2000). Density of Freshly Fallen Snow in the Central Rocky Mountains. *Bulletin of the American Meteorological Society*, *81*(7), 1577–1587. doi:10.1175/1520-0477(2000)081<1577:DOFFSI>2.3.CO;2

Keylock, C. J. (2003). The North Atlantic Oscillation and snow avalanching in Iceland. *Geophysical Research Letters*, *30*(5), 30–33. doi:10.1029/2002GL016272

LaChapelle, E. R. (1966). Avalanche Forecasting – A Modern Synthesis. *International Symposium on the Scientific Aspects of Snow and Ice Avalanches - IAHS Publication*, *69*, 350–356.

Landrø, M. (2013). Avalanche problems ; an important part of the Norwegian forecast , and a useful tool for the users. In *Proceedings issw 2013*.

Laternser, M. C. (2002). *Snow and avalanche climatology of Switzerland* (Doctoral dissertation).

Lazar, B., Greene, E., & Birkeland, K. W. (2012). Avalanche Problems & Public Advisories. *The Avalanche Review*, *31*(2), 1, 14–15, 23.

Matre, L. M. (2014). Hold deg til løypene - i dag er det skredfare. Retrieved November 18, 2016, from http://www.itromso.no/nyheter/vaer/article9333813.ece

McClung, D. M. (2013). The effects of El Niño and La Niña on snow and avalanche patterns in British columbia, canada, and central Chile. *Journal of Glaciology*, *59*(216), 783–792. doi:10.3189/2013JoG12J192

McClung, D. M. & Schaerer, P. (2006). *The Avalanche Handbook* (3rd ed.) (C. Hosler, Ed.). Seattle: The Mountaineers Books.

Mock, C. J. & Birkeland, K. W. (2000). Snow Avalanche Climatology of the Western United States Mountain Ranges. *Bulletin of the American Meteorological Society*, *81*(10), 2367–2392. doi:10.1175/1520-0477(2000)081<2367:SACOTW>2.3.CO;2

Mott, R., Schirmer, M., Bavay, M., Grünewald, T., & Lehning, M. (2010). Understanding snow-transport processes shaping the mountain snow-cover. *Cryosphere*, *4*(4), 545–559. doi:10.5194/tc-4-545-2010

Müller, K., Landrø, M., Haslestad, A., Dahlstrup, J., & Engeset, R. V. (2015). *Systematisk snødekkeundersøkelse*.

Nordahl, E. (2010). *Toppturer i Troms* (2nd ed.). Oslo, Norway: Fri Flyt AS.

Puschmann, O. (2005). *Nasjonalt referansesystem for landskap - beskrivelse av Norges 45 landskapsregioner*. Norsk institutt for jord- og skogkartlegging. Ås, Norway. Retrieved from http://www.

skogoglandskap.no/publikasjon/nj%7B%5C_%7Drapport%7B%5C_%7D10%7B%5C_%7D05/publication%7B%5C_%7Dview

Resvoll, J. & Johansen, J. I. (2016). Aldri før har snøen kommet så sent i Tromsø. Retrieved September 17, 2017, from https://www.nrk.no/troms/aldri-for-har-snoen-kommet-sa-sent-i-tromso-1.13238988

Roch, A. (1949). *Report on snow and avalanche conditions in the U.S.A.* Swiss Federal Institute for Snow and Avalanche Research. Davos, Switzerland.

Saloranta, T. M. (2012). Simulating snow maps for Norway: Description and statistical evaluation of the seNorge snow model. *Cryosphere*, *6*(6), 1323–1337. doi:10.5194/tc-6-1323-2012

Schweizer, J. (2008). Snow avalanche formation and dynamics. *Cold Regions Science and Technology*, *54*(3), 153–154. doi:10.1016/j.coldregions.2008.08.005

Schweizer, J. & Bruce Jamieson, J. (2010, September). Snowpack tests for assessing snow-slope instability. *Annals of Glaciology*, *51*(54), 187–194.

Schweizer, J. & Wiesinger, T. (2001). Snow profile interpretation for stability evaluation. *Cold Regions Science and Technology*, *33*(2-3), 179–188. doi:10.1016/S0165-232X(01)00036-2

Sharma, S. S. & Ganju, A. (2000). Complexities of avalanche forecasting in Western Himalaya - an overview. *Cold Regions Science and Technology*, *31*(2), 95–102. doi:10.1016/S0165-232X(99)00034-8

Simenhois, R. & Birkeland, K. W. (2009). The Extended Column Test: Test effectiveness, spatial variability, and comparison with the Propagation Saw Test. *Cold Regions Science and Technology*, *59*(2-3), 210–216. doi:10.1016/j.coldregions.2009.04.001

Statham, G., McMahon, B., & Tomm, I. (2006). The avalanche terrain exposure scale. In *Proceedings issw 2006* (1, pp. 491–497).

Sturm, M., Holmgren, J., & Liston, G. E. (1995). A seasonal snow cover classification system for local to global applications. *Journal of Climate*, *8*(5), 1261–1283. doi:https://doi.org/10.1175/1520-0442(1995)008<1261:ASSCCS>2.0.CO;2

The Canadian Avalanche Association. (2014). *Observation Guidelines and Recording Standards for Weather, Snowpack and Avalanches*.

The Norwegian Geotechnical Institute. (2016). *Dødsulykker i snøskred 2003–2013*. Norwegian Geotechnical Institute. Oslo, Norway.

The Norwegian Geotechnical Institute. (2017a). Bratte områder Norge. Retrieved June 30, 2017, from https://skredkart.ngi.no

The Norwegian Geotechnical Institute. (2017b). Ulykker med død. Retrieved June 26, 2017, from https://www.ngi.no/Tjenester/Fageksperti se-A-AA/Snoeskred/snoskred.no2/Ulykker-med-doed

The Norwegian Meteorological Institute. (2016). Klimaet i Norge. Retrieved November 9, 2016, from http://met.no/Klima/Klima%7B%5C_%7Di%7B%5C_%7DNorge/

The Norwegian Water Resources and Energy Directorate. (n.d.). Snøskredskolen [The Snow Avalanche School]. Retrieved September 25, 2017, from http://www.varsom.no/snoskredskolen/

The Norwegian Water Resources and Energy Directorate. (2015). ATES — Avalanche Terrain Exposure Scale.

The Norwegian Water Resources and Energy Directorate. (2016). Små snøskred som plutselig blir store. Retrieved November 9, 2016, from http://www.varsom.no/Nytt/Sma-snoskred-som-plutselig-blir-store/

The Norwegian Water Resources and Energy Directorate. (2017). The Avalanche bulletin - Varsom. Retrieved September 16, 2017, from http://www.varsom.no/snoskredvarsling/

Tremper, B. (2008). *Staying Alive in Avalanche Terrain* (2nd ed.) (E. Moore, Ed.). Seattle: The Mountaineers Books.

Van Herwijnen, A. & Birkeland, K. W. (2014). Measurements of snow slab displacement in Extended Column Tests and comparison with Propagation Saw Tests. *Cold Regions Science and Technology*, *97*, 97–103. doi:10.1016/j.coldregions.2013.07.002

Visit Tromsø. (2016). Northern Lights in Tromsø - 10 reasons to go. Retrieved November 9, 2016, from https://www.visittromso.no/en/content/northernlights-10-reasonstogototromso

Wahlgren, T. (2016). Tildeles 166.000 kroner til skiltprosjekt. Retrieved January 26, 2017, from http://www.framtidinord.no/nyheter/2016/04/14/Tildeles-166.000-kroner-til-skiltprosjekt-12599894.ece

Wakonigg, H. (1975). Die Schneeverhältnisse des östereichischen Alpenraumes. *Wetter und Leben*, *27*, 193–203.

COLOPHON

This document was typeset using the typographical look-and-feel `classicthesis` developed by André Miede. The style was inspired by Robert Bringhurst's seminal book on typography "*The Elements of Typographic Style*". `classicthesis` is available for both LaTeX and LyX:

https://bitbucket.org/amiede/classicthesis/